Biodegradable Amphiphilic Block Copolymers:

Synthesis, Characterization and Properties Evaluation

Yasser Assem

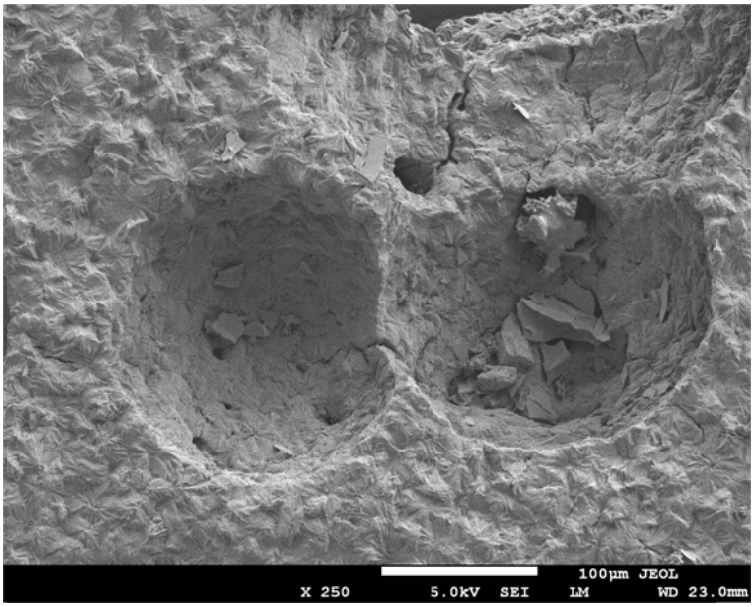

Marburg/Lahn- Germany 2011

Biodegradable Amphiphilic Block Copolymers:

Synthesis, Characterization and Properties Evaluation

Dissertation

For the doctor's degree of natural sciences

Submitted to
Chemistry department
Philipps-University of Marburg

By

Yasser Assem

From Cairo/Egypt

Marburg/Lahn- Germany 2011

Biodegradable Amphiphilic Block Copolymers:

Synthesis, Characterization and Properties Evaluation

Dissertation

zur Erlangung des Doktorgrades
der Naturwissenschaften
(Dr. rer. nat.)

dem Fachbereich Chemie
der Philipps-Universität Marburg

vorgelegt von

Yasser Assem

aus Kairo/Ägypten

Marburg/Lahn-Deutschland 2011

Vom Fachbereich Chemie der Philipps-Universität Marburg als Dissertation am /08/2011 angenommen

Erstgutachter: Prof. Dr. Andreas Greiner

Zweitgutachter: Prof. Dr. Seema Agarwal

Tag der mündlichen Prüfung: 25.08.2011

Table of Contents

Acknowledgements

First of all, I would like to express my sincere gratitude to my direct supervisor Prof. Dr. Andreas Greiner for giving me the chance to achieve my Ph.D. in his working group, and also for his continuous support during my research work. He has always been available for advice.

In German, the supervisor is called (Doktorvater), which means doctor´s father. This meaning reflects a true feeling towards Prof. Greiner. Many thanks Prof. Greiner for everything you have done for me.

My special thanks go to Prof. Dr. Seema Agarwal for her valuable guidance and advices. If I have a problem in my research, analytics or in the lab; an ideal solution is always available in her mind. I will never forget the common words that are always repeated by her (Do not worry, It is very easy). I would like to thank her also for the suggestion of the topic of chapter 4 (pH-responsive polymers).

I would like to show my gratitude to Mrs. Edith Schmidt for taking care of my official and personal documents and for being ever-so polite and helpful.

I am grateful to all the members of our working group for their constant support and advice. My special thanks go to my lab colleagues: Christian Heel, Urlich Meyberg, and Rüdiger Ellinghaus for their cooperation and for providing me with a good working environment. Special thanks again go to Christian Heel for plenty of work with GPC measurements. Thanks to Elisabeth Giebel for her help to achieve the mechanical testing. Special thanks to Ilka Paulus for the help in thermal analysis measurements and useful discussion.

I would also like to thank Mr. Uwe Justus and Lisa Hamel for their help in handling several kinds of instruments and helping to solve a lot of technical problems. I also appreciate Lisa for the IR measurement.

I would like to thank Martina Gerlach and Anna Bier for the ordering of chemicals and glassware and thereby ensuring that my work goes on smoothly.

My sincere thanks also go to Mr. Michael Hellwig for his help in operating the scanning electron microscope.
Many thanks to Haithem Abdelaal and Mohamed Abdel-majeed for their help in WAXRD measurements.

My special thanks go to Urlich Meyberg and Kathrin Buble for German translation of the summary. I want also to thank Christian Knierim for the correction of the English summary.

I am thankful to Dr. Amr Mohammed for helping me to correct my Ph.D. thesis.

Many thanks to all friends I met in Germany, Fuad Alrimawi- Gaza, Sajid Malek-Pakistan, Hesham Salem-Iraq, Brahim Mouddan-Morocco, Ayat Al-massaeda-Jordon, Tarek Afifi, Mohamed Elawady, Ahmed Fawzy, Haithem Abdelaal, Mohamed Abdelmajeed (elsahhah), Amr Mohammed, Hassan Ghareeb from Egypt for the nice and beautiful days we spent together in Germany as well as the difficult and black days (: D

Many thanks to all members of Egyptian cultural office in Berlin for their support and encouragement.

My sincere gratitude to my wife Eng. Amina Hamdy and my kids: Ammar (Mora), Mohamed (Hamoksha), and Abdelrahman (Bido), and ….? for their support and encouragement.

Last but not the least; I owe my deepest gratitude to my parent for their unconditional love and support. Without their blessings, this achievement would not have been possible.

List of symbols and abbreviations

Arranged alphabetically

a.u.	Arbitrary units
cm	centimeter
cm^{-1}	Wavenumber
cmc	Critical micelle concentration
Conc.	Concentrated
Da	Dalton
dL_b	Strain at break
DSC	Differential scanning calorimetry
e.g.	For example
et al.	et alii
FTIR	Fourier transform infrared spectroscopy
g	gram
GPC	Gel permeation chomatography
h	Hour
HCl	Hydrochloric acid
HMBC	Heteronuclear multiple bond correlation
HMQC	Heteronuclear multiple quantum correlation
i.e.	That is to say
J/g	Joule/gram
min	Minute
mL	Milliliter
Mn	Number average molecular weight
mol	Mole
Mp	Molecular weight at peak

MPa	Mega Pascal
MPEO	Methoxy poly(ethylene oxide)
MPEO2	Methoxy poly(ethylene oxide) (Mn 2000)
MPEO5	Methoxy poly(ethylene oxide) (Mn 5000)
Mw	Weight average molecular weight
nm	Nanometer
NMR	Nuclear magnetic resonance
Pa	Pascal
PBA-b-MPEO5	polybutylene adipate-b- methoxy poly(ethylene oxide) (Mn 5000)
PBS	polybutylene succinate
PBS-b-MPEO5	polybutylene succinate-b-methoxy poly(ethylene oxide) (Mn 5000)
PDI	Polydispersity index
PE	Polyester
PEG	Poly(ethylene glycol)
PEO	Poly(ethylene oxide)
PHA	polyhexylene adipate
PHA-b-MPEO2	polyhexylene adipate-b-methoxy poly(ethylene oxide) (Mn 2000)
PHA-b-MPEO5	polyhexylene adipate-b-methoxy poly(ethylene oxide) (Mn 5000)
PHS-b-MPEO5	polyhexylene succinate-b-methoxy poly(ethylene oxide) (Mn 5000)
PLA	Polylactide
PPA	Polyphosphoric acid
PVA	Poly(vinyl alcohol)

PGA	Poly(glycolic acid)
RPM	Revolution per minute
SD	Sulfadimethoxine
SEM	Scanning electron microscope
T	Temperature
Tcc	cold crystallization temperature
Tg	Glass transition temperature
TGA	Thermogravimetric analysis
THF	Tetrahydrofuran
Tm	Melting point
UV	Ultraviolet
vol.	Volume
WAXD	Wide angle X-ray diffraction
Wt %	Weight percentage
ΔH	heat of fusion
σ_b	Stress at break
σ_m ,	Stress maximum

Chapter 1

Introduction and Scientific background

1.1. Aim of the work

The main aim of this work is to prepare biodegradable amphiphilic diblock copolymers by melt polycondensation. These diblock copolymers are composed mainly of two segments, hydrophilic segment and hydrophobic segment. The hydrophilic segment is methoxy poly(ethylene oxide) (MPEO) of two different molecular weights (5000 and 2000 g/mol). The hydrophobic segment is polyester of adipate/hexandiol, succinate/butandiol or a mixture therefrom. Furthermore, to characterize the obtained materials, and to evaluate the physical properties including molecular weight, glass transition temperature, mechanical properties. Then hydrolytic and enzymatic degradation profile of the prepared material will be also investigated. Another aim is to obtain a pH responsive polymer by loading the obtained polymers with a pH responsive moiety, namely Sulfadimethoxine (SD). Finally measuring of critical micelle concentration (cmc) of SD loaded polymers as well as the virgin polymers by using fluorescence spectroscopy is also targeted.

The thesis includes 6 chapters: ***Chapter 1*** contains introduction, scientific background and literature survey. ***Chapter 2*** contains the synthesis of the aforementioned amphiphilic block copolymers with full characterization using different analytical tools including (GPC, thermal analysis, X-rays and different spectroscopic tools). ***Chapter 3*** includes the data of the hydrolytic and enzymatic degradation of the synthesized block copolymers. ***Chapter 4*** represents the trial of immobilizing a pH-dependent, bioactive ingredient onto the Polymer backbone. ***Chapter 5*** contains the data of the Determination of critical micelles concentration (cmc). ***Chapter 6*** contains the used materials, experimental techniques, and analytics of the polymers. Last part contains references and summary in English and German.

1.2. Scientific Background

1.2.1. Problem definition

Applications of polymeric materials are increasing day by day, in every place in our diary life; it is somewhat difficult to find any article or a material that does not include a kind of polymeric material in its body. These materials without doubt make our life easy and happy, this is of course the white side of the coin or in other words the filled half of the cup, but as a scientific people we should also pay attention to the black side of the coin i.e. the empty half of the cup and trying to find an answer to the question: what will happen to these polymeric material after usage?. To answer this question we should be aware of the nature and characteristics features of the final product of the polymeric materials. They are durable, resistant to various forms of degradation and in more dramatic case they are crosslinked and do not soluble in all solvents (tires for example). These specific properties of polymers make the disposal of these polymers a big challenge. As a consequence, a lot of efforts have been taken since the early 1990s to develop novel polymers that have the same properties as conventional polymers but are more susceptible to degradation and hence are more environmental friendly.

1.2.2. Degradable and biodegradable polymers

The term ‘‘degradable polymers’’ is difficult to define exactly because of confliction and confusion. The American Society for Testing and Materials (ASTM) defined the degradable polymer as the polymer that undergoes a significant change in its chemical structure under specific environmental conditions, resulting in a loss of some properties (e.g. integrity, molecular weight, structure or mechanical strength).[1,2] Degradation occurs randomly at any point of the polymer chain, leading to a drastic change in molecular weight, or could be along the chain ends (depolymerization) by which monomers are liberated. Different ways of degradation include: ***thermal degradation*** that uses heat and /or reduced pressure (autoclave) to degrade the polymer [3,4] ***mechanical degradation*** in which extruders and roll mills are used [5], ***photo-degradation*** that takes place by action of natural daylight [6] , ***oxidative degradation*** in which degradation takes place by oxidation [7-9], ***degradation by ultrasonic waves*** [10], ***degradation by high-energy radiation*** [11], ***hydrolytic degradation*** like for example alkali hydrolysis [12], and most importantly

biodegradation in which degradation takes place by natural bacteria, fungi, and other microorganisms that present in the environment. [2,13] Polymers that undergo to biodegradation are coined as ***biodegradable polymers***.

1.2.3. Degradation mechanism.

Because the back bone of the polymer chains are mainly C-C bonds, most of the synthetic polymers are durable and resistant to various kinds of degradation. However, polymers could be degraded if their backbone contains functional groups like ester, carbonate, anhydride, acetal, amide, or hydroxyl-esters, as these groups are susceptible to either hydrolytic degradation or biodegradation by micro-organisms. [14-17]

At first the polymers containing these hetero atoms are degraded by effect of hydrolytic hydrolysis or enzymatic hydrolysis into oligomers or even small molecules with functional groups such as for instance carboxylic acids and/or alcohol in case of polyester degradation .[18] It is generally stated that the enzymatic degradation occurs only on the surface of the solid polymer as the enzyme cannot penetrate into the bulk of the solid substrate. The degradation starts from the amorphous or relatively less-ordered area instead of the more rigid crystalline interior. After hydrolysis of the surface, the produced small fragments are washed away by water, and enzyme can attack another new layer. Therefore, the molecular weight of the substrate does not change theoretically, only the loss of weight of the solid material could be observed. Hydrolytic hydrolysis (basic or acidic) takes place also from the surface preferring amorphous area. However, small basic or acidic reagent can diffuse into the solid substrate and lead to in-depth degradation. Therefore, the molecular weight of the material decreases, but the total weight of solid cannot be detected very fast. Metabolism of the resulting small molecules by microorganisms into CO_2, and biomass is crucial for perfect and complete biodegradability. Thus, a biodegradable polymer has the ability to be broken down by biological means into natural raw materials and then disappear into the nature. Because of the co-existence of both biotic and non-biotic effects, the entire mechanism of polymer degradation can also be known as environmental degradation.[19]

It is worth to mention that, environmental factors not only help the polymer to degrade, but they also play an essential role in affecting the activity of different microorganisms. Factors such as humidity, pH, temperature, salinity and the presence, or the absence of oxygen, have important influences on the microbial degradation of polymers. In addition, the chemical structure and the chemical composition of the polymer are major parameters in polymer degradation. It is well known that, polymers (especially, the end use articles) usually do not exist as one homogeneous component but they can contain different polymers (blends) or low molecular weight additives like plasticizers. Polymers of different structures such as copolymers which consist of random, alternate or block copolymers, and branched or crosslinked polymers can affect the degradation behavior of that polymer. Besides, the crystallinity and crystal morphology of a polymer depends on the processing parameters and it can be changed with time. These mentioned parameters play the major role that determines the degradation behavior of a polymer. [2,20]

Some polymers with C-C backbone can be coined as biodegradable polymer. These polymers contain usually pendent groups on the main polymeric chains, which can undergo (photo, thermo or enzymatic) oxidation and the resulting product can be oxidized further to oligomers or even small molecules such as a naturally occurring polymer, polyisoprene (Natural rubber). Others are synthetic vinyl polymers like poly(vinyl alcohol)[21-23] and poly(vinyl methyl ether) [24-26] as represented in Figures 1.1 and 1.2.

Depending on how far water/enzyme can diffuse inside the polymer matrix, erosion of the polymer can occurs either on the surface of the polymer matrix or in the bulk. In bulk erosion, degradation takes place throughout the whole of the sample by taking water inside the matrix, in surface erosion, the polymer is eroded from the surface in which polymers do not allow water to penetrate into the material and erode layer by layer. Examples of the polymers that undergo surface erosion are polyanhydrides and poly (ortho) esters. Herein, erosion proceeds at constant velocity at any time during erosion. However, bulk eroding polymers such as polylactides (PLA), polyglycolides (PGA), poly (lactic-*co*-glycolic acid) (PLGA), and polycaprolactones (PCL), have no constant erosion velocity. Polymer erosion plays an important role in many essential and important processes such as the control release of drugs from polymer implants. By knowing the kind of erosion a polymer undergoes, it can be effectively used for the design of drug delivery systems.[2, 27]

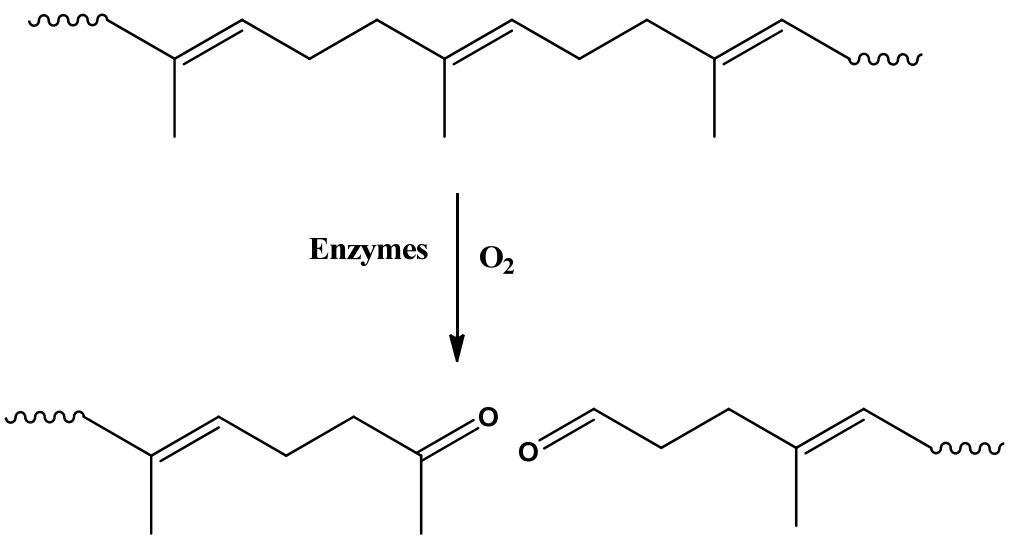

Figure 1.1. Proposed mechanism of enzymatic degradation of Natural Rubber

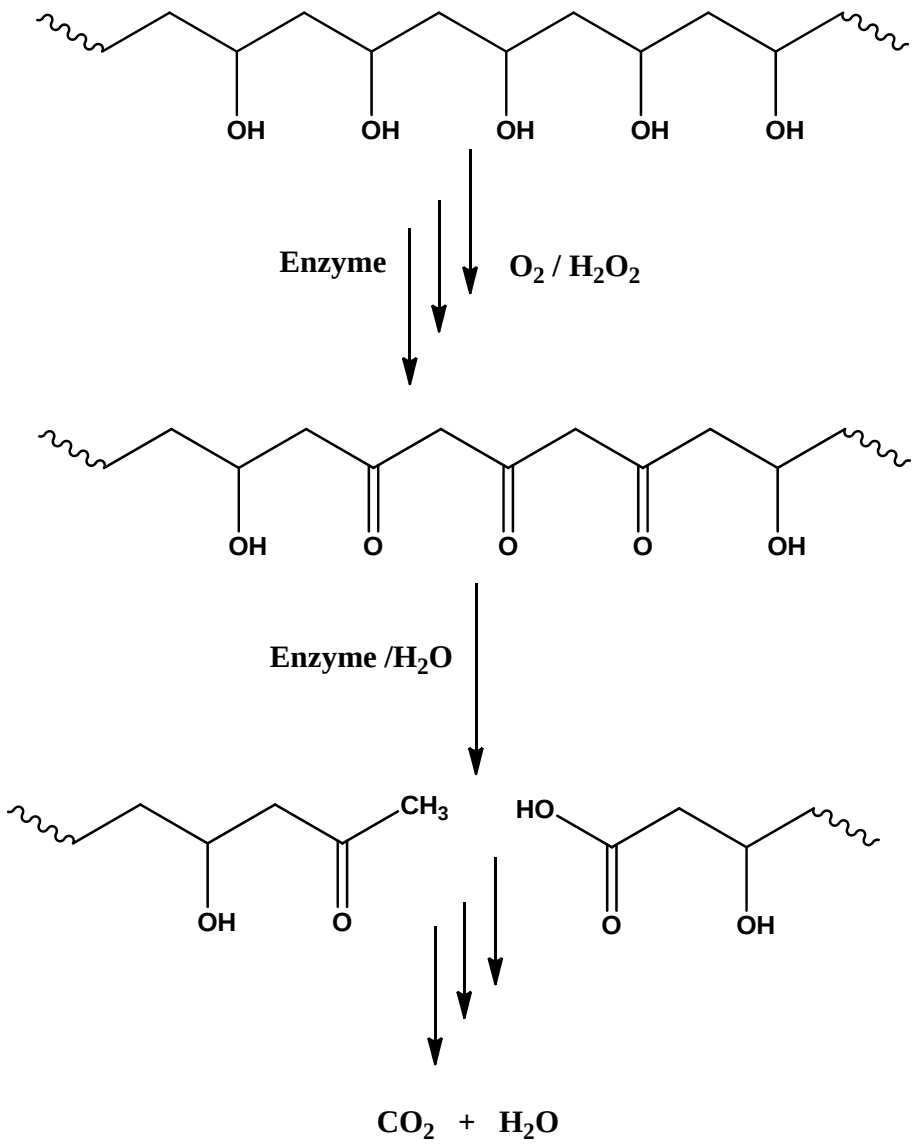

Figure 1.2. Proposed mechanism of enzymatic degradation of polyvinyl alcohol.

1.2.4. Classification of biodegradable polymers

There are many ways to classify biodegradable polymers. They can be sorted according to their chemical composition, synthesis method, processing method, economic importance, application, etc. Each of these classifications provides different and useful information. According to their origin, biodegradable polymers can be classified into two groups[28]: ***i- natural polymers***, polymers coming from natural resources and ***ii- synthetic polymers***, polymers synthesized from crude oil.

Polymers from natural origins include sub-groups:

1. Polysaccharides (e.g., starch, cellulose, lignin, chitin)
2. Proteins (e.g., gelatin, casein, wheat gluten, silk and wool)
3. Lipids (e.g., plant oils including castor oil and animal fats)
4. Polyesters produced by micro-organisms or plants (e.g., polyhydroxy-alcanoates, poly-3-hydroxybutyrate)
5. Polyesters synthesized from bio-derived monomers (polylactic acid)
6. Miscellaneous polymers (natural rubbers, composites).

Biodegradable polymers from mineral origins include four sub-groups:

1. Aliphatic polyesters (e.g., polyglycolic acid, polybutylene succinate, polycaprolactone)
2. Aromatic polyesters or blends of the two types (e.g., polybutylene succinate terephthalate)
3. Polyvinyl alcohols
4. Modified polyolefins (polyethylene or polypropylene with specific agents sensitive to temperature or light).

1.2.5. Biodegradable polyesters

Polyesters represent a large family of polymers having in their structure the potentially hydrolysable ester bond. The polyesters can be classified following the composition of their main chain as aliphatic and aromatic polyesters. Aliphatic polyesters are one of the most promising biodegradable materials for industrial and biomedical uses with relatively good mechanical properties and processability. A wide range of aliphatic polyesters can be designed by using various reactants and changing the synthesis conditions to meet specific requirements such as hydrophobicity, crystallinity, degradability, solubility, glass transition temperature, melting temperature and so on.[28] Commercially available degradable polyester found their applications as flexible and tough thermoplastics in industrial, agricultural and biomedical applications. Ikada el al in his review gave some information about the degradation rates of different polyesters as listed in table 1.1[29]

Table 1.1 Rate of degradation of various biodegradable polymers

Polymer	Structure	Mw	Degradation rate
Poly(glycolic acid)	Crystalline	-	100% in 2-3 months
Poly(L-lactic acid)	Semi-crystalline	100-300	50% in 1-2 years
Poly(glycolic acid-*co*-L-lactic acid)	Amorphous	40-100	100 % in 50-100 days
Poly(ε-caprolactone)	Semi-crystalline	40-80	50 % in 4 years
Poly(L-lactic acid-*co*-ε-caprolactone)	Amorphous	100-500	100 % in 3-12 months
Poly(orthoester)	Amorphous	100-150	60% in 50 weeks

1.2.6. Classification of degradable polyesters

Aliphatic polyesters can be categorized into two kinds depending on the monomers used in the synthesis. The 1st category is polyhydroxyalkanoate (PHA), a polymer of hydroxy carboxylic acid (HO-R-COOH). These acids can be divided further into α, β, ω-hydroxy acids based on the position of OH group with respect to the COOH group. The 2nd one is poly(alkylene dicarboxylate), which are produced by condensation reaction between prepolymers having hydroxyl or carboxyl terminal groups using chain extenders such as diisocyanate. A detailed classification of the aliphatic polyesters as well as the type of degradation is given in Table 1.2.

Table 1.2 Different classes of aliphatic polyester combined with degradation method. [29,30]

Chemical Structure / Name		Example	Degradability
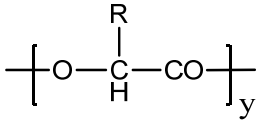 Poly(α-hydroxy acid)	R =H	Poly(glycolic acid) (PGA)	Chemical Hydrolysis
	R = CH_3	Poly(L-lactic acid) (PLLA)	
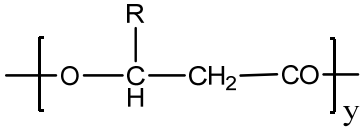 Poly(ß-hydroxyalkanoate	R = CH_3	Poly(ß-hydroxybutyrate)	
	R = CH_3, C_2H_5	Poly(β-hydroxybutyrate-*co*-β-hydroxyvalerate) (PHBV)	Enzymatic Hydrolysis
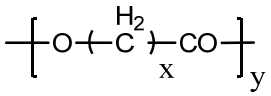 Poly(ß-hydroxyalkanoate)	Y = 3	Poly(γ-butyrolactone)	Enzymatic Hydrolysis
	Y = 4	Poly(δ-valerolactone)	
	Y = 5	5 Poly(ε-caprolactone)	
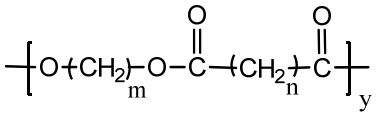 Poly(alkylene dicarboxylate)	m = 2, n = 2	Poly(ethylene succinate) (PES)	Enzymatic Hydrolysis
	m = 4, n = 2	Poly(butylene succinate) (PBS)	
	m = 4, n = 2,4	Poly(butylene succinate-co-butylene adipate) (PBSA)	

1.2.7. Synthetic routes for polyesters

Polyesters are generally synthesized by a step-growth process, i.e., polycondensation from a mixture of diol and diacid (or diacid derivatives) as shown in Figure 1.3. This method required instant elimination of the water from the polymerization system to avoid the hydrolysis [31].

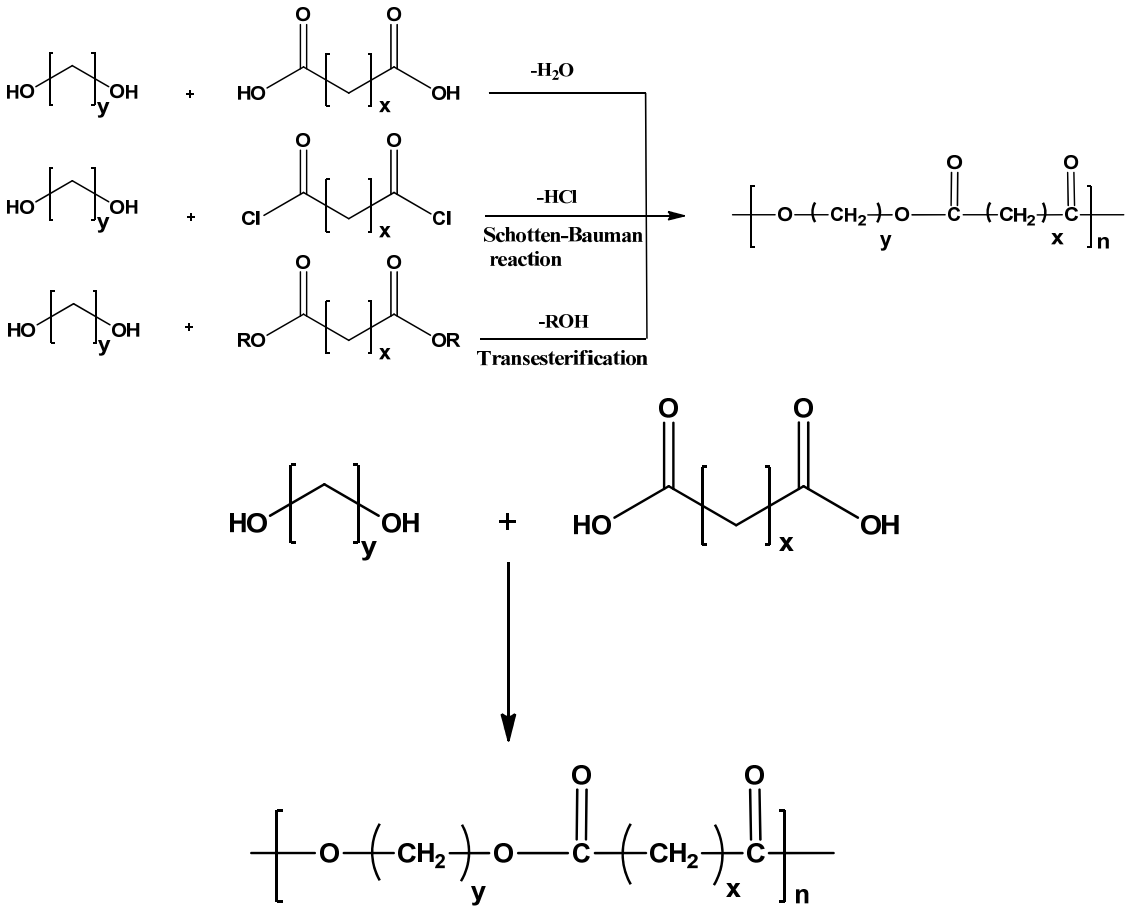

Figure 1.3. Synthetic route of aliphatic polyester by polycondensation.[31]

Ring-opening polymerization (ROP) of cyclic esters and related compounds in presence of a catalyst such as stannous octoate is an alternative method for the synthesis of aliphatic polyesters[32-37] (Figure 1.4).

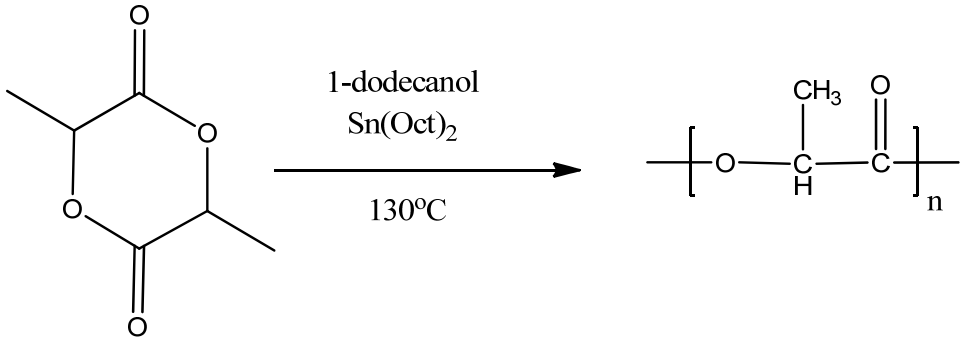

Lactide
3,6-dimethyl-1,4-dioxane-2,5-dione

Figure 1.4. Synthesis of polylactic acid by Ring Opening Polymerization of lactide.

Enzyme-catalyzed polymer synthesis is another approach using enzyme to catalyze polymerization process and now being used by many researchers [38-40], for example enzyme-catalyzed polycondensation and ring opening polymerization are now being used for preparation of homopolymers, random copolymers and block copolymers [41-46]

1.2.8. Applications of Biodegradable polymers

Aliphatic polyesters are utilized in various application fields particularly in medicine application, flexible packaging and in agriculture as briefed in the coming sections[20].

1.2.8.1. Biomedical uses

Controlled Drug Delivery is considered as one of the most important and versatile application of these polymers. Controlled drug delivery has applications not only in medicine but also in veterinary and agrochemical active ingredients from pesticides to contraceptives that can be delivered by sustained release with the ultimate biodegradation of the carrier medium. ***Tissue culture and tissue engineering*** is also a very interesting field of application that exploits aliphatic polyester to produce biodegradable networks that are effective as wound dressings, tubular conformations for intestine or vascular grafts and skin substitutes. Another use is in ***Surgical fixation*** (sutures, clips, bone pins and plates), where PGA and PLA have been used to produce strong filament and were shown to degrade rapidly. The use of biodegradable implants for ***the fixation of fractured bones and joints*** has been established and contrasted with the use of metal pins and clips. About 40 different biodegradable polymers and copolymers are currently being used as alternatives of metal implants. [47, 48]

1.2.8.2. Biodegradable plastics for packaging

Poly(3-hydroxybutyrate) (PHB) and the copolymer poly(3-hydroxybutyrate-co-3-hydroxyvalerate) (PHBV), which are produced in plant cells and can be synthesized biochemically by fermentation, are commercialized under trade name Biopol, and were originally intended as biodegradable substitutes for oil-based polyolefin in plastic containers, films and bottles[49], for packaging shampoo, and motor oil containers, and paper-coating materials. The main disadvantages of the use of biodegradable polymers for bulk packaging is the difference in the price of these polymers compared with that of bulk produced, oil-based plastics. Current low oil prices, increased recycling capacity and improved technologies for the separation of plastics and make the use of biodegradable polymers for most packaging requirements still uneconomic.[20,50]

1.2.8.3. Other uses

Biodegradable polymers have been used for the sorption of oil-based aromatic compounds from low carbon sand by microbial polyesters[20,51], more than 1994 patient cited the use of poly(caprolactone) filaments blended with other biodegradable polymers as a biodegradable carrier for denitrifying bacteria in water purification. Biodegradable materials can be effectively used for agricultural applications where core materials like pesticides or pheromones can be released into the environment in a controlled manner and the polymeric material gets completely degraded with time.

1.3. Block copolymers

Block copolymers are an interesting class of polymeric materials which composed of two different polymer segments that are chemically bonded.[52] These segments are in most cases, thermodynamically incompatible giving rise to a rich variety of microstructures in bulk and in solution. The mode of arrangement of the block segments can vary from diblock or triblock copolymers, with two or three segments respectively, to multiblock copolymers containing many segments. A schematic representation of various block copolymer architectures are given in Figure 1.5 including graft and radial block copolymers. A variety of morphologies and properties can be achieved with microphase separated block copolymers.

1.3.1. General Synthetic Methods for Block copolymers

Various synthetic approaches have been utilized to prepare block copolymer, ***anionic polymerization*** [53] which has been discovered more than 50 years ago is considered as one of the most efficient method to prepare well defined block copolymers. Anionic polymerization is characterized by the absence of termination and chain transfer reactions, carbanions (or, in general, anionic sites) remain active after complete consumption of monomer, giving the possibility of block copolymer formation, in the simplest case, by introduction of a second monomer into the polymerization mixture giving chance for the preparation of linear block copolymers. Successful examples are AB diblock copolymers of styrene and isoprene or butadiene, with predictable composition and molecular weights as well as narrow molecular weight have been synthesized by sequential addition of monomers.

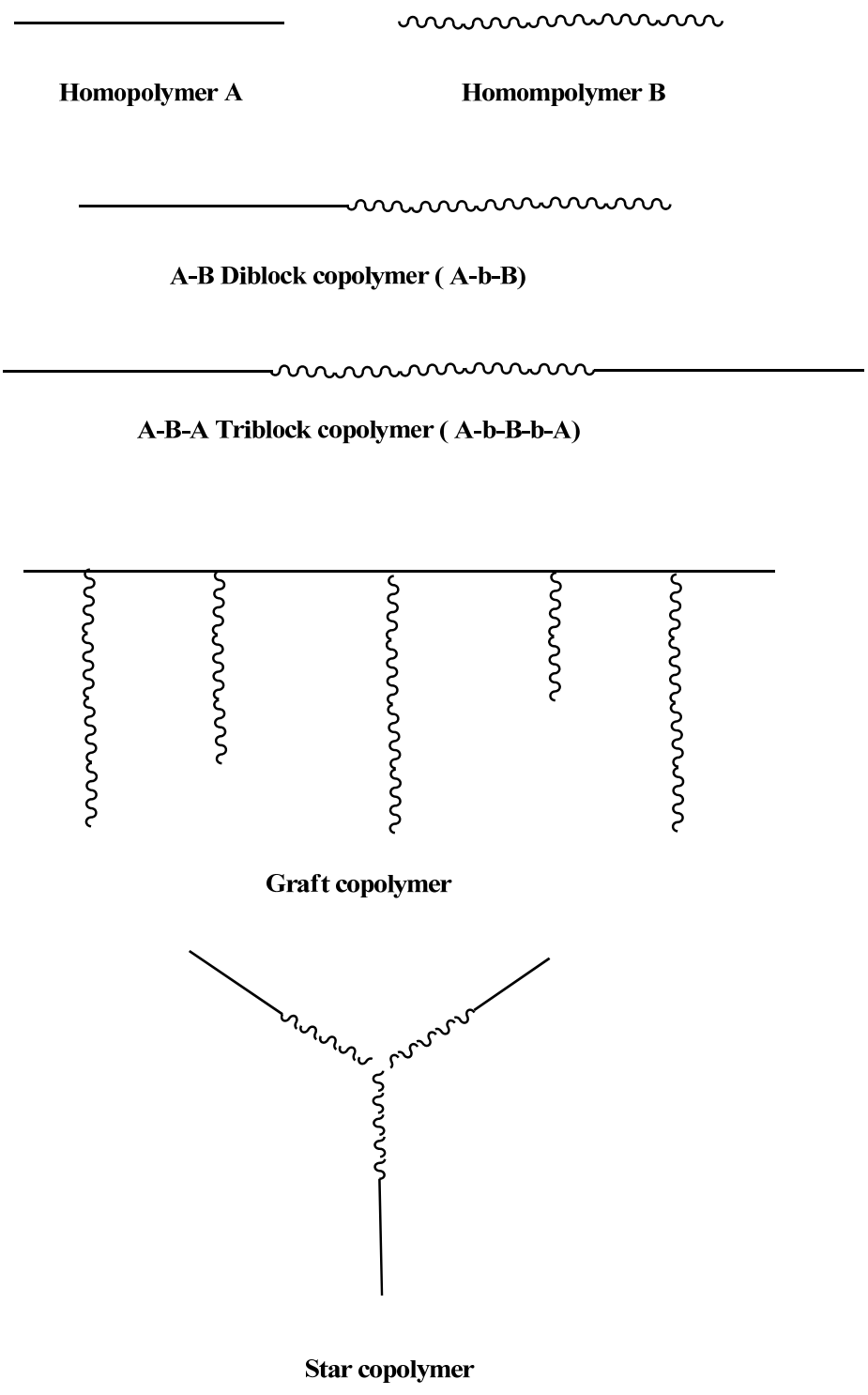

Figure 1.5 Architecture of different block copolymers[52]

Cationic polymerization [54] was also used to prepare diblock copolymers from styrene and isobutylene, however it is suffering from several problems which is out of the scope of this thesis to be discussed in details. ***Controlled radical polymerization***[55] is an important topic nowadays in polymer chemistry that comprises different mechanisms to produce living polymers with well-defined architectures. Nitroxide mediated radical polymerization (NMP) [56], atom transfer radical polymerization (ATRP)[57], and reversible addition-fragmentation chain transfer polymerization (RAFT)[58] have been utilized extensively to prepare different polymer architectures including various block copolymers.

1.3.2. Synthesis of block copolymers by coupling of end-functionalized prepolymers

Diblock and triblock copolymers have been synthesized by using a direct coupling between end functionalized prepolymers. Poly(p-phenyleneethylene)-b-poly(ethylene oxide) rod-coil block copolymers were also synthesized by direct coupling of carboxy-terminated PPE and hydroxyl-terminated PEO. A large numbers of amphiphilic block copolymers comprising aliphatic polyesters and poly(ethylene oxide) have been also prepared by the same approach, where hydrxoy/carboxy-terminated aliphatic polyester was prepared then coupled directly with mono or di hydroxyl poly(ethylene oxide) to synthesize di and triblock copolymers.[59]

1.4. Poly(ethylene glycol) based block copolymers

Poly(ethylene glycol) (PEG) is a hydrophilic, non-toxic, flexible polymer that has a lot of applications as a biocompatible material. At high molecular weights PEG is also referred to as poly(ethylene oxide) (PEO). Amphiphilic block copolymers comprising PEG as a hydrophilic segment and aliphatic polyester (PE) as the hydrophobic segment taking the benefit of both biocompatibility of PEG and biodegradability of the polyesters have been gained and still much attention by a lot of researchers. Huge amount of scientific articles and reviews have been published including the synthesis and applications of the PE-b-PEG, especially in pharmaceutical and medical fields [60-64]. An example of the aliphatic polyester used is polylactic acid (PLA). PLA is characterized by ease of biodegradability, nontoxicity and biocompatibility [50,65-70]. Just by adjusting the ratio of both segments, modulation of biodegradation rate and hydrophilicity could be achieved. The synthesis of poly(lactic- glycolic acid) (PLGA) and poly(ethylene glycol) block copolymer with high molecular weight was reported by Ferruti et al.[71] At first acid chloride end groups of PEG were prepared by reacting poly(ethylene glycols) with phosgene. Then a polycondensation of the resulting α,ω-bis(chloroformates) with PLGA oligomers was conducted. It was found that, the length of PEG segment is a main factor to control the desolation rate of PLGA-b-PEG [71,72]. It is possible to use different catalysts in the polycondensation process for the synthesis PLGA-b-PEG as reported by Deng et al.[73] They used $SnCl_2 \cdot 2H_2O$ as a catalyst in the synthesis of the block copolymers of DL-lactic acid and PEG, while, Kricheldorf et al. used metal oxide and stannous octoate to synthesize poly(L-lactic acid)-b-poly(ethylene glycol) (PLLA-b-PEG) [74] and in another experiment they have also prepared the copolymers from L-lactide and PEG using potassium tert-butoxide in toluene at 80 °C.[75] Bulk polymerization reaction using aluminium triisopropoxide as catalyst was used to prepare ABA triblock copolymer containing hydrophilic PEO segments and hydrophobic PLA or PLGA segments. After formation of the initiator complex between PEO and the catalyst, the PLA and PLGA blocks are attached by ring opening polymerization[76]. The degradation of ABA tri-block copolymers was rapid with comparison of its random copolymers. [77] Ma et al. [78] used ring opening polymerization to prepare ABA block copolymers of DL-lactide and poly(ethylene glycol). Anionic polymerization initiated with potassium poly(ethylene glycol)ate as a microinitiator was used to prepare poly(DL-lactic acid)-b-PEG-b-poly(DL-lactic acid) (PDLLA-

b-PEG-b-PDLLA) as reported by Zhu et al.[79] Hu et al. reported the effect of incorporation of ether linkages into PLLA chains on the time of biodegradation as well as on the behavior of protein adsorption [80]. It was found that, incorporation of PEG segments increases the copolymer polarity; consequently a reduction of protein adsorption takes place. Studying the viscoelastic properties of an aqueous dispersion of PLA-b-PEG were reported by Hagan et al.[81] They have also estimated the chain length of PEG (nearly 6.4 nm) and suggested that this value will give an indication of the steric stability of the particle. Preparation of PLA-b-PEG with biotinylated PEG end groups (final polymer termed PLA-b-PEG-biotin) was reported by Black et al. [82], they aimed to facilitate the fabrication of complex biomaterial surfaces. PLA-b-PEG-biotin was found to be biodegradable and resistant to non-specific protein adsorption, and the biotin moiety allows surface chemical engineering to be achieved using avidin–biotin interactions, which is a rapid method of immobilizing biomolecules at biomaterial surfaces under aqueous conditions. PEGs based block copolymers containing polycaprolactones as the hydrophobic segments were also reported. For example poly(ε-caprolactone)-block-poly(oxyethylene)-block-poly(ε-caprolactone) (PCL-b-POE-b-PCL) and PLA-b-POE-b-PLA have been synthesized without any catalyst at 185 and 140°C, respectively by ring-opening polymerization [83]. It was found that with the increase of molar percentage of oxyethylene unit in the chain, hydrophilicity of copolymer increases, and PLA-b-POE-b-PLA is more hydrophilic than the PCL-b-POE-b-PCL having the same molar composition. Protein-C loaded nanospheres were formed from these triblocks copolymers[83]. Li et al[84] prepared four kinds of core-shell nanoparticles from di-block copolymer of methoxy poly(ethylene glycol)-b-polycaprolactone (MPEG-b-PCL) and tri-block copolymer of polycaprolactone-b-poly(ethylene glycol)-b-polycaprolactone (PCL-b-PEG-b-PCL). The block copolymers were synthesized by ring opening copolymerization using stannous octate at 130 ^{o}C. The prepared nanoparticles were evaluated as a drug carrier and antitumor drug. Histoculture Drug Response Assay (HDRA), a more predictive method usually used to evaluate chemosensitivity was firstly applied in this study to evaluate the antitumor potency of polymeric nanoparticles. It was found that all the four kinds of copolymers exhibited remarkable antitumor effects.[84]

Recently, triblock copolymers of poly(ε-caprolactone)-*block*-poly(ethylene glycol)-*block*-poly(ε-caprolactone) (PCL-b-PEG-b-PCL) containing biotin moiety at the junction points were prepared by a combination of click chemistry and ring-opening polymerization.[85] Alkyne-functionalized PEG was used as macroinitiators in ring opening polymerization of ε-caprolactone to give the target block copolymers PCL-b-PEG-b-PCL. By employing click chemistry, biotinylated triblock copolymers were prepared and the structure was proofed by gel permeation chromatography and ^{1}H NMR. The triblock copolymer chains can self-assemble into micelles in aqueous solution, where, the PCL blocks form the cores of the micelles while, the hydrophilic PEG blocks form the coronae. The biotin moieties are distributed at the interface of the micelles. Upon addition of avidin to the micellar solution, micelles aggregated together forming micellar aggregates due to the interaction between avidin and biotin.[85] Chen et al. prepared amorphous amphiphilic triblock copolymers of poly (3-hydroxybutyrate)–poly(ethylene glycol)–poly(3-hydroxybutyrate) (PHB–PEG–PHB) using the ring-opening copolymerization of *β*-butyrolactone monomer. These triblock copolymers can form biodegradable nanoparticles with core–shell structure in aqueous solution. Comparing to the poly(ethylene oxide)–PHB—poly(ethylene oxide) (PEO–PHB–PEO) copolymers, these nanoparticles exhibited much smaller critical micelle concentrations and better drug loading properties, which indicated that the nanoparticles were very suitable for delivery carriers of hydrophobic drugs.[86, 87]

Star block copolymers from multi-arm PEO and L-lactide or L-lactide/glycolide were reported by Kissel et al.[88] In this example, solution polymerization in toluene using aluminium triethylene as a catalyst was used to synthesize biodegradable star block copolymers containing a hydrophilic 4- and 8-arm branched poly(ethylene oxide) (PEO) central unit and hydrophobic poly(L -lactide) (PLLA) or poly(L -lactide-co-glycolide) (PLLG). The degradation of these polymers was assayed in phosphate buffer saline [(PBS), pH 7.2, 37°C. Slow mass erosion was observed with the constant ratio of PEO/PLLG within the first 20 days, however, acceleration of the degradation was observed after 20 days which attributed to the slower cleavage of the PEO-PLLG bond. Synthesis of star shaped poly (ethylene oxide) (PEO), poly(L -lactide) (PLLA) and PEO-poly(ε-caprolactone) block copolymers was reported by Choi et al. [89] At first multi-arm PEOs with various numbers of arms with a fixed molecular weight (M_w 10 000) were synthesized by anionic polymerization of ethylene oxide and used as a core block. Then ring-

opening polymerization using multiarm PEOs as initiator in the presence of stannous octoate as a catalyst was used to prepare star-shaped PEO-PLLA and PEO-PCL block copolymers. Swelling behavior of star-block copolymers suggests that the water uptake depend on the molecular architecture and the phase mixing of PEO segment with PLLA or PCL segment [89]. Water uptake was higher in PEO-PLLA than PEO-PCL and with increasing number of arms in copolymer under the same conditions, due to more hydrophobic nature and higher crystallinity of PCL compared to PLLA block. Two melting endotherms for PEO-PCL block copolymers in the DSC thermogram indicates two immiscible separated phases of PCL and PEO, in contrast to the results from PEO-PLA block copolymers of similar PEO contents and molecular architecture. Decrease in crystallinity in star block copolymers was due to phase mixing, which was increased with an increase in the number of arms. Intrinsic viscosity of star-block copolymers was decreased with degree of branching because in good solvent, polymer chains are fully extended due to the thermodynamically favorable interactions between polymer and solvent.

Synthesis of a star polymer in which the core of the star polymer is polyamidoamine (PAMAM) dendrimer and arms of the star are amphiphilic block copolymer is reported by Wang et al.[90] The inner block in the arm is hydrophobic poly (ε-caprolactone) (PCL), and the outer block in the arm is hydrophilic poly(ethylene glycol) (PEG). The star-PCL polymer was synthesized first by ring-opening polymerization of ε-caprolactone with a PAMAM-OH dendrimer as initiator. The PEG polymer was then attached to the PCL terminus by an ester-forming reaction. The star structure of the polymers was confirmed by conventional analytical tools as SEC, ^{1}H NMR, FTIR, TGA, and DSC. The micelle formation of the star copolymer (star-PCL−PEG) was studied by fluorescence spectroscopy. Hydrophobic dyes and drugs can be encapsulated in the micelles.[90]

In another study, by the same authors, they compared the structures and the amphiphilic properties of two types of arms in the star polymers. The first type, stPCL-PEG_{32}, is composed of a polyamidoamine (PAMAM) dendrimer as the core with arms having poly(ε-caprolactone) (PCL) and poly(ethylene glycol) $(PEG)_{32}$ as an inner lipophilic block and outer hydrophilic block respectively. The second type, stPLA-PEG_{32}, is similar but with poly(l-lactide) (PLA) as the inner hydrophobic block. It was found that the stPCL-PEG_{32} is having higher potency to

encapsulate the hydrophobic anticancer drug (etoposide) micelles than that of stPLA-PEG_{32} and better release kinetics and it is more suitable as a potential drug delivery carrier.[91]

Recently, $A_{14}B_7$ miktoarm star copolymers composed of 14 poly(ε-caprolactone) (PCL) arms and 7 poly(ethylene glycol) (PEG) arms with β-cyclodextrin (β-CD) as core moiety were synthesized by the combination of controlled ring-opening polymerization (CROP) and "click" chemistry. ^{1}H NMR, FT-IR, and SEC-MALLS analyses confirmed the well-defined $A_{14}B_7$ miktoarm star architecture. In aqueous solution these amphiphilic miktoarm star copolymers are able to self-assemble into multi-morphological aggregates that were characterized by dynamic light scattering (DLS) and transmission electron microscopy (TEM).[92]

Another type of the Poly(ethylene glycol) based block copolymers is that comprising hydrophobic segment which is composed of polyester prepared from the dicarboxylic acids and diol by melt polycondensation. In fact the availability of the literature concerning this topic is less if compared with the block copolymers that comprising lactide/caprolactone as the hydrophobic segments. Khoee et al. prepared amphiphilic triblock copolymers of poly (butylene adipate)–poly(ethylene glycol)–poly(butylene adipate) (PBA–PEG–PBA) with different PBA molecular weights. Nanoparticles from these block copolymers were prepared by self-assembly of the amphiphilic copolymers in the aqueous solution. These nanoparticles were loaded with the hydrophobic drug quercetin. It was observed that block copolymers with higher molecular weight of polyester are crucial for optimum drug release.[93]

Multiblock copolymers based on poly (ethylene glycol), butylene terephthalate, and butylene succinate units were synthesized by a two-step melt polycondensation reaction aiming to develop a new series of degradable polymers for controlled release applications[94].

The release of two model proteins, lysozyme and bovine serum albumin (BSA), from films of these block copolymers was evaluated and correlated to the swelling and degradation characteristics of the polymer matrices.[94, 95]

Multiblock copolymers of poly[(butylene terephthalate)-*co*-poly(butylene succinate)-*block*-poly(ethylene glycol)] (PTSG) were synthesized with different poly(butylene succinate) (PBS) molar fractions and varying the poly(ethylene glycol) (PEG) segment length, and were evaluated

as biomedical materials. The *in vivo* biocompatibility of these samples was also measured subcutaneously in rats for 4 weeks. The assessments indicated that these poly (ether ester) copolymers are good candidates for anti-adhesion barrier and drug controlled-release applications[96]. Series of poly (oxyethylene-*b*-butylene succinate) (POBS) ionomers were prepared using stepwise polycondensation of succinic acid and mixed monomers of sodium sulfonated poly(ethylene glycol) (SPEG) and 1,4-butanediol. The composition and chemical structure of these segmented ionomers were determined by ^{1}H NMR spectroscopy. Enzymatic hydrolysis of POBS copolymer occurs more rapidly than homo poly (butylene succinate) and was drastically accelerated with increasing ionic contents. The authors attributed this behavior to the presence of the ionic group, which not only reduced the crystallinity but also improved hydrophilicity on the POBS surface.[97]

Block copolymers based on poly(ethylene glycol) (PEG) of two molecular weights and aliphatic dicarboxylic acids (decanedioic and dodecanedioic) were prepared and the surface properties of aqueous solutions were studied. The surface activity of the polyesters and their ability to form micellar assemblies has been confirmed in water. The experiment confirmed that micellization of polyesters is accompanied by the association of more hydrophobic (aliphatic) constituents forming the micelle interior. The hydrophilic fragments (ethylene oxide groups) are involved in the formation of micelle exterior.[62 ,98] Amphiphilic triblock copolymers of poly (propylene succinate) (PPSu) and PEG with different hydrophobic/hydrophilic ratios were synthesized by melt polycondensation technique using a facile one-pot procedure. The synthesized copolymers were used to prepare core–shell nanoparticles with hydrophobic PPSu and hydrophilic PEG forming the core and shell, respectively. The drug loading efficiency and drug release properties of the mPEG–PPSu nanoparticles were investigated using two model drugs: the hydrophilic Ropinirole and the hydrophobic Tibolone. Hydrophobic/hydrophilic balance is playing the essential role to investigate the drug loading/releasing efficiency of the nanoparticles. It was found that hydrophobic drug Tibolone was loaded at much higher rate. Drug release characteristics also depended on drug hydrophilicity: the hydrophilic Ropinirole was released at a much higher rate than the hydrophobic Tibolone.[99]

1.5. Applications of Poly(ethylene glycol) based block copolymers

It is needless to say that the most important field of application of the amphiphilic block copolymer comprising polyethylene glycol is the drug delivery as already discussed in the aforementioned survey, where biodegradable nanoparticles are prepared from these block copolyesters and used in drug carriers, peptide, protein and DNA delivery,[60,63,64,99,100]

Other applications are also reported, for example biodegradable nanofibers by electrospinning[101], the representative electrospun polymers were poly-(ethylene glycol-block-ε-caprolactone)[101], poly(lactide-b-ethylene glycol-b-lactide)[102], poly(ethylene glycol-*co*-lactide)[103]. Recently, in our lab, biodegradable nanofibers of Poly(hexamethylene adipate)-PEO block copolymers (PHA-b-PEO) were obtained by green electrospinning i.e. electrospinning from aqueous suspension, at first PHA-b-PEO with different PEO contents were synthesized and processed to aqueous suspensions with high solid contents by solvent displacement. This suspension was mixed with a small amount of high molecular weight PEO and Brij78 and electrospun into corresponding nanofibers.[104]

Chapter 2

Synthesis and characterization of biodegradable amphiphilic diblock copolymers

Synthesis of amphiphilic diblock copolymers composed of methoxy poly(ethylene oxide) of different molecular weights and different aliphatic polyesters was targeted by polycondensation. These diblock copolymers are consisting mainly of two blocks. The hydrophobic block is polyester of adipate/hexandiol, succinate/butandiol or a mixture therefrom, while the hydrophilic block is methoxy poly(ethylene oxide) with different molecular weights (5000 and 2000 g/mol).

2.1. Synthesis and structural characterization of the block copolymers.

The targeted amphiphilic block copolymers with different hydrophobic/hydrophilic molar ratio were prepared by polycondensation in one pot reaction over two steps. At first the reactants (adipic acid/Succinic acid, 1,6-hexandiol/1,4 butandiol and MPEO (M. wt 5000 or 2000 g/moL)) and catalyst were mixed together and left to react for about 6 hours at 190 ^{o}C in an oil bath until the amount of expelled water becomes constant. In order to increase the molecular weight, temperature was increased to 230 ^{o}C in presence of polyphosphoric acid (usually used as thermal stabilizer) under application of vacuum for 40 h. During the reaction, the viscosity was markedly increased and the stirring ability of the magnet stirrer bar became less and less. At the end of the reaction, a viscous transparent yellow liquid is obtained that solidified upon cooling. The obtained polymer is dissolved in large amount of Chloroform or THF and precipitated in n-Pentane or n-Hexane, to obtain finally a white powder that is dried in vacuum oven at ambient temperature for 72 hours. Block copolymers with different molar ratios were prepared by the same procedures. The prepared block copolymers are polyhexylene adipate-b-methoxy poly(ethylene oxide) ***(PHA-b-MPEO5 and PHA-b-MPEO2)***, polybutylene succinate-b-methoxy poly(ethylene oxide) ***(PBS-b-MPEO)***, polyhexylene succinate-b-methoxy poly(ethylene oxide) (PHS-b-MPEO) and finally polybutylene adipate-b-methoxy poly(ethylene oxide) ***(PBA-b-MPEO)***. Figure 2.1 represents the schematic procedures of the block copolymer synthesis.

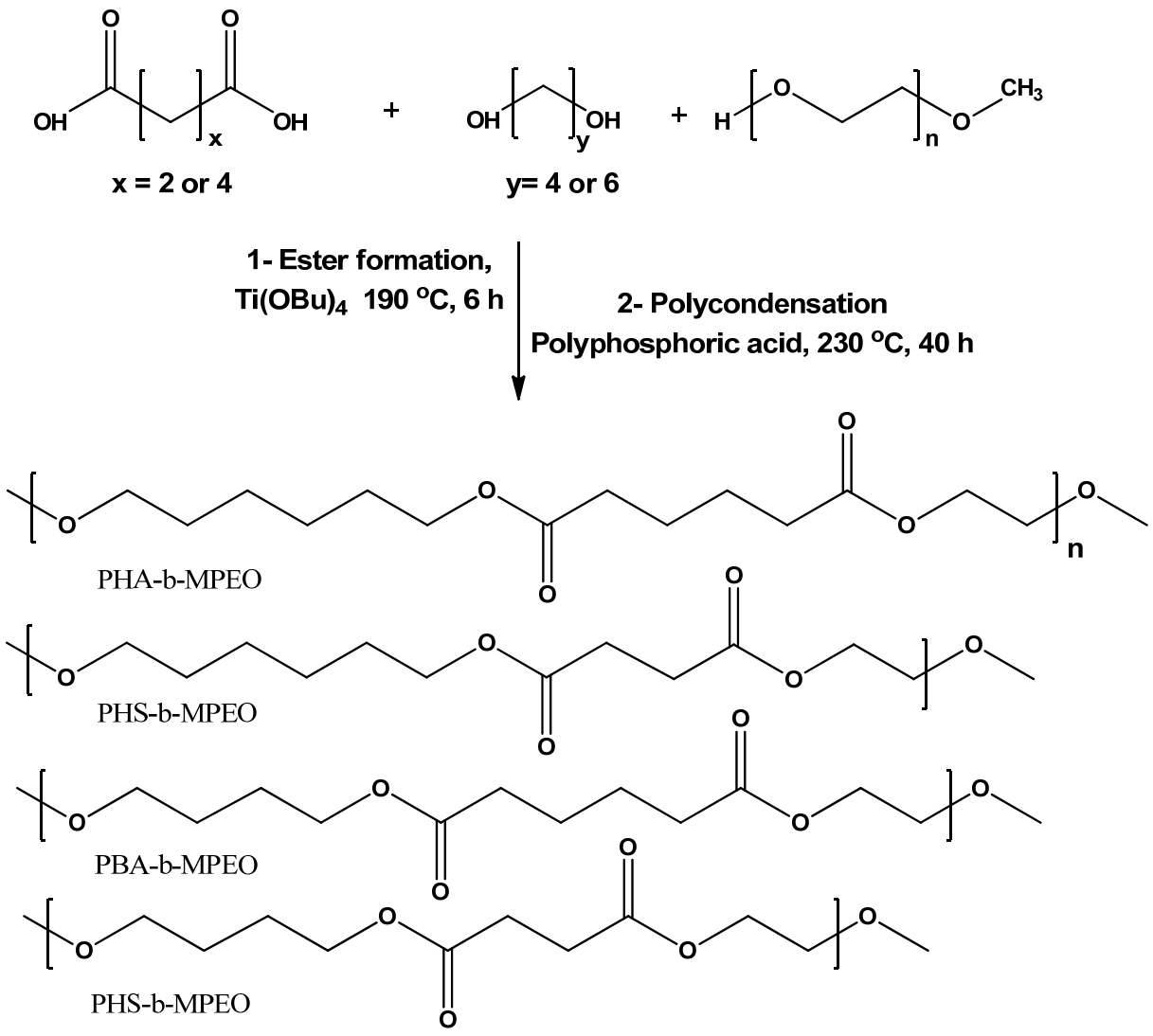

Figure 2.1. Synthetic route used for the diblock copolymers preparation

2.1.1. Structural characterization

The structure of the prepared block copolyesters was proven and characterized using NMR and IR spectroscopy. The block copolymers with feed molar ratio 1:1 were taken as representative examples for the detailed discussion, as all samples of each category have the same structure, only they differ in the integration values of different peaks. *I should mention here that, a separate section for detailed discussion of the purification had come after NMR characterization section, because understanding of the structure of the polymer is crucial in the purification step. Also the spectroscopic analysis was done for samples before and after purification, but charts of purified sample were used for final Structural characterization in this section.*

2.1.1.1. Detailed NMR characterization

Figure 2.2 shows the respective ^{1}HNMR of block copolymer PHA-b-MPEO5 as a representative example. The ^{1}H NMR peak assignments are done in accordance with the literature.[104] The four protons (13, 14 Fig 2.2) of MPEO appear at ppm 3.6, while the protons of the hydrophobic segments of the block copolymer could be assigned as follow, four terminal protons of hexandiol moiety (1, 6 Fig 2.2) at ppm 4.06, four internal protons of the hexandiol moiety (3, 4 Fig 2.2) at ppm 1.37, four terminal protons of adipate moiety (8, 11 Fig 2.2) at ppm 2.3, eight internal protons of both hexandiol moiety and adipate moiety (2,5,9,10 Fig 2.2) at ppm 1.65.

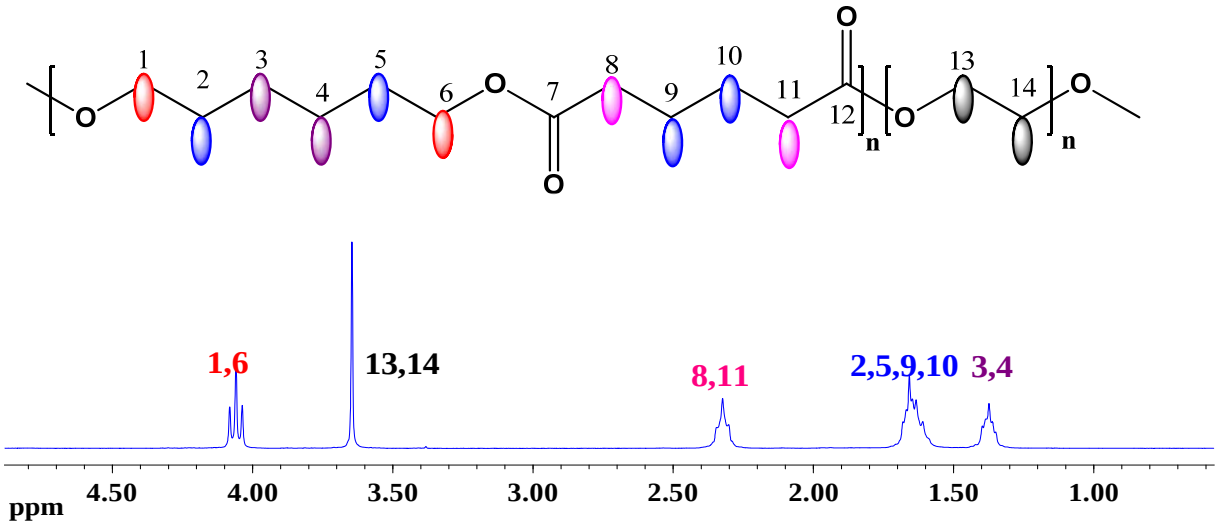

Figure 2.2. ^{1}HNMR of PHA-b-MPEO5, feed molar ratio 1:1 (Table 2.1, run 3).

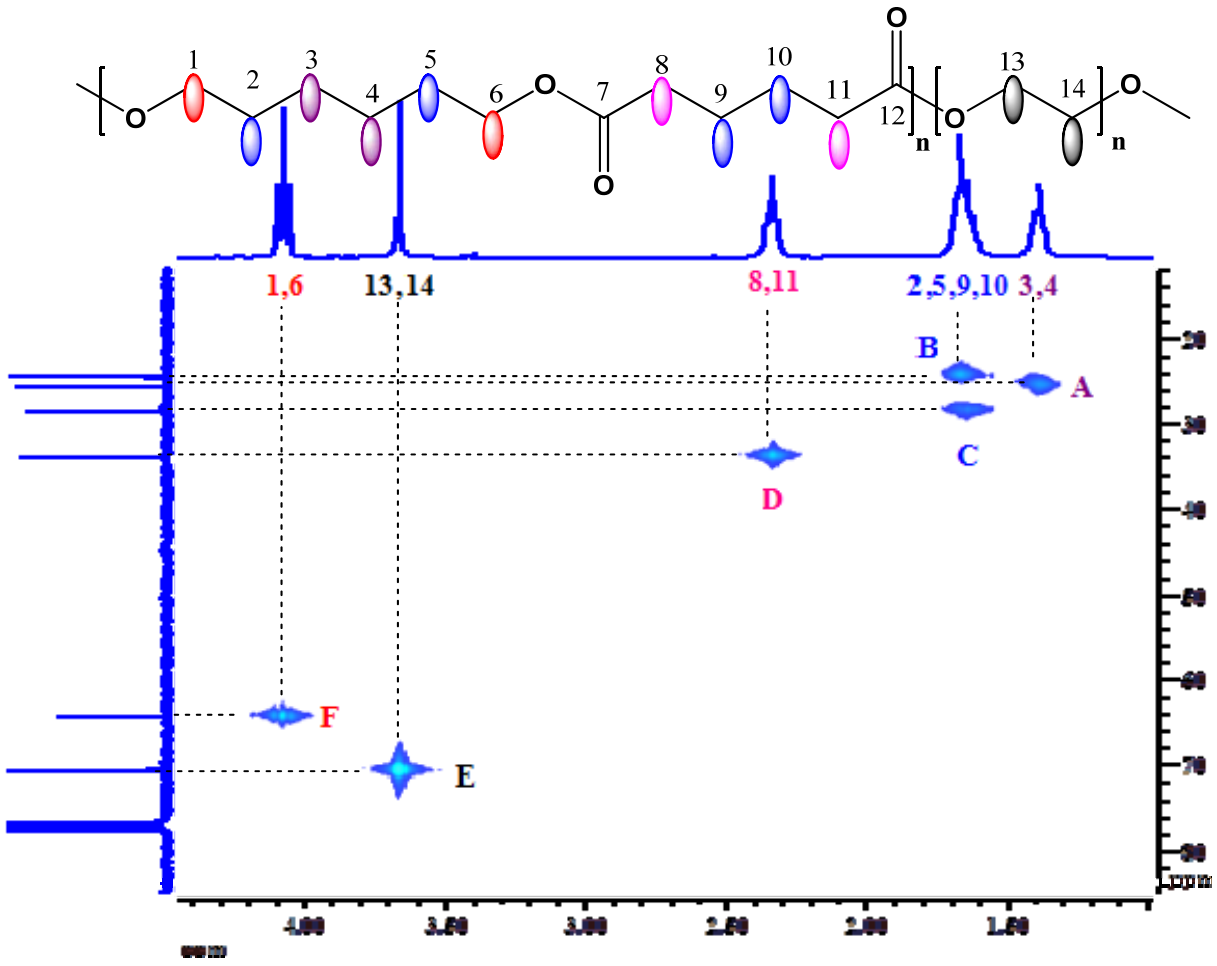

Figure 2.3. 2D ^{1}H-^{13}C HMQC (Heteronuclear multiple quantum correlation) NMR for PHA-b-MPEO5 (Table 2.1, run 3).

For ^{13}C NMR peak assignments, 2D HMQC (hetero nuclear multiple quantum correlation) NMR studies were used. The representative 2D HMQC NMR spectrum is shown in the figure 2.3. The peak in ^{13}C NMR spectrum at ppm 70.5 is assigned unambiguously for the two carbons of MPEO as they show clear correlation with its protons at ppm 3.6 (zone E Fig 2.3). Similarly the peaks at ppm 33.9 and ppm 64.3 are assigned for the terminal carbon atoms of adipate moiety and hexandiol moiety respectively (zones D, F Fig 2.3) as they show clear cross peaks with their protons at ppm 2.3 and 4.06 respectively. The Peak at ppm 25.6 correlate with the four internal protons of hexandiol moiety at ppm 1.37 (zone A Fig 2.3), finally the remaining two peaks at ppm 24.4 and 28.5 show correlation with the eight protons at ppm 1.65 (zones B and C Fig 2.3), this means these two peaks are corresponding to the four internal carbon atoms carrying eight

internal protons of both hexandiol moiety and adipate moiety (2,5,9,10 Fig 2.3).With only 2D HMQC, it was not possible to differentiate between these two peaks. For their exact assignment, 2D HMBC (hetero nuclear multiple bond correlation) NMR studies were used. The representative 2D HMBC NMR spectrum is shown in the figure 2.4. The peak at ppm 28.5 in ^{13}C NMR showed a very strong correlation at zone B with peaks at ppm 4.06 (four terminal protons of hexandiol moiety 1, 6 Fig 2.4), i.e. with its neighbor so that it could be assigned for the carbons 2,5 (Fig 2,4), confirming this assignment is the correlation at zone A between carbons 3,4 (ppm 25.6) and the same 4 protons 1,6. The two carbon peaks at ppm 24.5 showed a very strong and clear correlation (C) with four terminal protons of adipate moiety (8, 11 Fig 2.4) at ppm 2.3, which confirm the assignment of these two carbon as 9, 10 (Fig 2.4).

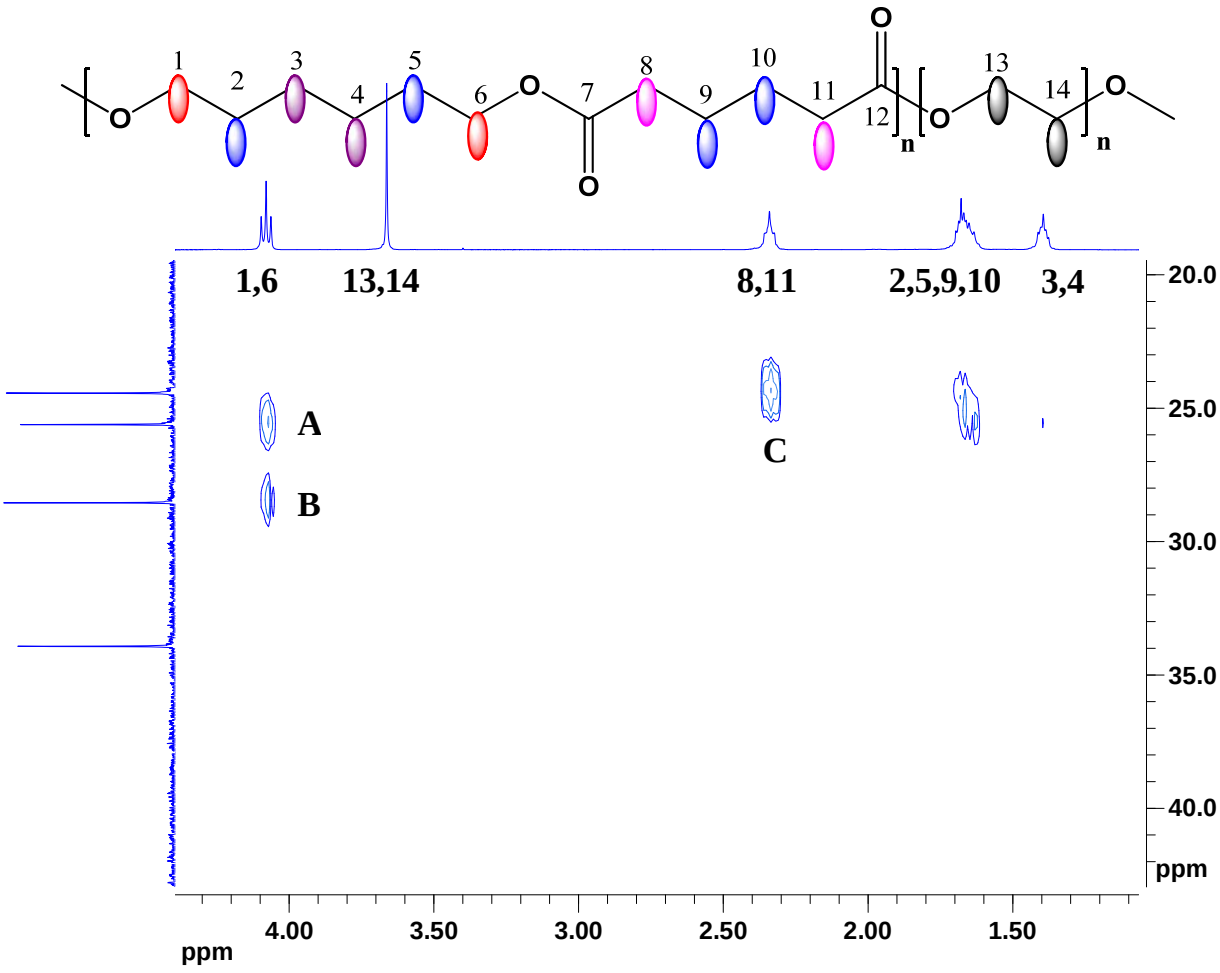

Figure 2.4. A part of 2D 1H-13C HMBC (Heteronuclear multiple bond correlation) NMR for PHA-b-MPEO5, feed molar ratio 1:1 (Table 2.1, run 3).

Finally the peak at ppm 173.4 is clearly assigned for the carbonyl groups of the adipate moiety. The ^{13}C NMR with correct peak assignments as deduced from HMQC and HMBC are shown in figure 2.5.

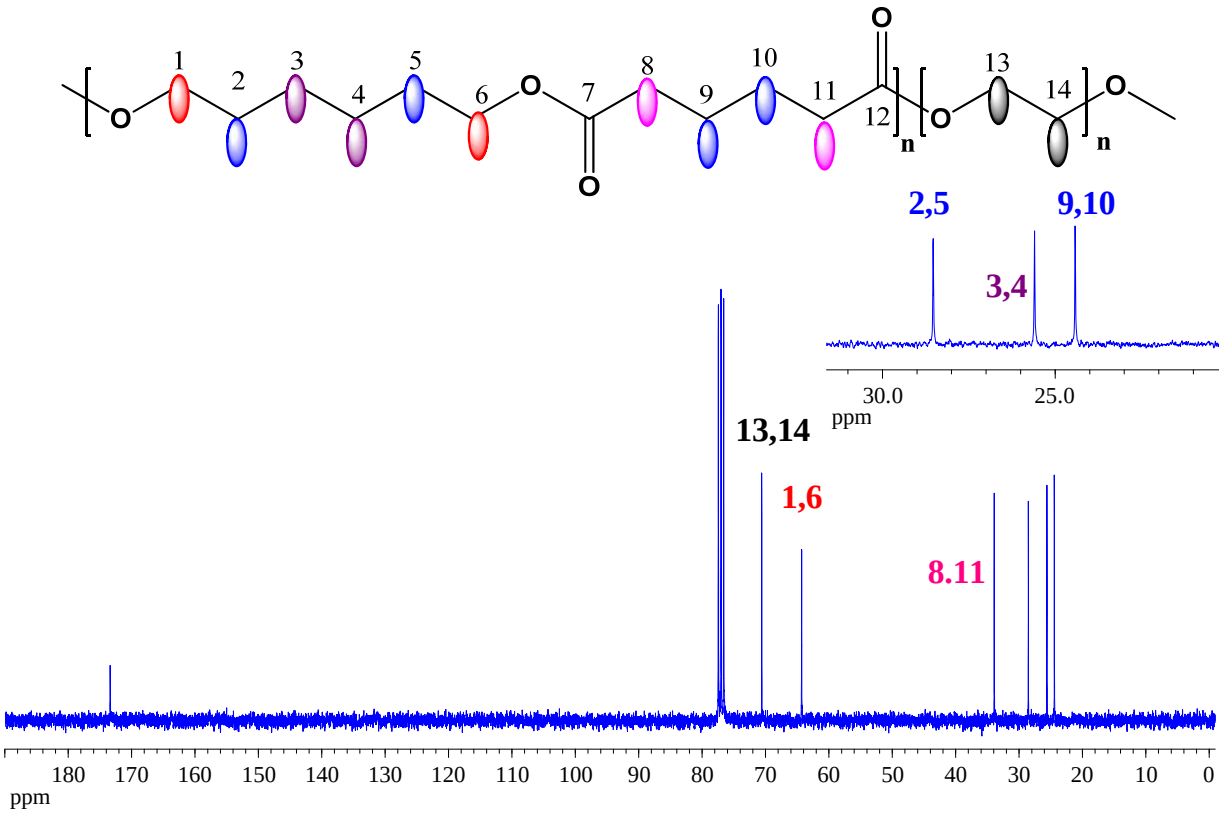

Figure 2.5. ^{13}CNMR of the Polyhexylene adipate-block-methoxy poly(ethylene oxide), feed molar ratio 1:1 (Table 2.1, run 3).

By the same way, the structure of all block copolyesters were elucidated and represented in figure 2.6

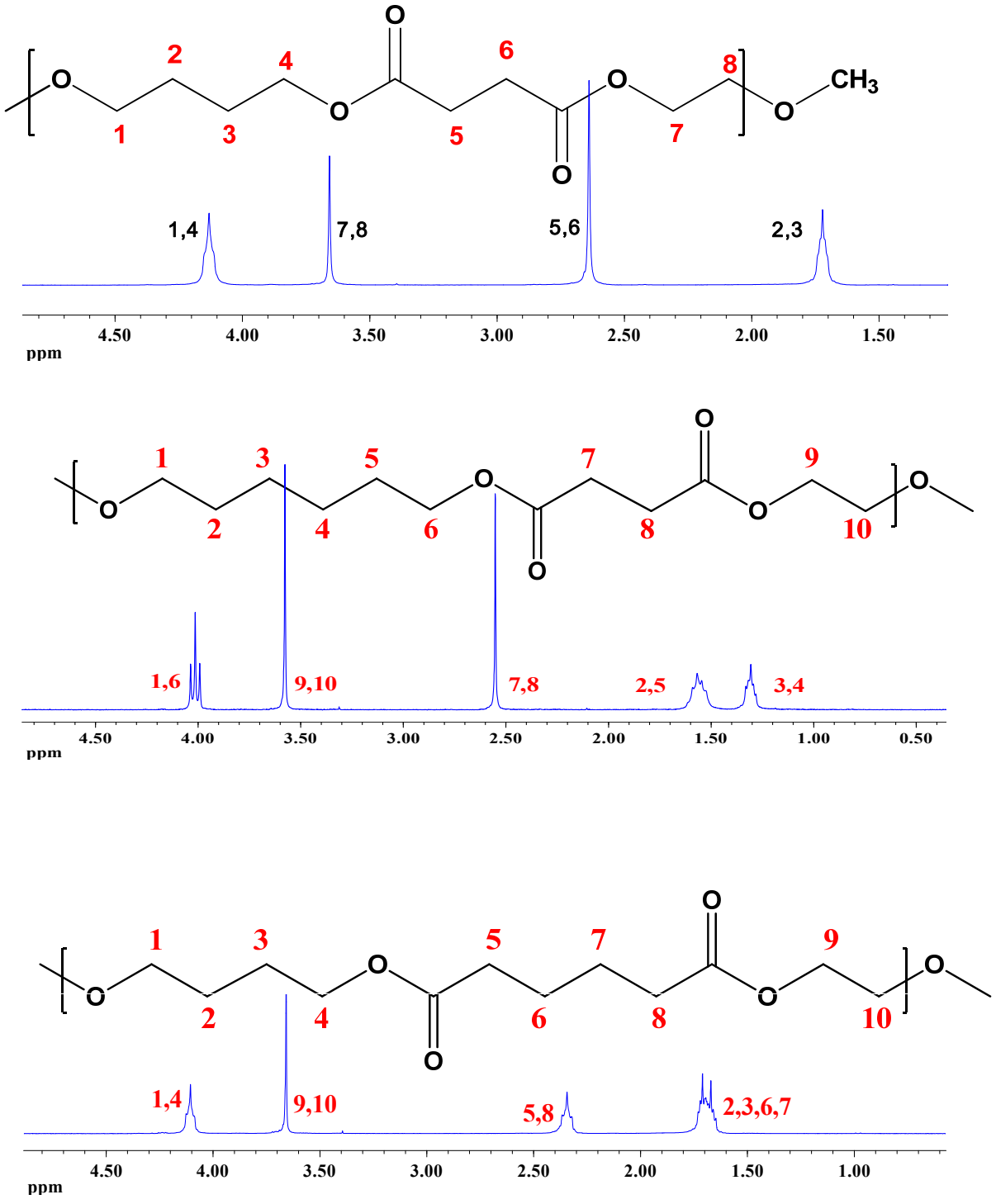

Figure 2.6. [1]HNMR of PBS-b-MPEO, PHS-b-MPEO and PBA-b-MPEO (Table 2.1, runs 13,16,17).

2.1.1.2. Detailed IR characterization

IR spectroscopy for the same polymers investigated by NMR is also performed. A representative example polymer with feed molar ratio 1:1 is chosen. The characteristic bands could be assigned as follow; C=O stretching band of the ester group occurs at 1730 cm^{-1}, CH_2 stretching occurs at 2880 cm^{-1}, 2940 cm^{-1} (symmetrical and asymmetrical respectively), CH_2 bending occurs at 1464 cm^{-1} (scissoring,), 730 cm^{-1} (rocking), 1360-1250, 1110 (twisting-wagging), C-O stretching band occurs at 1175 cm^{-1} as shown in figure 2.7a. An overlay of IR charts of all block copolymers is shown in figure 2.7b. No noteworthy difference in the peak assignment of the all polymers.

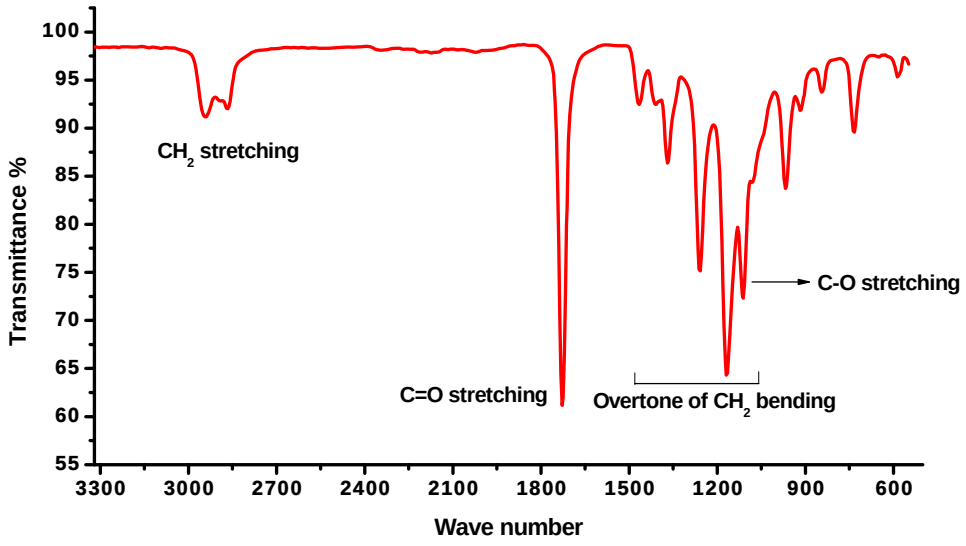

Figure 2.7a. FTIR of PHA-b-MPEO5 (Table 2.1, run 3).

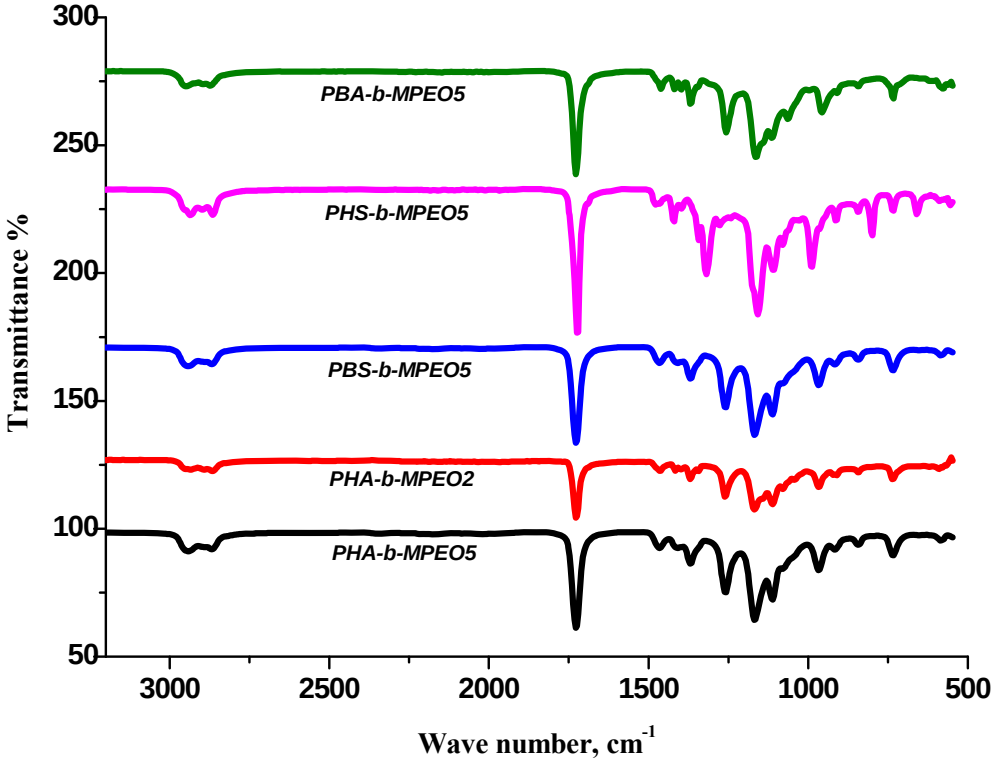

Figure 2.7b. an overlay of FTIR of all prepared block copolymers (Table 2.1 runs 3, 8, 13, 16, 17).

2.1.2. Purification and final molar ratio determination

Before I go further in studying the structural properties and characterization of these block copolymers, purification of the obtained block copolymers should be done correctly, as the determination of the final molar ratio is mainly depending upon how pure is the polymer. Generally the obtained polymers are precipitated in n-pentane or n-Hexane, the main problem is that, the unreacted MPEO has the same behavior, i.e. it is co-precipitated with the block copolyester. To find out a solution for this problem, three solvents are chosen to test the solubility and precipitate-ability of both the block copolyester and MPEO. These three solvents are water, methanol and ethanol; these solvents were chosen depending on the hydrophilic/hydrophobic balance. Accordingly and as a representative example, 0.5 g of MPEO

(Mn 5000 g/mol) as well as 0.5 g of PHA-b-MPEO5 with feeding molar ratio 1:1 was dissolved independently in 30 mL of each solvent. The solubility of MPEO in these solvents can be arranged as follow H_2O > methanol > ethanol as shown in figure 2.8. For the chosen polymer, apparently and under this condition (0.5 g/30 mL solvent) it is not soluble in all of these solvents, however for more clarification of this behavior, the polyester in each solvent was filtered then the filtrate was evaporated and the residue was dried and analyzed by ^{1}HNMR. Figure 2.9 represents the ^{1}HNMR of the filtrate residue of the three solvents. From this figure it is clearly seen that water is the best solvents for the purification as the filtrate residue is composed mainly of MPEO and very less amount of the polyester itself, on the other hand the selected polymer was more and more in case of methanol and ethanol filtrate residue, however polymers with higher amounts of hydrophilic segments i.e. MPEO form milky suspension in water (actually they acts like surfactants) and it was found that it's very difficult to re-gather the polymer again. Based on these findings, I generally used water as a precipitating solvent in the purification of polyester containing more hydrophobic segments, while those containing more hydrophilic segments (MPEO) are purified using methanol as a precipitating solvent. Table 2.1 show the conversion, initial molar ratio and experimental molar ratio of the final purified block copolyester.

Figure 2.8. Solubility of MPEO in H_2O, Methanol and Ethanol from left to right respectively. The order of solubility is H_2O > methanol > ethanol.

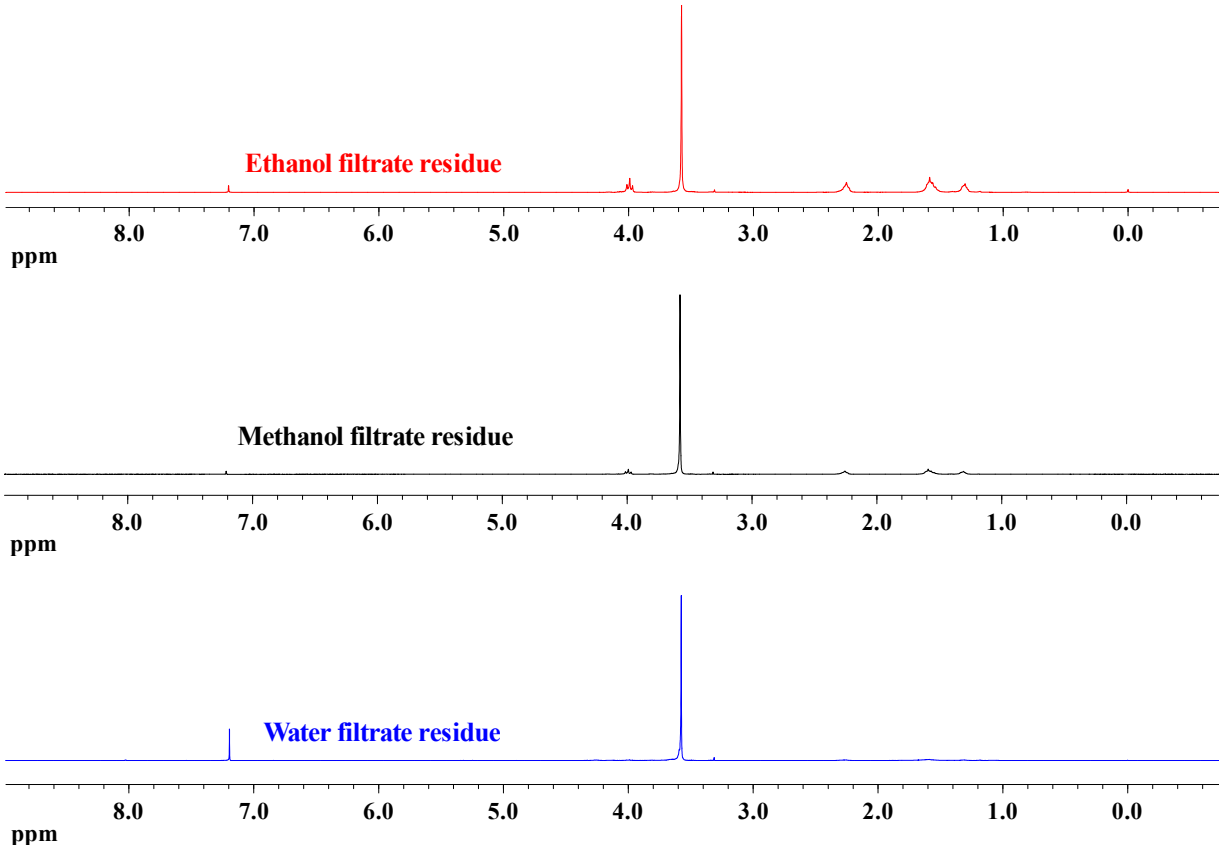

Figure 2.9. ^{1}HNMR overlay of the filtrate residue resulting from dissolving of PHA-b-MPEO5 molar feed ratio is 1:1(Table 2.1, runs 3) in H_2O, Methanol and Ethanol. The intensity of the peaks between 1.0 and 3.0 ppm that represent the hydrophobic segments of the block copolymer are increased in the order; Ethanol > Methanol > H_2O i.e. water has very less amount of polymer residue.

From the data in table 2.1, one can observe that by increasing of the amount of MPEO in the feed molar ratio, the deviation of the experimental molar ratio is also increased. This behavior could be attributed to the fact that, the viscosity of the reaction medium becomes high as the polycondensation reaction proceeds further and consequently the movement of MPEO polymer chains becomes difficult and they could not contribute easily in the polycondensation reaction via their chain end groups. Conversions are satisfactory with average value of 85 %. It is also worth to mention that the experimental molar ratio was calculated from the ^{1}HNMR charts by comparing the integral intensity of the four protons of MPEO at ppm 3.60 with the 4 terminal protons of diol moiety at ppm 4.06. Figure 2.10 represents the relation between the increases of

MPEO amount in the polycondensation and the deviation of experimental molar ratio from the feed molar ratio, while figure 2.11 show an overlay of both the unpurified and purified sample with the integration values of peaks that utilized in calculating the molar ratio.

Table 2.1. Feed molar ratios, Experimental molar ratio and Conversion of PHA-b-PMPEO.

Run	Feed molar ratio	Experimental molar ratio	Yield,	Deviation from feed molar ratio,
	MPEO:PE	MPEO:PE	%	%
		PHA-b-MPEO5		
1	¼:1	0.90:4	87	10
2	½:1	0.83:2	88	17
3	1:1	0.81:1	85	19
4	2:1	1.35:1	83	32.5
5	4:1	1.90:1	85	52.5
		PHA-b-MPEO2		
6	¼:1	0.90:4	87	10
7	½:1	0.85:2	88	15
8	1:1	0.80:1	86	20
9	2:1	1.20:1	85	40
10	4:1	2.10:1	83	48
		PBS-b-MPEO5		
11	¼:1	0.90:1	85	10
12	½:1	0.90:2	87	10
13	1:1	0.90:1	85	10
14	2:1	1.70:1	82	15
15	4:1	3.08:1	80	23
		PHS-b-MPEO5		
16	1:1	0.87:1	87	13
		PBA-b-MPEO5		
17	1:1	0.88:1	83	12

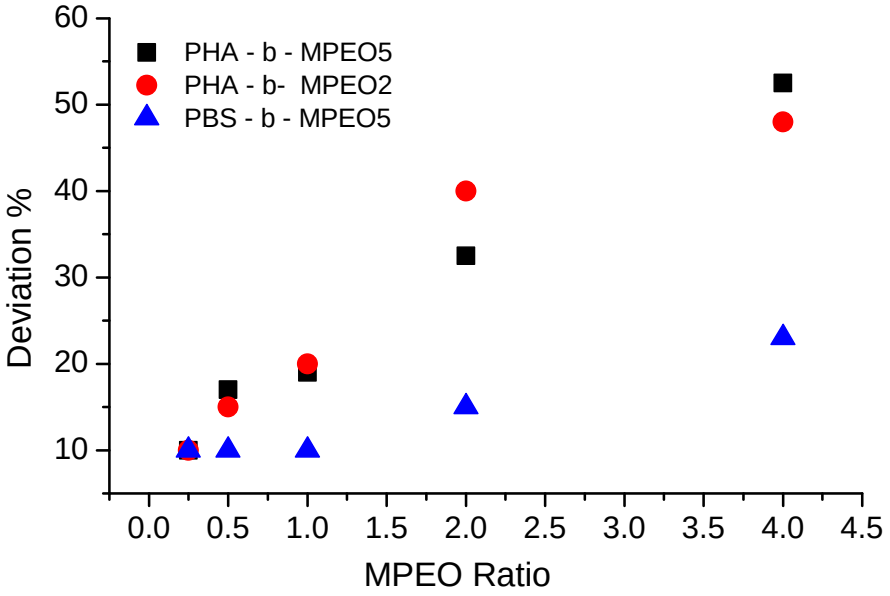

Figure 2.10 MPEO ratios vs. deviation of experimental molar ratio from feed molar ratio. As the MPEO contents increases, the deviation from the feed molar ratio increases.

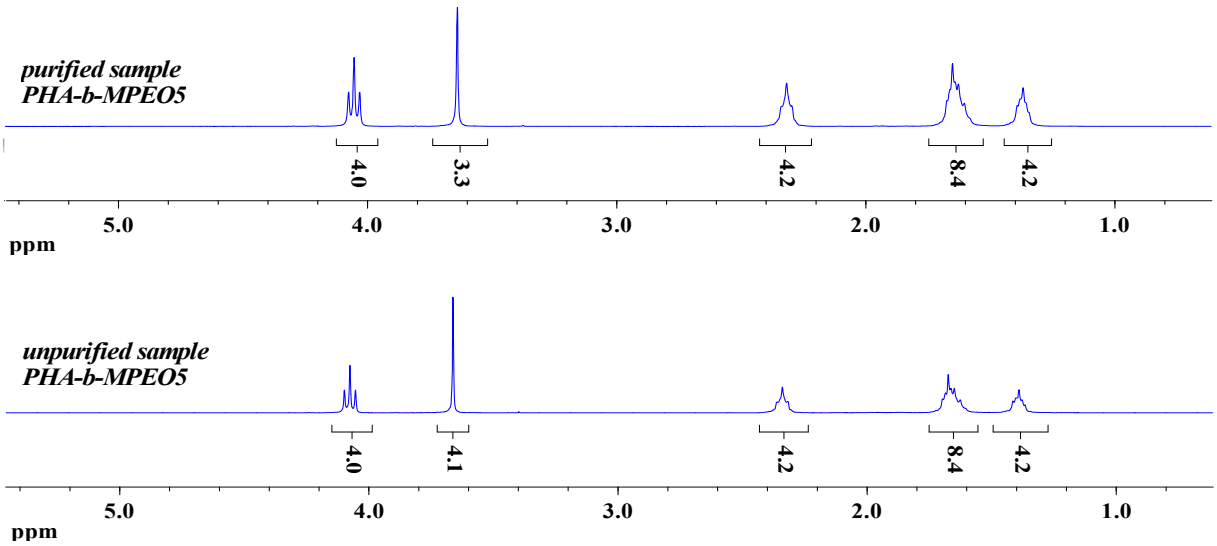

Figure 2.11. [1]HNMR overlays of both unpurified and purified samples with focusing on the integration values of the peaks used to determine the molar ratio (Table 2.1 runs 3).

2.2. Molecular weight determination

Molecular weights (Mn, Mw) as well as molecular weight distribution (PDI) of the resulting copolymers were determined by $CHCl_3$ GPC. The results are shown in table 2.2

Table 2.2 Molecular weights and polydispersty values as determined by chloroform GPC using PMMA as calibration standards and toluene as internal reference.

Sample	Mn	Mw	PDI	MPEO/PE (feed molar ratio)
			PHA-b-MPEO5	
1	18000	36000	2.02	¼:1
2	16000	31000	1.90	½:1
3	16000	34000	2.20	1:1
4	15000	28000	1.92	2:1
5	8300	14000	1.62	4:1
			PHA-b-MPEO2	
6	21000	38000	1.88	¼:1
7	14000	29000	2.03	½:1
8	14000	30000	2.06	1:1
9	8000	16000	1.90	2:1
10	11000	17000	1.57	4:1
			PBS-b-MPEO5	
11	18000	39000	2.16	¼:1
12	20000	44000	2.13	½:1
13	18000	47000	2.58	1:1
14	16000	27000	1.75	2:1
15	14000	25000	1.79	4:1
			PHS-b-MPEO5	
16	12000	26000	2.16	1:1
			PBA-b-MPEO5	
17	8000	16000	1.99	1:1

For PHA-b-MPEO5, moderate molecular weight was obtained for most of the polymers, ranging from 15000 to 18000 g/mol (runs 1-4, Table 2.2). For the block copolyester that contains more MPEO segments, (run 5, Table2.2) the obtained molecular weight is somewhat lower, this low value may be because in presence of higher amount of MPEO in the reaction medium, MPEO has bigger chance to react with the growing PHA chains at earlier stage, i.e. before PHA forms longer chains, resulting in a fixed MPEO chain length and lower PAH chain length and the overall molecular weight is reduced. The same behavior could be clearly observed for the remaining block copolyester PHA-b-MPEO2, PBS-b-MPEO5. All the obtained block copolyesters have mono-modal GPC curves as shown in figure 2.12, with slight shift of the polymers containing larger amount of MPEO to higher elution volume, i.e. lower molecular weight region.

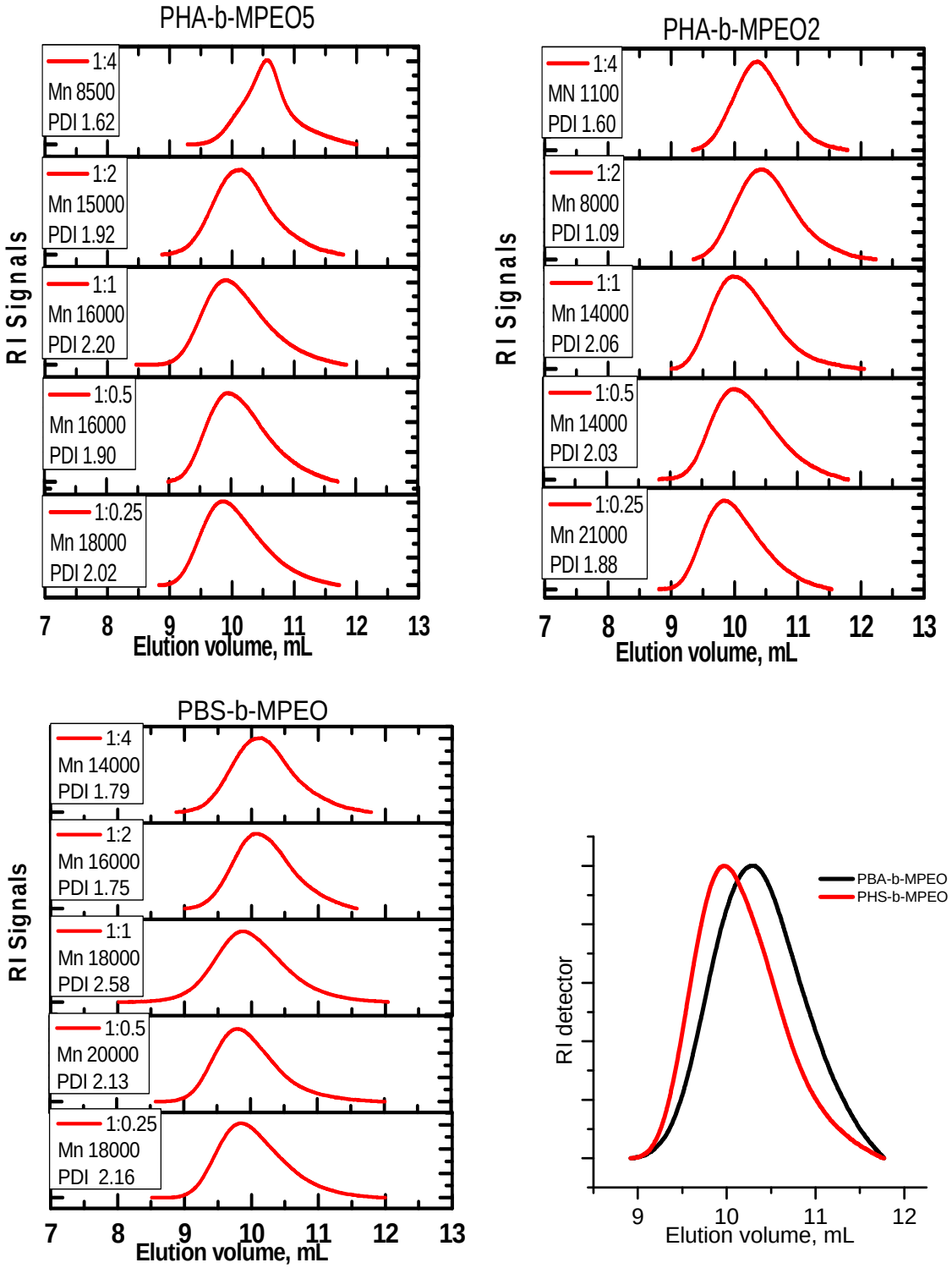

Figure 2.12 GPC Elugrams of the whole type of Block copolymers give uni-modal curves. Increasing of MPEO is from down to up with slight shift to lower molecular weight region.

2.3. Thermal analysis

2.3.1. Thermal gravimetric analysis (TGA)

The thermal properties of the prepared block copolymers were investigated by TGA and DSC. At first the thermal stability of polyesters was studied using thermo gravimetric analyzer. Thermogravimetric curves are shown in Figure 2.13. Analytical data of homopolymers polybutylene succinate (PBS) and polyhexylene adipate (PHA) are also represented, where they will be useful to compare their properties with those of the block copolymers. One-step degradation is observed in all curves. Also the initial decomposition temperature (0 % decomposition) is ranging from 320 to 350 ^{o}C, indicating high thermal stability of the whole block copolymer categories. Temperatures at 0 % and 5 % decomposition are listed in table 2.3. Slight decrease in the decomposition temperature ($T_{0\%}$) for adipate based polymers by increasing the MPEO ratio (runs 1-10) while it is mostly unchanged in case of succinate based polymers. De-polymerization of linear aliphatic polyester gives at lower temperatures cyclic and linear esters or lactones, while at higher temperatures, the formed esters decomposes further to give vinyl and carboxyl groups by ester scission and by cyclic elimination mechanism.[105,106] Plage et. al. reported that the chain length of the diol subunits of polyesters play the main role in the thermal decomposition of polyesters, while the impact of the dicarboxylic acid one is less important.[107] They studied the decomposed fragments of several aliphatic polyesters by means of pyrolysis-field ionization mass spectroscopy in order to investigate the degradation mechanisms. In polyester containing succinate and adipate subunits, it was found that the main degradation products were propionaldehyde and cyclic succinic anhydride in the case of succinate subunits, while in case of adipate subunits butyrodiketene, cyclopentanone and a cyclic anhydride of stable seven-membered ring were recognized.[107]

Table 2.3 Thermal decomposition temperature at 0 and %5 decomposition of the prepared block copolymers as well as the homopolymers.

PE/MPEO, feed ratio	$T_{0\%}$,°C	$T_{5\%}$,°C
PHA-b-MPEO5		
¼:1	346	369
½:1	319	372
1:1	326	372
2:1	324	358
4:1	320	377
PHA-b-MPEO2		
¼:1	355	377
½:1	340	374
1:1	319	368
2:1	319	370
4:1	320	365
PBS-b-MPEO5		
¼:1	326	367
½:1	338	363
1:1	335	354
2:1	335	354
4:1	327	368
PHS-b-MPEO5		
1:1	320	361
PBA-b-MPEO5		
1:1	318	362
Homopolymers		
PHA	322	362
PBS	333	364
MPEO2	344	380

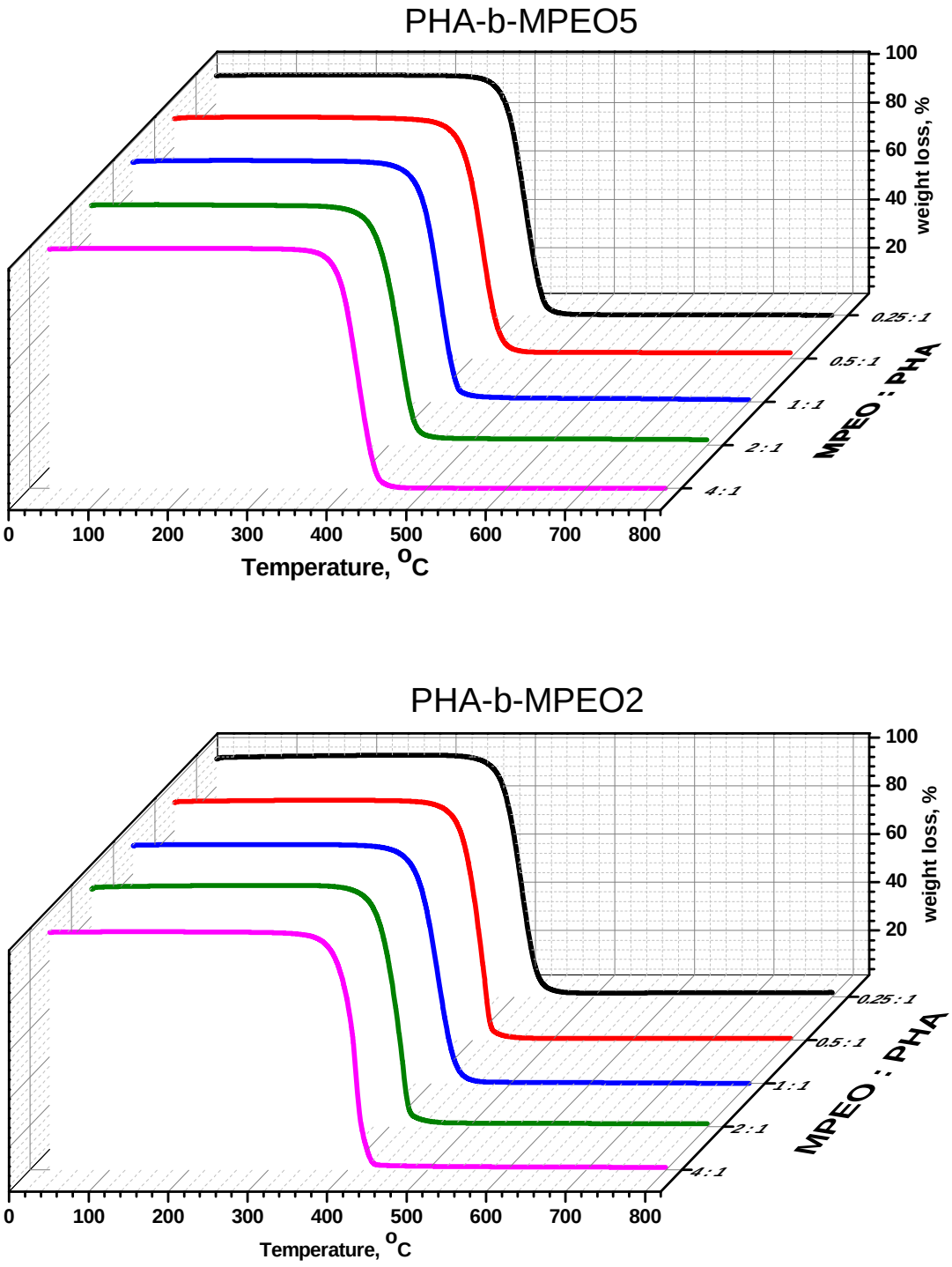

Figure 2.13. TGA thermograms of the prepared block copolymers as well as the homopolymers.

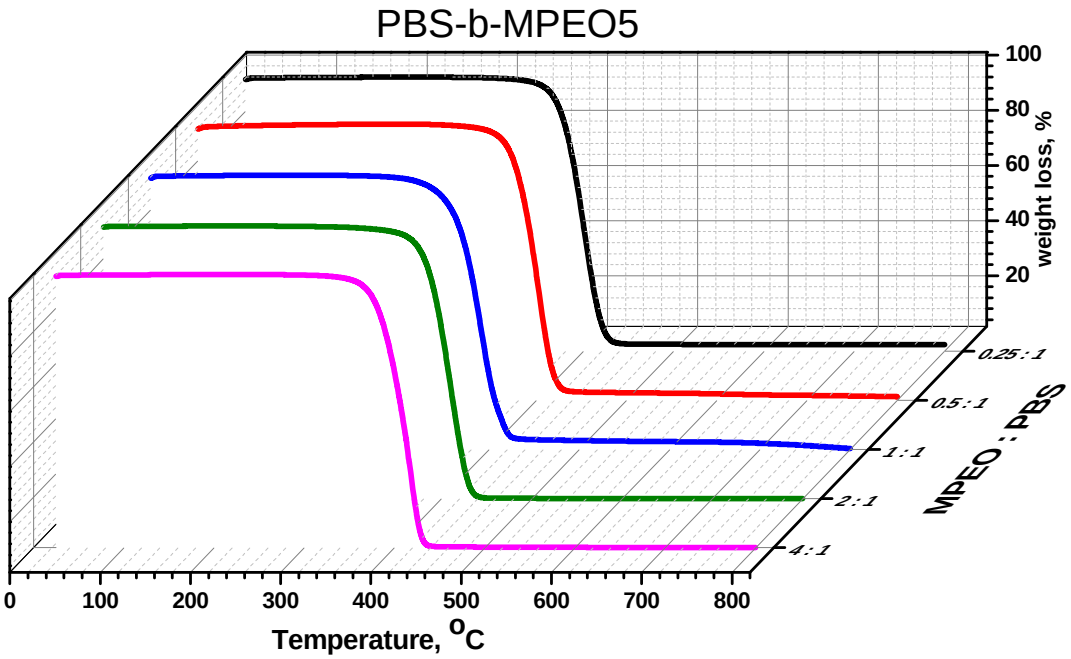

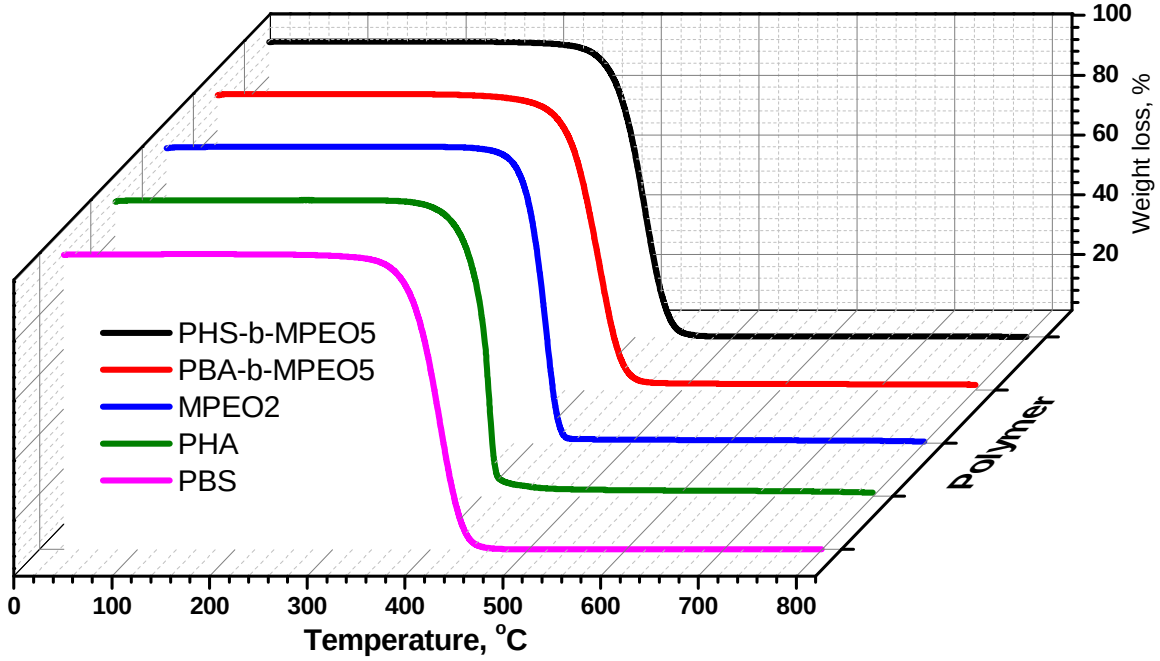

Figure 2.13. ***continued***

2.3.2. Differential scanning calorimetry (DSC)

DSC measurement conditions were varied depending on the type of the polymers. For PHA-b-MPEO5/2 i.e. adipate based polymers the endothermic/exothermic cycles were as follow, the samples were heated in the first heating cycle from –100 ^{o}C to 100 ^{o}C at a heating rate 20 ^{o}C/min. The samples were cooled again to –100 ^{o}C with cooling rate -20 ^{o}C/min and again heated in the second heating cycle till 100 ^{o}C. In case of remaining polymers the heating cycles were as follow; the first heating cycle from –150 ^{o}C to 150 ^{o}C at a heating rate 20 ^{o}C/min. The samples were cooled again to –150 ^{o}C with a cooling rate -20 ^{o}C/min and again heated in the second heating cycle till 150 ^{o}C. The glass transition temperatures (Tg), melting points (Tm), cold crystallization temperatures (Tcc) and heat of fusion (ΔH) were taken from the second heating/cooling cycle as listed in table 2.4. To investigate the behavior of all our polymers in DSC measurements, cooling / heating curves of the homopolymers as well as MPEO were also measured and shown in figure 2.14 with labeled peaks of Tg, Tm and Tcc. Figure 2.14 shows the DSC heating and cooling curves of methoxy poly(ethylene oxide) (MPEO2), the homopolymers polyhexylene adipate (PHA) and polybutylene succinate (PBS) at a rate of 20 ^{o}C/min. In the heating cycle for all polymers an endothermic peak that represents Tm are observed at 56, 60, and 116 °C for MPEO, PHA and PBS respectively, in addition an exothermic peak (Texo) at 94 °C could be observed for PBS exactly as observed by Miyata et.al.[108] He rationalized the extra exothermic behavior of PBS during the heating cycle to the recrystallization of the polymer during heating as evidenced by x-ray analysis at different temperatures.[108] Tg could be obtained only for the semi-crystalline polymers PHA and PBS at -60 and -37 °C respectively, while for PEO it was not possible to detect any Tg, as PEO is mostly crystalline polymer (70-80 %)[109], however it was detected at -57 ^{o}C in the literature.[110] In the 2nd cooling cycle from 150 to -150 ^{o}C, crystallization exothermic peaks (Tcc) of all polymers MPEO, PHA and PBS could be observed at 33, 36 and 67 ^{o}C respectively. Based on these findings, the block copolymers PHA-b-MPEO and PBS-b-MPEO and the mixture therefrom PBA-b-MPEO and PHS-b-MPEO could be studied.

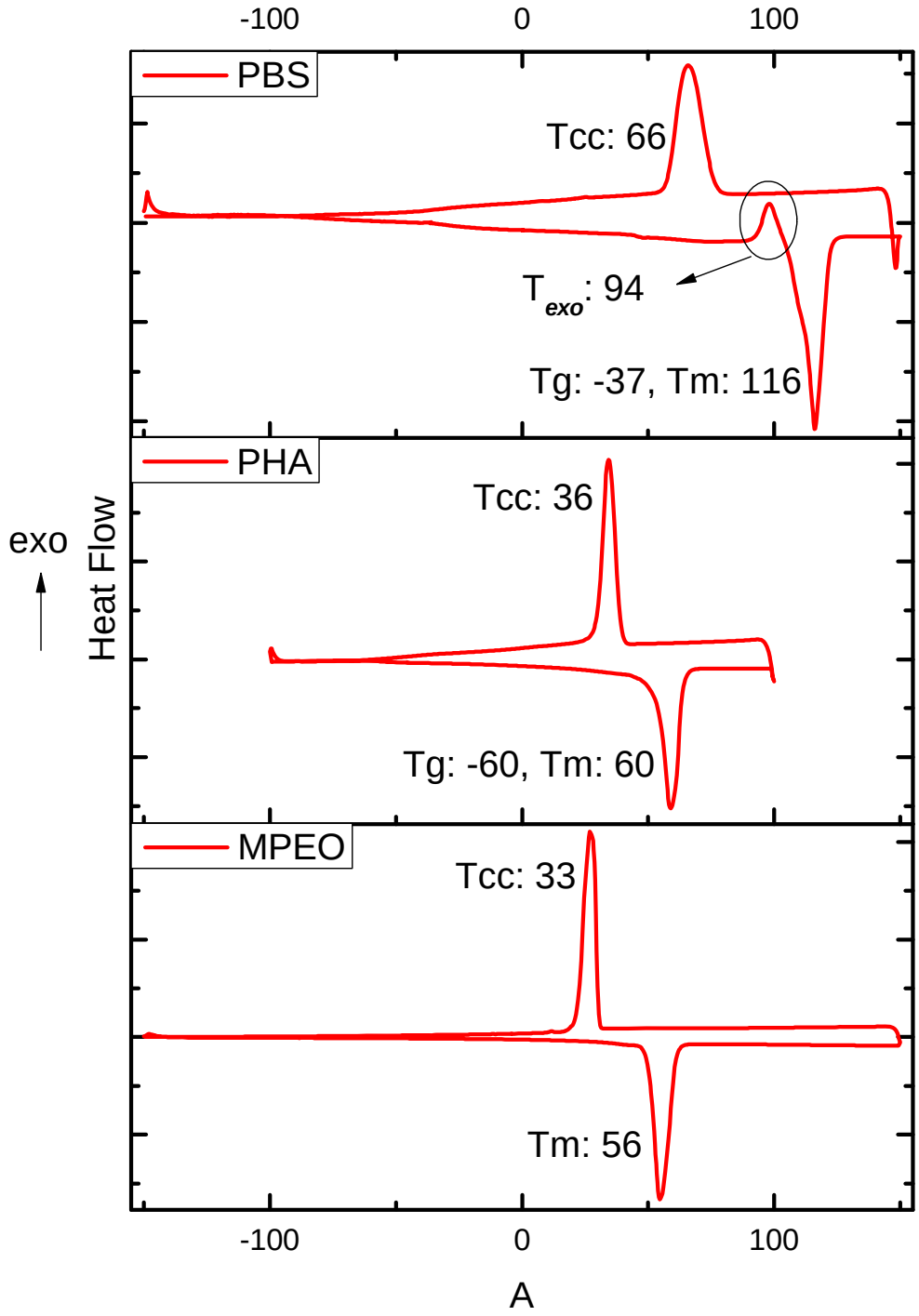

Figure 2.14. DSC Thermograms of MPEO2 and homopolyesters PHA and PBS.

Table 2.4. Thermal Characteristic data of the prepared block copolymers and homopolymers as extracted from DSC measurements.

MPEO/PE	MPEO segment				PE segment			
feed ratio	Tg °C	Tm °C	Tcc °C	Δ Hm J/g	Tg °C	Tm °C	Tcc °C	Δ Hm J/g
PHA-b-MPEO5								
¼:1	---	40	---	---	-56	59	37	63
½:1	---	42	-8	---	-58	58	38	65
1:1	---	42	-6	---	-58	57	38	57
2:1	---	32	17	---	-58	55	37	65
4:1	---	32	16	---	-56	54	35	63
PHA-b-MPEO2								
¼:1	---	34	-16	---	-60	58	38	67
½:1	---	34	-16	---	-60	59	37	60
1:1	---	34	-10	---	-59	57	37	62
2:1	---	21	-14	---	-60	51	32	60
4:1	---	41	17	---	-53	51	33	61
PBS-b-MPEO5								
¼:1	---	---	---	---	-37	115	67	65
½:1	---	35	---	---	-40	113	66	72
1:1	---	29	---	4.5	-44	112	64	64
2:1	---	45	21	47	-44	112	66	64
4:1	---	57	30	76	-40	113	56	51
PHS-b-MPEO5								
1:1	---	45	-5	---	-49	51	14	60
PBA-b-MPEO								
1:1	---	45	---	---	-59	55	23	54
Homopolymers								
PHA	---	---	---	---	-60	58	35	75
PBS	---	---	---	---	-37	116	67	89
MPEO2	---	54	33	140	---	---	---	---

To analyze the data in table 2.4, step by step we first discuss the individual category of each polymer, and then we will correlate the results with each other if there is a correlation. Also both segments of the block copolymers are investigated. The adipate based block copolymers are discussed first. it is clearly observed from the data in table 2.4 that for the hard hydrophobic segments i.e. PHA segments Tg, Tcc and heat of fusion (Δ Hm) are in the same range and no observable effect of the chain length (Mn) and MPEO % on the Tg. But a reduction in melting point Tm (from 59 to 54 in case of MPEO5, runs 1-5 and from 59 to 51 in case of MPEO2, runs 6 to10) was observed as the amount of MPEO was increased. This reduction in melting point may be because the MPEO homopolymer itself has lower melting than PHA; therefore it lowers the overall melting point of the block copolymer when it exists in larger amounts. Also if we recall the Mn values, where polymers containing more MPEO have lower value, then we can explain the reduction in melting points. For MPEO segments, Tm is barely calculated from the observed shoulder in the DSC curves as shown in figure 2.15. The values of Tm of MPEO segments are at stake and should be taken with caution because a) they were calculated from broad melting peaks b) they interfere with the melting peaks of PHA. In block copolymers with fewer amounts of MPEO and due to the comparable values of Tm of both MPEO and PHA, a merging of the two peaks could be possible during the heating cycle (Fig 2.15). Tg values as aforementioned for homopolymer MPEO were not detected but it was reported in the literature at -57 ^{o}C [110] nearly as those of PHA and also could interfere with those of PHA segments as also shown by Ferrutti et al and many others.[71,109,111,112] Figure 2.16 shows the DSC thermograms of both heating and cooling cycles of PHA-b-MPEO5/2 for the molar ratio 4:1 1:1 and 1:4 MPEO/PHA, where the distinction of the two segments is clearer in polymers containing more MPEO and Tcc of both segments could be observed without leisurely. The presence of two melting points indicate a kind of phase separation between the two segments, however a merging of the two melting is greatly enhanced because both segment have comparable melting points (MPEO 50-54 ^{o}C, PHA 55-60 ^{o}C). Anyhow the presence of two melting points confirms the formation of diblock copolymer as the dominant component of our polymer.

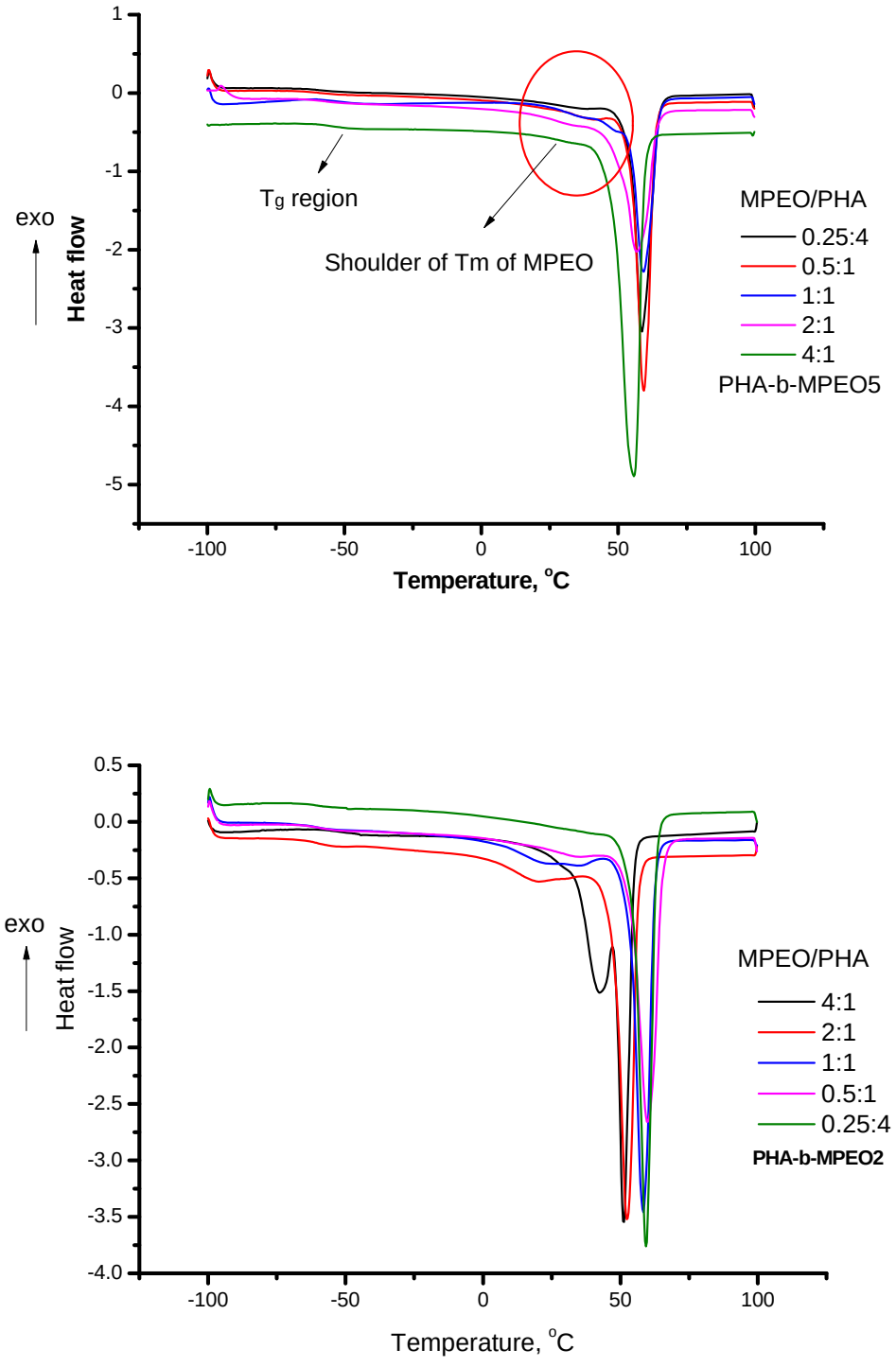

Figure 2.15. DSC curves of adipate based block copolymers

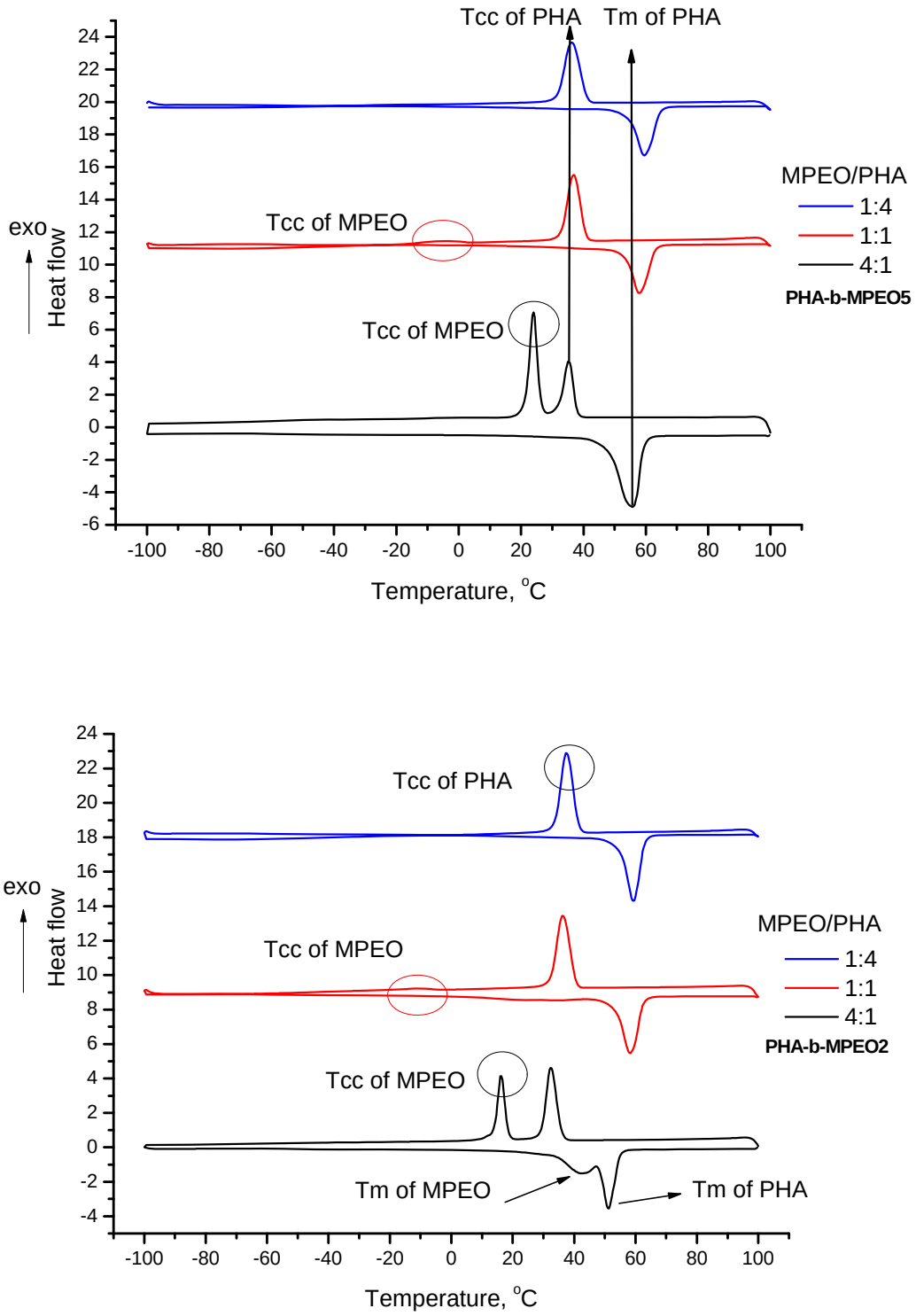

Figure 2.16. DSC overlays of Heating and cooling cycles of adipate based block Copolymers

The same behavior could be observed in the succinate based system, the thermograms are shown in figure 2.17. Tm of succinate moiety is ranging from 112-116 ^{o}C, while those of MPEO segments are in the range from 30-57 ^{o}C. These disparate melting values make the phase separation distinct and could be observed easily in both heating and cooling cycles. It is worth to mention also that the T***exo*** that observed in the homopolymers PBS is always associated with the endotherm of all succinate based polymers. For the block copolymers PBA-b-MPEO5 and PHS-b-MPEO5, the DSC thermogram is shown in figure 2.18. The melting points at around 55 ^{o}C is split into two peaks that represents the two segments, however the splitting is more distinct in case of PHS-b-MPEO5.

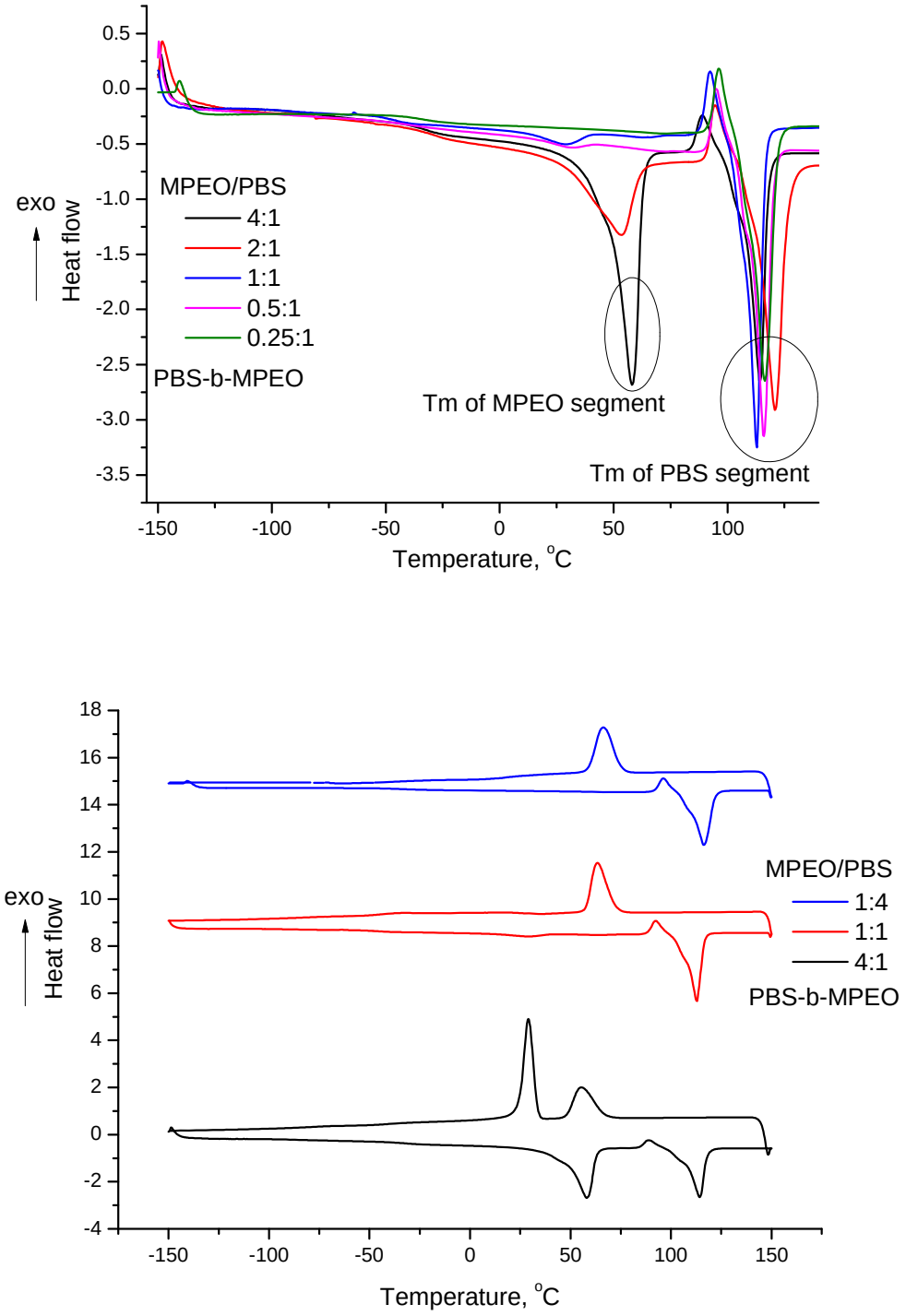

Figure 2.17. DSC curves and overlays of Heating and cooling cycles of succinate based block Copolymers

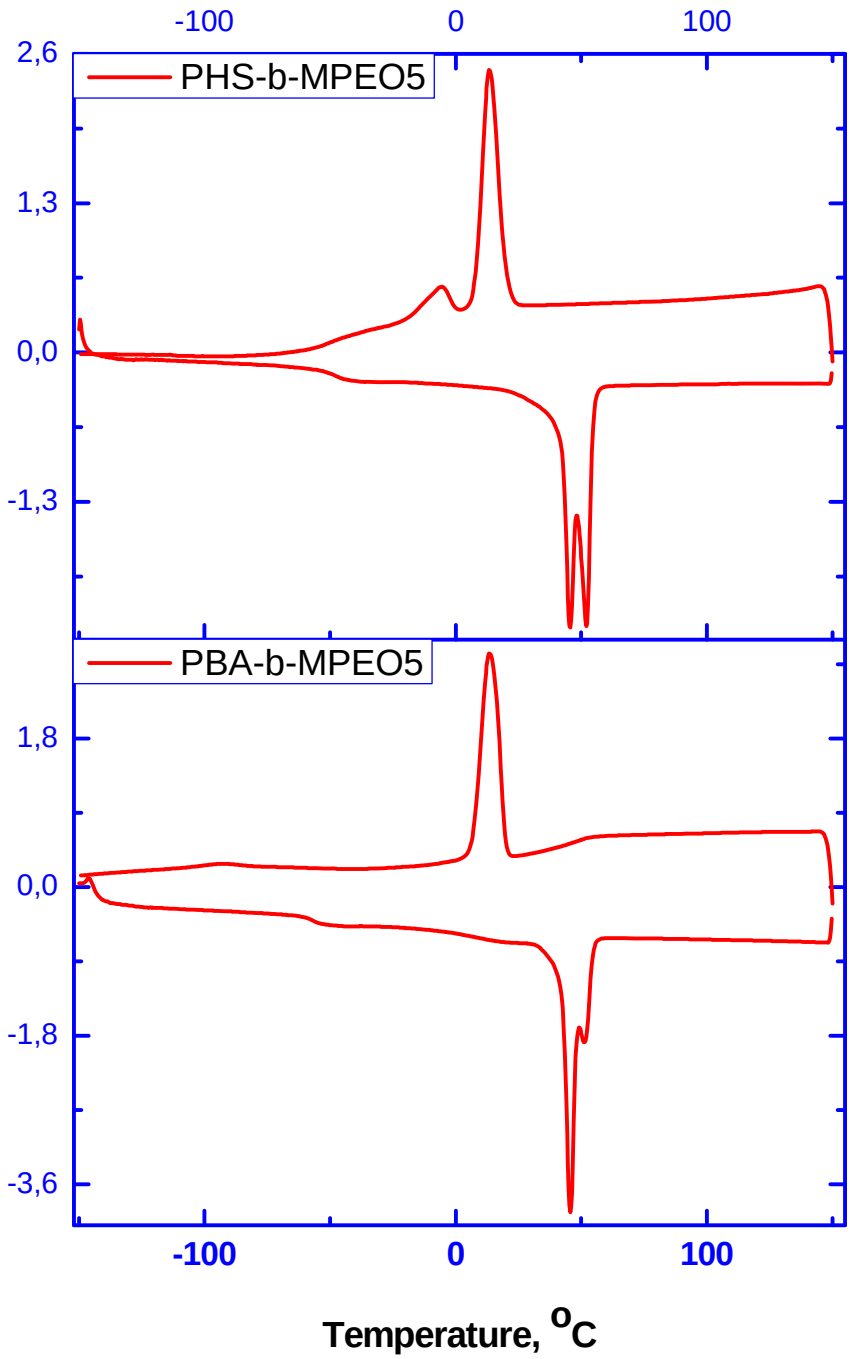

Figure 2.18. DSC curves of Heating and cooling cycles of PHS and PBA based block Copolymers

2.4. Wide Angle X-ray diffraction (WAXD)

The WAXD patterns were recorded in order to investigate the crystallinity of block copolymers. The sequence of studying the WADX analysis will be the same as that of DSC analysis. Figure 2.19 represents the X- ray of MPEO2 and homopolymers PHA and PBS. Many literatures have characterized the MPEO by XRD. [110,113] The characteristic peaks of MPEO occur at 2θ: 13.69, 15.1, 19.68, 23.81, 27.42 and 36.60°. Among these peaks, the most intensive three peaks are of 2θ: 19.68, 23.81, 27.42° as also shown by many references.[99,113] For homopolymer PHA, the characteristic peaks occur at 2θ: 21.60, 24.47, and 30.36°, while for PBS the characteristic peaks occur at 2θ: 19.87, 22.84, and 29.08°. For PHA-b-MPEO2/5, PBS-b-MPEO5, PBA-b-MPEO5 and PHS-b-MPEO5, I see it is useful to exhibit the whole range of the WAXD patterns as represented in figures 2.20-2.23, then some zooming is also presented in specific range of 2θ (15-30°) which contains the most crucial peaks that have been affected by changing the molecular structures of the block copolymers.

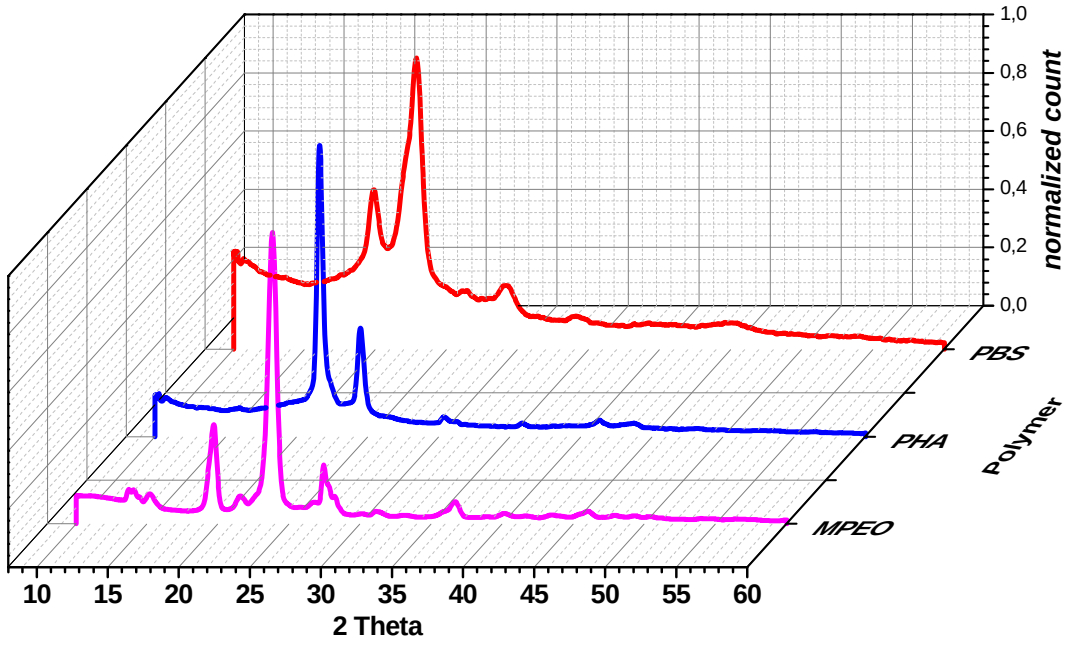

Figure 2.19. X-ray diffraction patterns of PEO and homopolymers PHA and PBS.

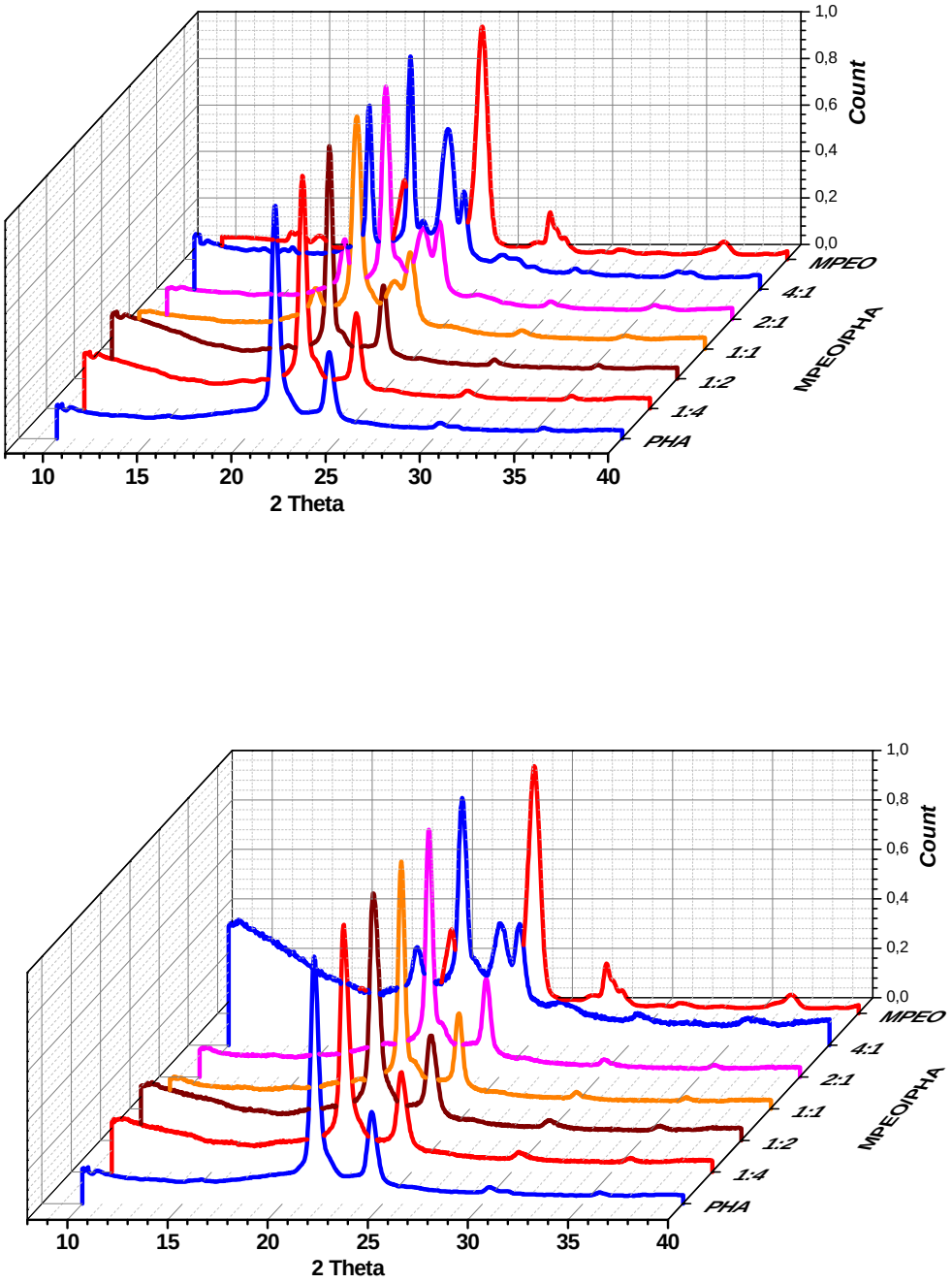

Figure 2.20. X-ray diffraction patterns of PHA-b-MPEO. Top (5000 Da) bottom (2000 Da).

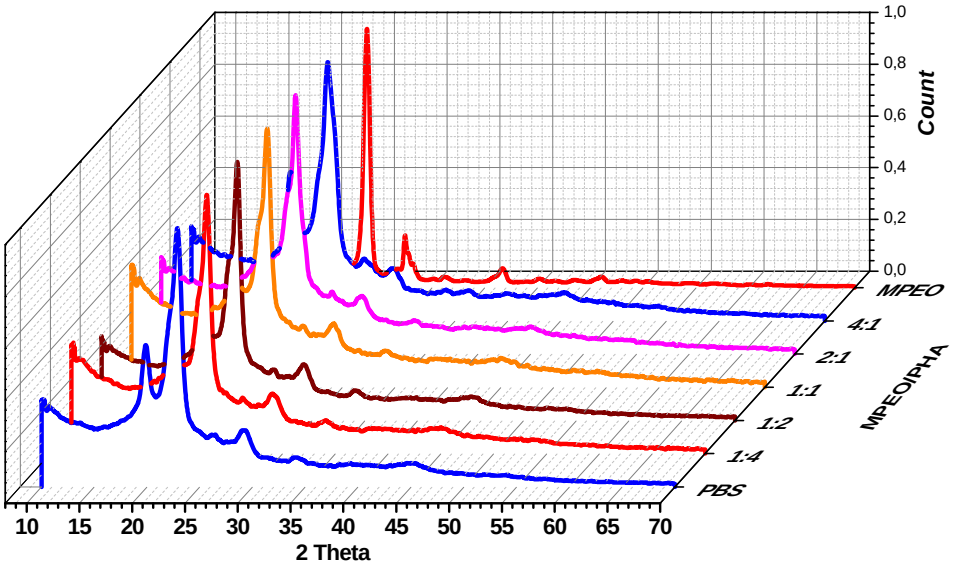

Figure 2.21. X-ray diffraction patterns of PBS-b-MPEO5.

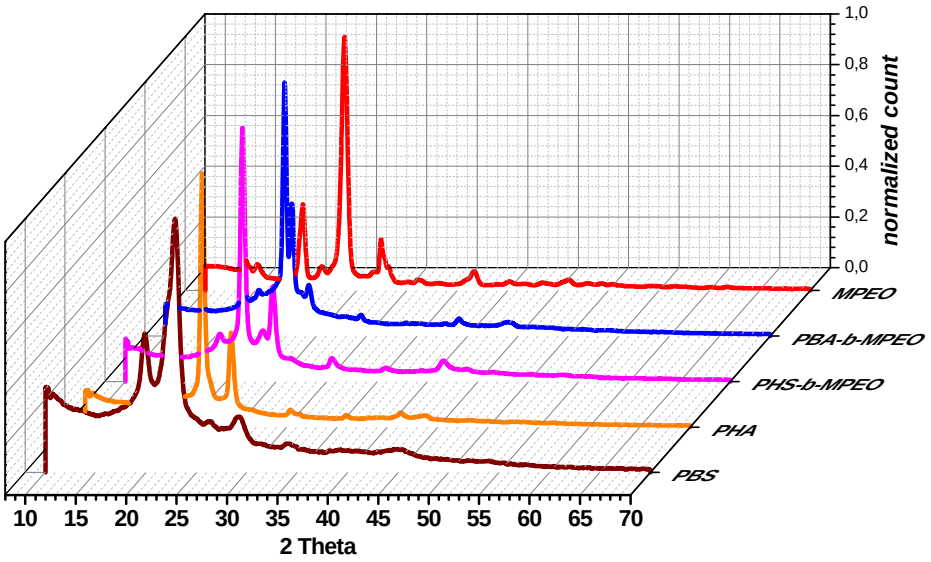

Figure 2.22. X-ray diffraction patterns of PBA-b-MPEO5 and PHS-b-MPEO5.

To take closer look to the WAXD patterns of the copolymers, a narrow range of these patterns is presented in figures 2.23-2.26. For example, the WXRD patterns of the block copolymers PHA-b-MPEO of both MPEO5 and MPEO2 are shown in figures 2.23 and 2.24. It is clearly observed that, by increasing the amount of PHA segments in the block copolymers, the main MPEO diffraction peaks exhibited differences in shape and position in which the intensity of the characteristic peaks at 2θ: 19.68 and 23.81° were decreased or even diminished at the least amount of MPEO in the block copolymers.

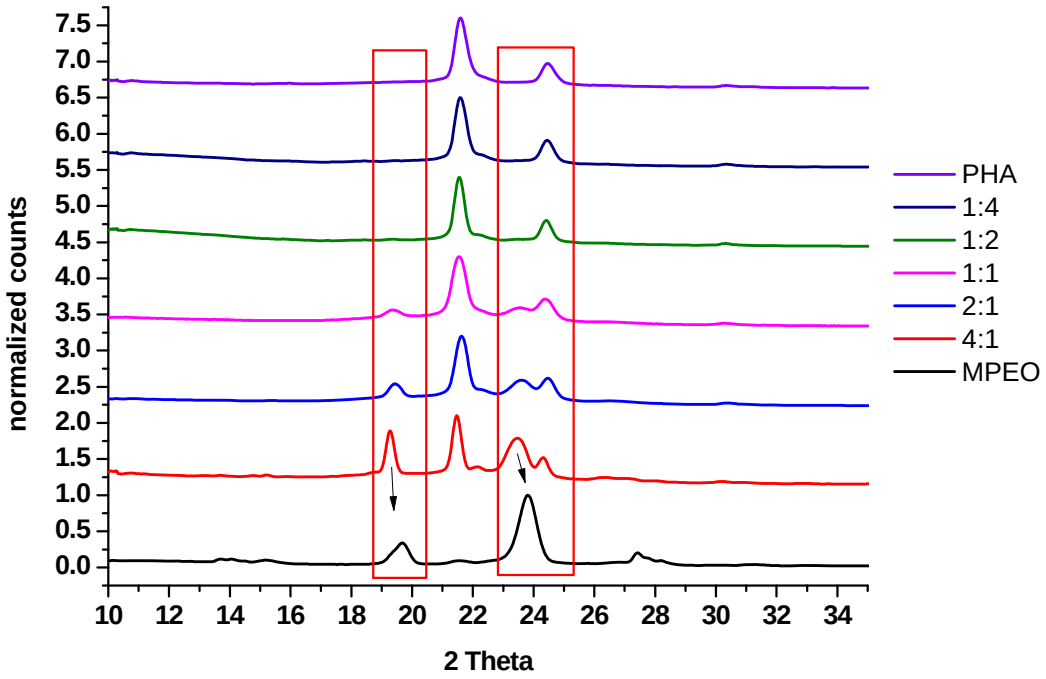

Figure 2.23. Part of X-ray diffraction patterns overlay of PHA-b-MPEO5.

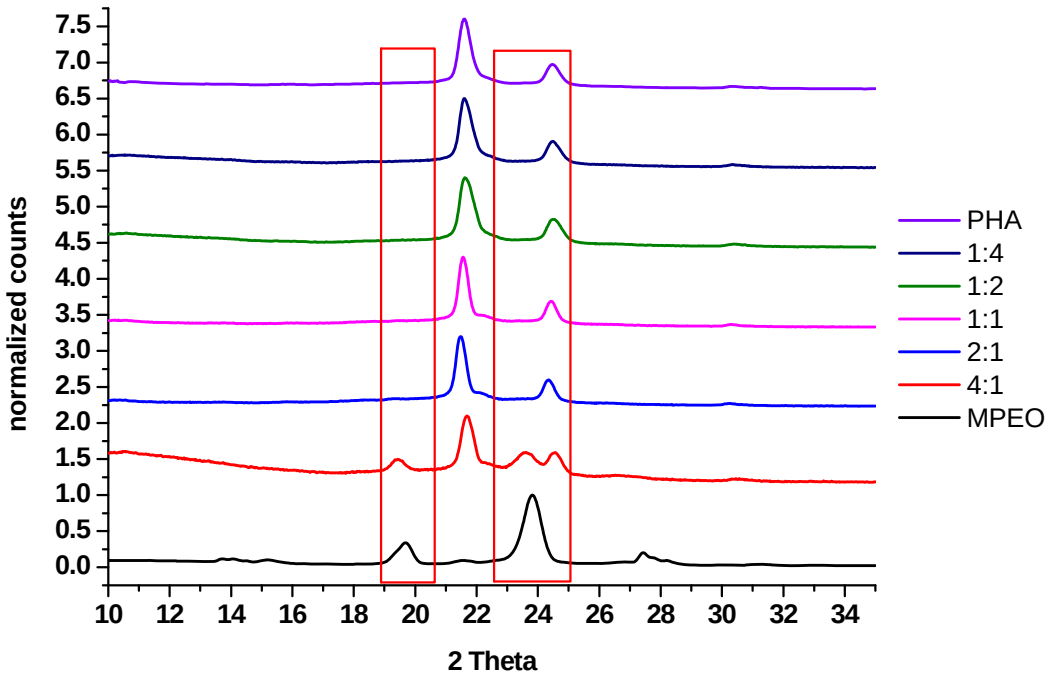

Figure 2.24 Part of X-ray diffraction patterns overlay of PHA-b-MPEO2.

The eye can observe easily a very little shift of the peaks of MPEO in the block copolymers to the left side of the pattern compared with the neat MPEO, i.e. to less 2θ values which reflect a change in the crystalline structure of the MPEO in these materials. The same behavior of PEO was observed by Silva et.al, he studied the crystal structure of a blend of Poly (ethylene oxide) and poly[bis[2-(20-methoxyethoxy) ethoxy] phosphazene], PEO/MEEP, the change in the crystalline structure was interpreted to the influence of MEEP side chains on the formation of a new crystalline arrangement in the blends.[110] By recalling the Tcc in table 2.7 (runs 1-10) values of the block copolymers segments, it is possible to correlate the less crystallinity of the whole polymers with decreasing the amount of MPEO by the absences of Tcc of MPEO as was shown in figure 2.16.

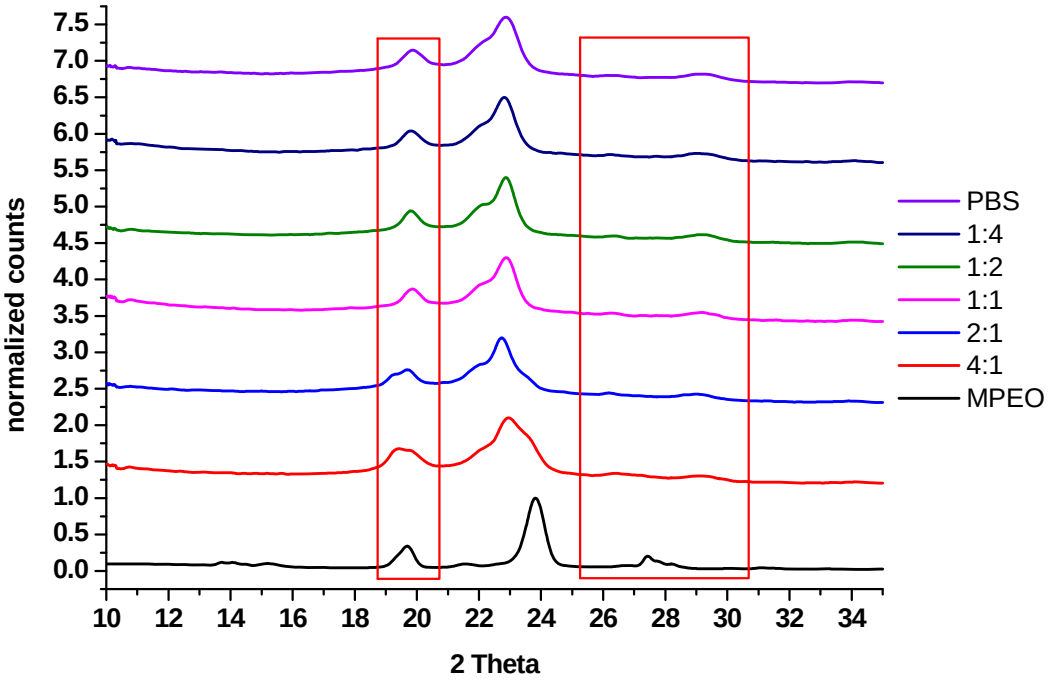

Figure 2.25 Part of X-ray diffraction patterns overlay of PBS-b-MPEO5

In case of PBS-b-MPEO5, the main two peaks of both segments occur at 2θ: 23.81 and 22.84° for MPEO and PBS respectively, this reflects some difficulties to differentiate between them. Also the two peaks at 2θ: 19.68 and 19.87 ° appears as one broad peak for three samples of the five as shown in figure 2.25, but bimodal peak or splitting of this broad peak could be observed in the copolymer that contains larger amounts of MPEO (4:1 and 2:1 MPEO/PBS). The intensity of MPEO peak at 2θ 27.42 ° and that of PBS peak at 2θ:29.08° also follow the same sequence and related to the amount of the two segments of the block copolymers. It is worth to mention that, the PBS-b-MPO copolymers that comprising less amount of MPEO have no Tcc of MPEO in the cooling cycle in the DSC curves as shown in figure 2.17 and Table 2.4 (runs 11-15) exactly as the case in PHA-b-MPEO block copolymers.

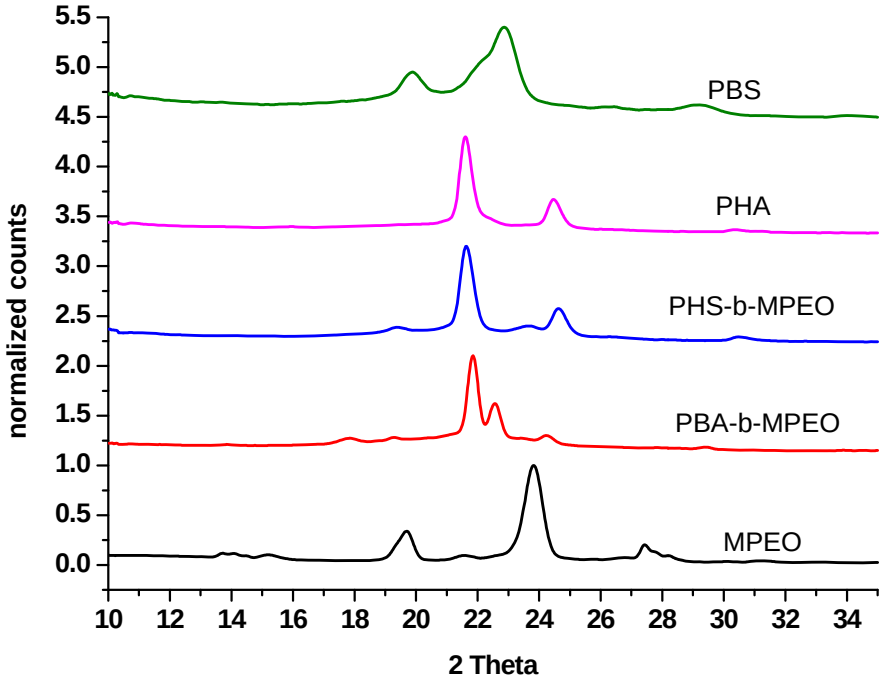

Figure 2.26 Part of X-ray diffraction patterns overlay of PBA-b-MPEO5 and PHS-b-MPEO5

For PHS-b-MPEO x-ray pattern, the main peaks occur at 2θ: 19.4, 21.62, 23.66 and 24.57°, while those of PBA-b-MPEO occur at 2θ: 13.84, 17.84, 19.29, 21.84, 22.56, 24.16 and 29.40°. Let us first take PHS-b-MPEO; the x-ray pattern is almost like that of the neat PHA, where the main peaks of both occur at 2θ: 21.62 and 24.6°. Two small peaks that occur at 2θ:19.4 and 23.66 at nearly the same position of those of MPEO and PBS. These means all segments of the block copolymers (MPEO, Hexylene/succinates) can contribute in the final shape of the crystal structure. However by recalling the DSC melting curve of PHS-b-MPEO5 (Fig 2.18) which shows sharp two melting peaks that represents the two segments of the block copolymers MPEO and PHS, this means the controversial peaks in the x-ray pattern is mainly due to the crystalline segments MPEO. For PBA-b-MPEO5, it seems that this block copolymer has unique crystal structure. The characteristic peaks that occur at 2θ: 13.84, 19.29 ° are similar to those of MPEO at the same position. Peaks at 2θ: 21.84 and 24.16 ° are similar to those of PHA homopolymers, peaks at 2θ: 22.56 and 29.40 ° are similar to those of PBS homopolymers. Finally a unique peak

at 2θ: 17.48^{o} that is considered as new peaks in the pattern and does not match with any peaks of the represented neat homopolymers.

Form the DSC and WXRD analysis, a clear correlation between the obtained results is observed. This correlation confirms the well-known phenomena of phase separation. Generally block copolymers undergo phase separation due to chemical incompatibilities between the different blocks that build up block copolymer molecules. This phase separation takes place when the inter-block segregation is sufficiently high. As a result, self-assemble of the block copolymer in the melt into a variety of ordered structures (e.g. spheres, cylinders, gyroid and lamellar structure Figure 2.27)[114] depending on the relative block lengths. These different structures can be controlled by changing the composition of the block copolymer. In our case the inter-block segregation is clearly increased in those block copolymers comprising excess amount of MPEO that make the whole system more heterogeneous and microphase separation could be observed in DSC and WAXD plots. Therefore the two crucial mechanisms that considered as the driving force for phase separation are inter-block segregation and crystallization. Any change between these two mechanisms results in both morphological and kinetic complexity as stated in more than one reference. [115-117]

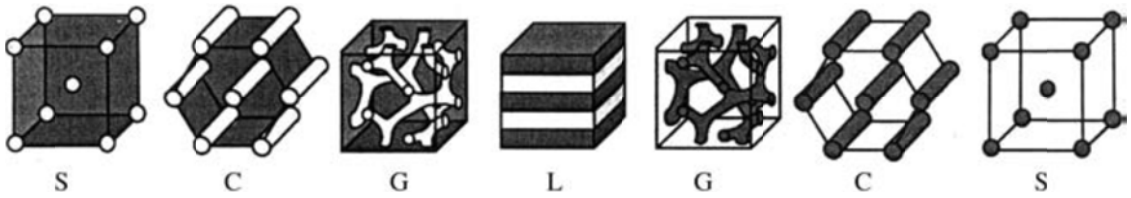

Figure 2.27. Schematic illustration of the nanostructures formed by an AB diblock copolymer in the bulk. The various phases are: S (spheres), C (hexagonally-packed cylinders), G (double gyroid), and L (lamellae). The white and grey domains represent the A and B blocks, respectively, as the fraction of A in the copolymer increases from left to right.[114]

2.5. Mechanical properties

The stress–strain properties of the block copolymers are shown in table 2.15 and figures 2.28. According to the obtained results, it is observed that by increasing the ratio of MPEO in the polymers, tensile strength and elongation are decreased, as for example in PHA-MPEO5. The whole block copolymers might be classified into three categories, 1st category is those samples containing less amount of MPEO (runs 1-2, 6-7, 11-12), where they have the best mechanical properties if compared with the remaining polymers, tensile strength(σ_b) is ranging from 1.6 MPa (run 6) to 1.0 MPa (run 12). Elongation (dL_b) values are ranging from 4 % (runs 2, 6) to 2.0 % (run 7). This values are markedly decreased when the MPEO ratio is increased to 1:1 (runs 3, 8, 13, 16, 17), which represents the 2nd category. Finally the 3rd category is those samples containing MPEO more than the PE moieties in the block copolymers (runs 4, 5, 9, 10, 14, 15). This latter category has very poor mechanical properties and the formed films are very brittle and could not be measured. These results could be attributed to the microphase separation caused by segments segregation that takes place in presence of sufficient amount of MPEO as discussed in the last section.

Table 2.5 Stress-Strain properties of the prepared block copolymers.

Run	Sample	σ_m MPa	σ_b MPa	dL_b %	E modulus MPa
		PHA-b-MPEO5			
1	¼:1	7.9	1.4	3.7	0.26
2	½:1	6.0	1.2	4.0	0.22
3	1:1	3.7	0.73	2.3	0.18
4	2:1	1.2	0.24	1.0	0.25
5	4:1			Very brittle	
		PHA-b-MPEO2			
6	¼:1	8.1	1.63	4.0	0.25
7	½:1	5.1	1.2	2.0	0.32
8	1:1	3.6	0.80	2.3	0.19
9	2:1	1.6	0.3	1.2	0.13
1017.03YA5	4:1			Very brittle	
		PBS-b-MPEO5			
11	¼:1	5.5	1.2	2.6	0.24
12	½:1	5.3	1.0	2.3	0.26
13	1:1	2.2	0.5	1.4	0.22
14	2:1			Very brittle	
15	4:1			Very brittle	
		PHS-b-MPEO5			
16	1:1	3.4	0.7	2.0	0.38
		PBA-b-MPEO5			
17	1:1	3.0	0.7	1.4	0.27

σ_m , σ_b (Stress maximum and at break), dL_b Strain at break

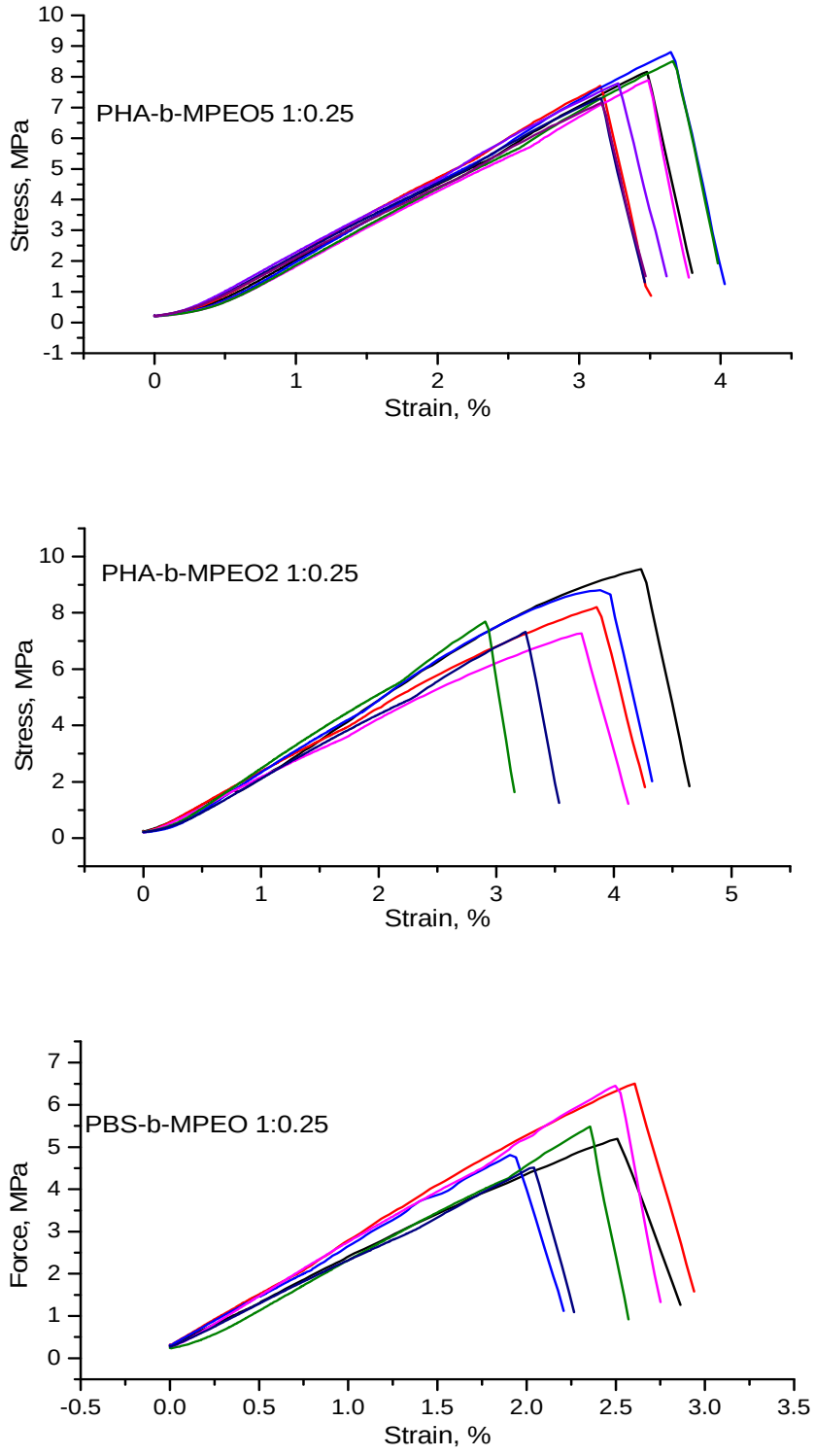

Figure 2.28a. Stress-strain curves of Block copolymer samples (runs 1, 6, 11 table 2.5)

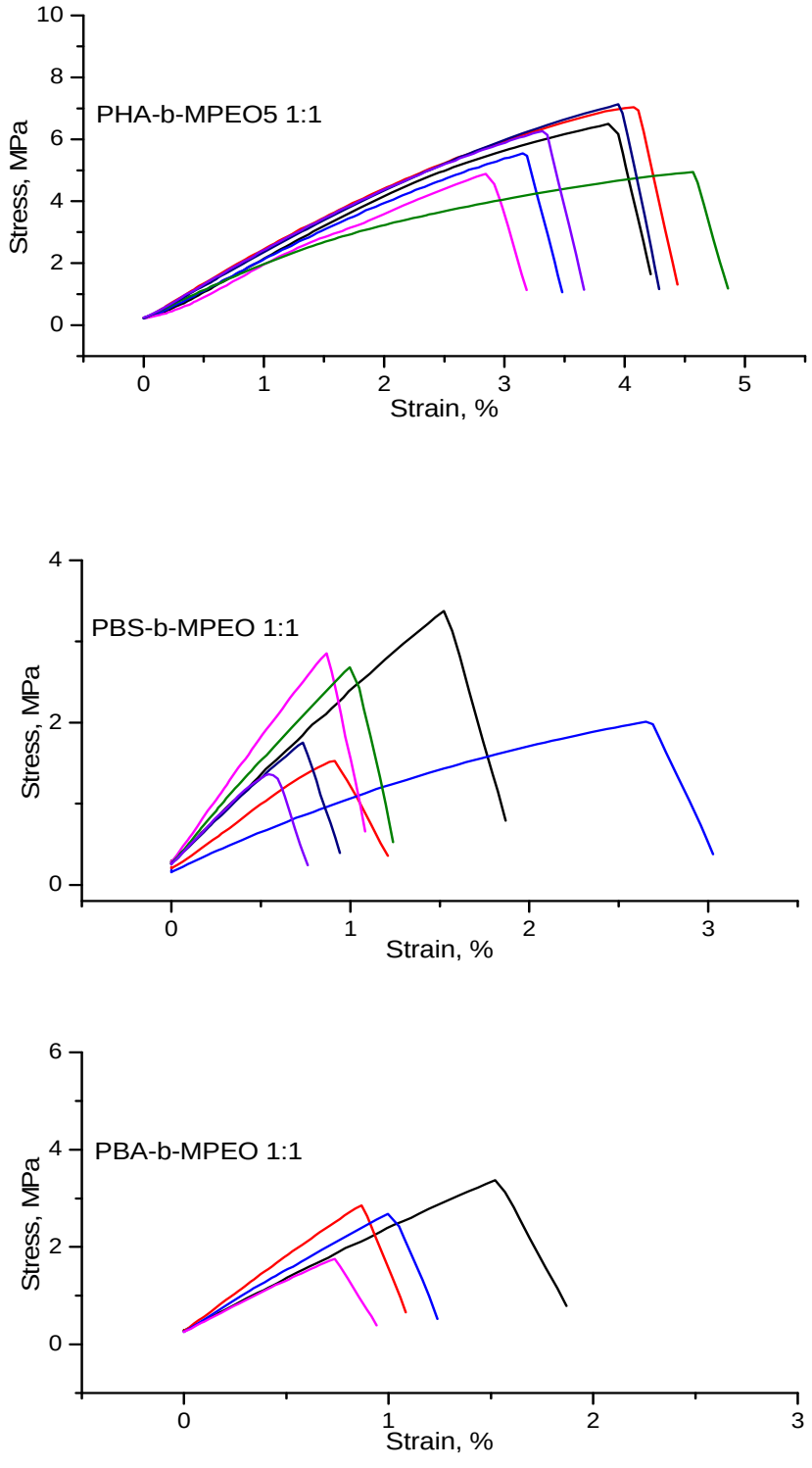

Figure 2.28b. Stress-strain curves of Block copolymer samples (runs 3, 13, 17 table 2.5)

2.6. Solubility in different solvents

Solubility of the block copolymers in polar solvents are achieved by preparing 1 % of polymer solution in different solvents. Results are shown in table 2. Chloroform, dichloromethane, THF; ethyl acetate and DMF are good solvents for most of block copolymers. In water and alcohols, the solubility is disparate, the entire polymers are sparingly soluble and the solubility is dependent on the hydrophilic/hydrophobic balance. The polymers are completely insoluble in non-polar solvents

Table 2. 6 Solubility of the prepared block copolymers in different solvents

run	MPEO/PE	H_2O	MeOH	EtOH	Isopropanol	DMSO	Acetone	$CHCl_3$	CH_2Cl_2	THF	Ethyl acetate	DMF
					PHA-b-MPEO5							
1	¼:1	S--	S--	S--	S--	S-	S-	S	S	S	S	S
2	½:1	S--	S--	S--	S--	S-	S	S	S	S	S	S
3	1:1	N	N	N	N	N	S	S	S	S	S	S
4	2:1	N	N	N	N	N	S--	S	S	S	S	S
5	4:1	N	N	N	N	N	S--	S	S	S	S	S
					PHA-b-MPEO5							
1	¼:1	S--	S--	S--	S--	S-	S-	S	S	S	S	S
2	½:1	S--	S--	S--	S--	S-	S-	S	S	S	S	S
3	1:1	N	N	N	N	N	S-	S	S	S	S	S
4	2:1	N	N	N	N	N	S--	S	S	S	S	S
5	4:1	N	N	N	N	N	S--	S	S	S	S	S
					PBS-b-MPEO5							
1	¼:1	S--	S--	S--	S--	S-	S-	S-	S-	S	S	S--
2	½:1	S--	S--	S--	S--	S-	S-	S-	S-	S	S	S--
3	1:1	N	N	N	N	N	S-	S-	S-	S	S	S--
4	2:1	N	N	N	N	N	S--	S-	S-	S	S	S--
5	4:1	N	N	N	N	N	S--	S-	S-	S	S	S--
					PHS-b-MPEO5							
	1:1	S--	S--	S-	S--	S-	S	S	S	S	S	S-
					PBA-b-MPEO5							
	1:1	S--	S--	S-	S--	S-	S	S	S	S	S	S-

S: soluble, N: non-soluble, S: sparingly soluble, S--: very less solubility

2.7. Conclusion

1- Full characterization of the prepared block copolymers has been achieved using 1 and 2D NMR, IR, TGA, DSC, X-ray and mechanical testing.
2- Moderate molecular weights are obtained and the polymers containing more hydrophobic segments have higher molecular weights.
3- Micropahse separation, a well-known phenomenon that occurs in amphiphilic block copolymers is used to interpret the melting behavior, crystal structure and mechanical properties of the prepared polymers.
4- Microphase separation could be observed clearly, when the MPEO amount in the block copolymer is high enough, so that chemical incompatibility is high and segregation between both hydrophilic and hydrophobic take place leading to the separation between two segments.
5- The prepared polymers are insoluble in non-polar solvents, while in polar solvent, the solubility is disparate, depending on type of the PE and the hydrophilic/ hydrophobic ratio

Chapter 3

Hydro and Biodegradation of the prepared block copolymers

3.1. Hydrolytic degradation

The hydrolytic degradation of the prepared block copolymers were done by dissolving 0.2 g of the polymer sample in 12 mL of 5 % KOH aqueous solution and left to stir for 24 at room temperature. After that the solution was neutralized by addition of equivalent concentration of HCl. The neutralized samples were stirred with equivalent amount of $CHCl_3$ to extract the polymer. The $CHCl_3$ phase was separated from the aqueous phase by separating funnel and subjected to rotary to evaporate the chloroform. The collected samples were dried in vacuum oven at 40 ^oC for 72 h. The samples were then analyzed by NMR and GPC. Results are shown in Tables 3.1 and Figure 3.1and 3.2. The degree of degradation was calculated from the ^{1}HNMR charts by comparing the integral intensity of the four protons of MPEO at ppm 3.60 with the protons of the hydrophobic segment at ppm 4.06 that represent the terminal diol protons in the different hydrophobic segments (i.e. PHA, PBS, PBA and PHS). For example, I found the integration of the adipate 4 protons peak at 4.06 was decreased from 3.9 of the virgin sample to 1.1 of the hydrolyzed one (Table 3.1 run 3). This means that the amount of the remaining adipate segment is about 28 % ((1.1/3.9)*100) and thus the degree of degradation is 100-28 = 72 %. By the same way all degradation % was calculated as shown from ^{1}HNMR overlay of PHA-b-MPEO5 ratio 1:1 and PHA-b-MPEO2 ratio 1:1 as representative examples in figure 3.1. All block copolymers are hydrolyzed under the alkaline conditions with higher % of degradation. Slight increase in the degradation % is observed with copolymers having higher hydrophobic segments. Molecular weight is drastically decreased to few hundreds, but the numerical values should be taken with caution as the GPC elugrams of the hydrolyzed samples are multi-modal due to the action of hydrolysis and presence of a lot of oligomeric short chains as also indicated by the drastic increase in polydispersities. But the important issue is that these elugrams occur at higher elution volume region i.e. the lower molecular weight region as shown in figures 3.2.

Table 3.1. Weight losses, molecular weights of the hydrolyzed block copolyesters in comparison with the virgin values and the degradation % of the hydrolyzed polyesters calculated from ^{1}HNMR after 24 h degradation time.

Run	MPEO/PE	Virgin sample		Hydrolyzed sample		Weight loss,	degradation
		Mn	PDI	Mn	PDI	%	%
				PHA-b-MPEO5			
1	¼:1	18000	2.02	1100	8.29	78	88
2	½:1	16000	1.90	870	3.04	78	76
3	1:1	16000	2.20	790	4.40	77	75
4	2:1	15000	1.92	1040	3.98	78	72
5	4:1	8300	1.62	2330	2.76	76	71
				PHA-b-MPEO2			
6	¼:1	21000	1.88	690	5.26	78	78
7	½:1	14000	2.03	920	2.11	79	85
8	1:1	14000	2.06	870	3.04	73	82
9	2:1	8000	1.90	850	2.50	76	75
10	4:1	11000	1.57	690	1050	78	72
				PBS-b-MPEO5			
11	¼:1	18000	2.16	2500	2.77	90	83
12	½:1	20000	2.14	3700	2.53	86	81
13	1:1	18000	2.58	1400	2.19	80	81
14	2:1	16000	2.14	1800	2.44	67	78
15	4:1	14000	2.04	3500	2.11	69	75
				PHS-b-MPEO5			
16	1:1.0	12000	2.16	2200	2.36	67	80
				PBA-b-MPEO5			
17	1:1.0	9000	1.99	1800	2.68	70	78

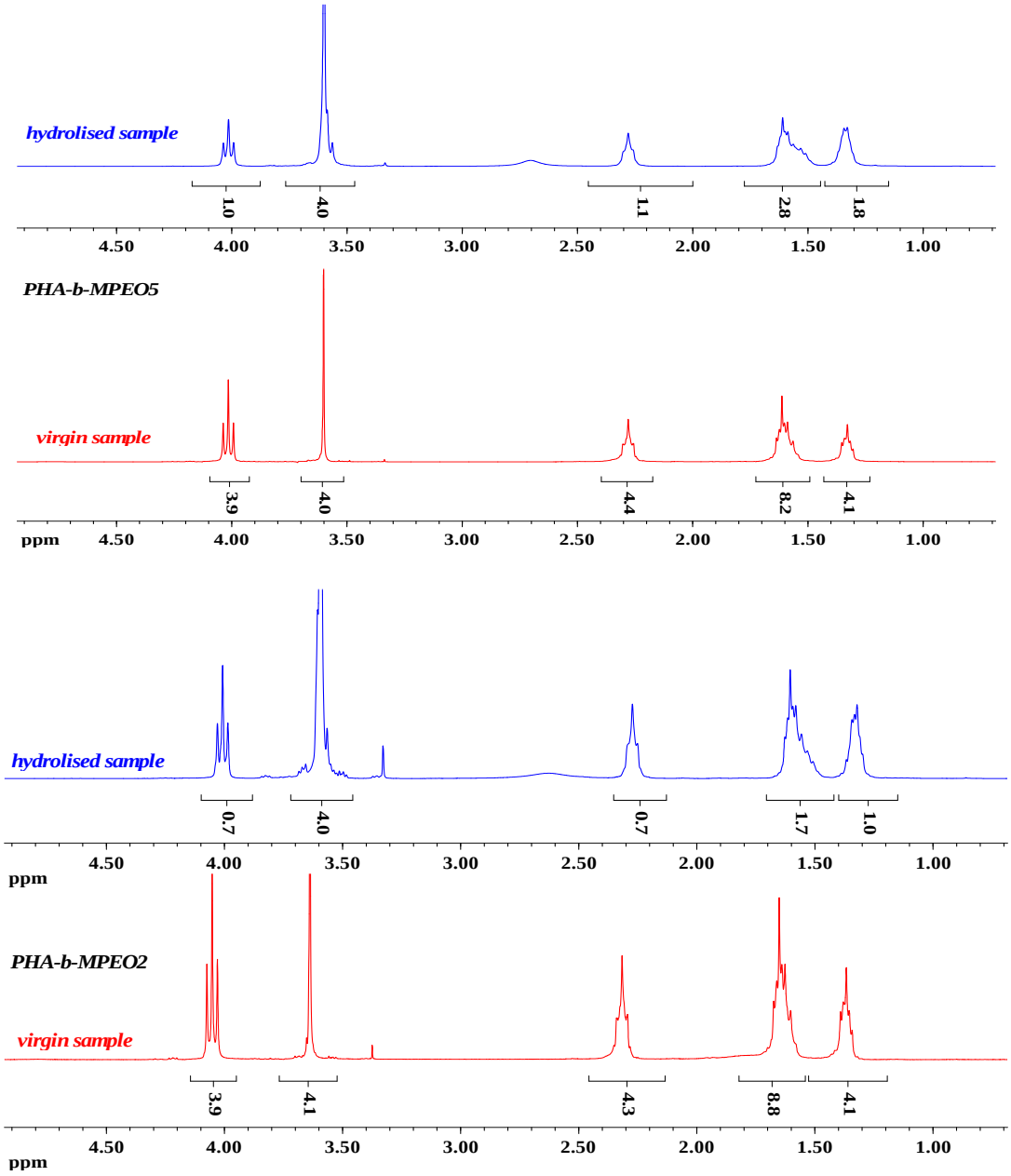

Figure 3.1. [1]HNMR overlays of both hydrolyzed and virgin PHA-b-MPEO (5000, 2000 1:1, Table 3.1 runs 1, 8) illustrating the integrals that used to calculate degradation %.

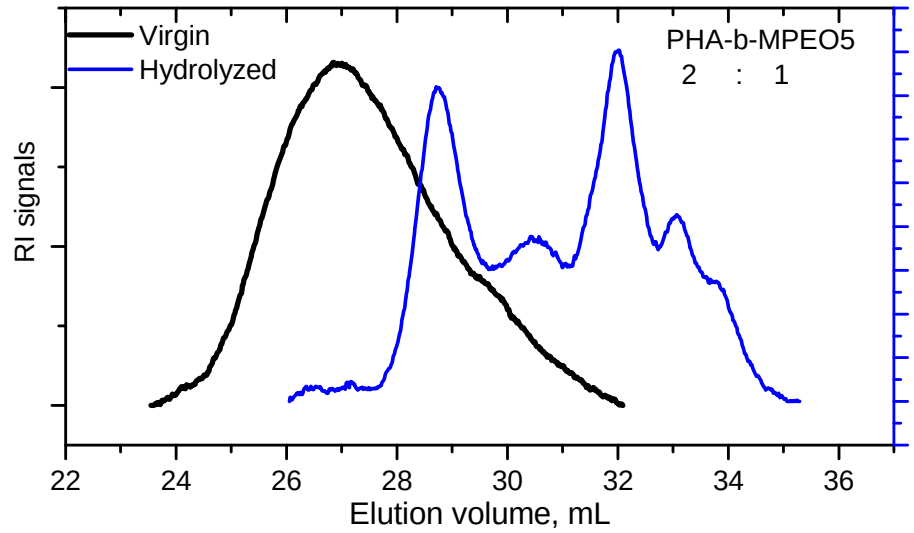

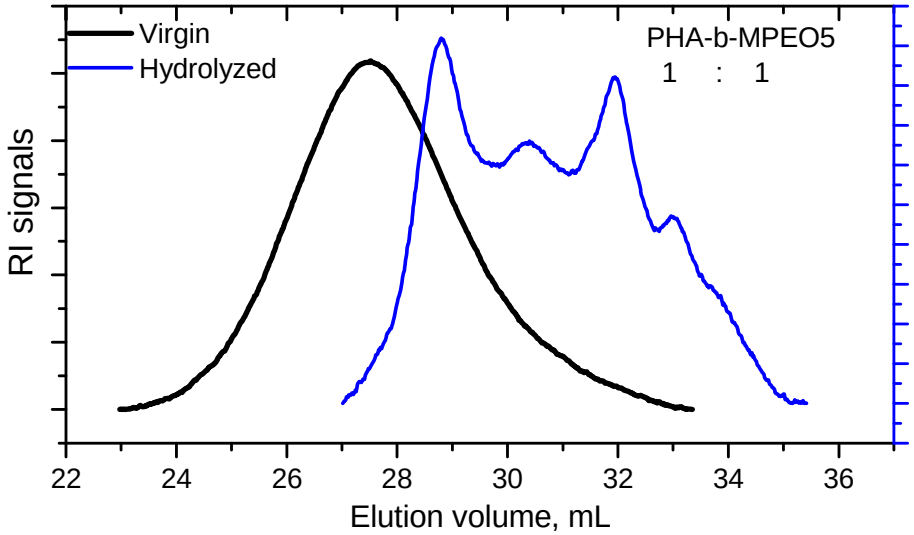

Figure 3.2 GPC overlays of both hydrolyzed and virgin PHA-b-MPEO5 (Table 3.1 runs 2-4)

As represented in figures 3.2 and 3.3 the hydrolyzed samples were eluted at higher volume with multi-peaks elugram that consisting of a fixed sharp peak at elution volume about 29 mL for PHA-b-MPEO5 (i.e. MPEO of 5000 Da) and 31 mL for PHA-b-MPEO2 (i.e. MPEO of 2000 Da). These sharp peaks represent the hydrolyzed MPEO from the block copolyester as confirmed

by the GPC elugrams of virgin MPEO5 and MPEO2, where they have nearly the same elution volume as of the aforementioned two sharp peaks.

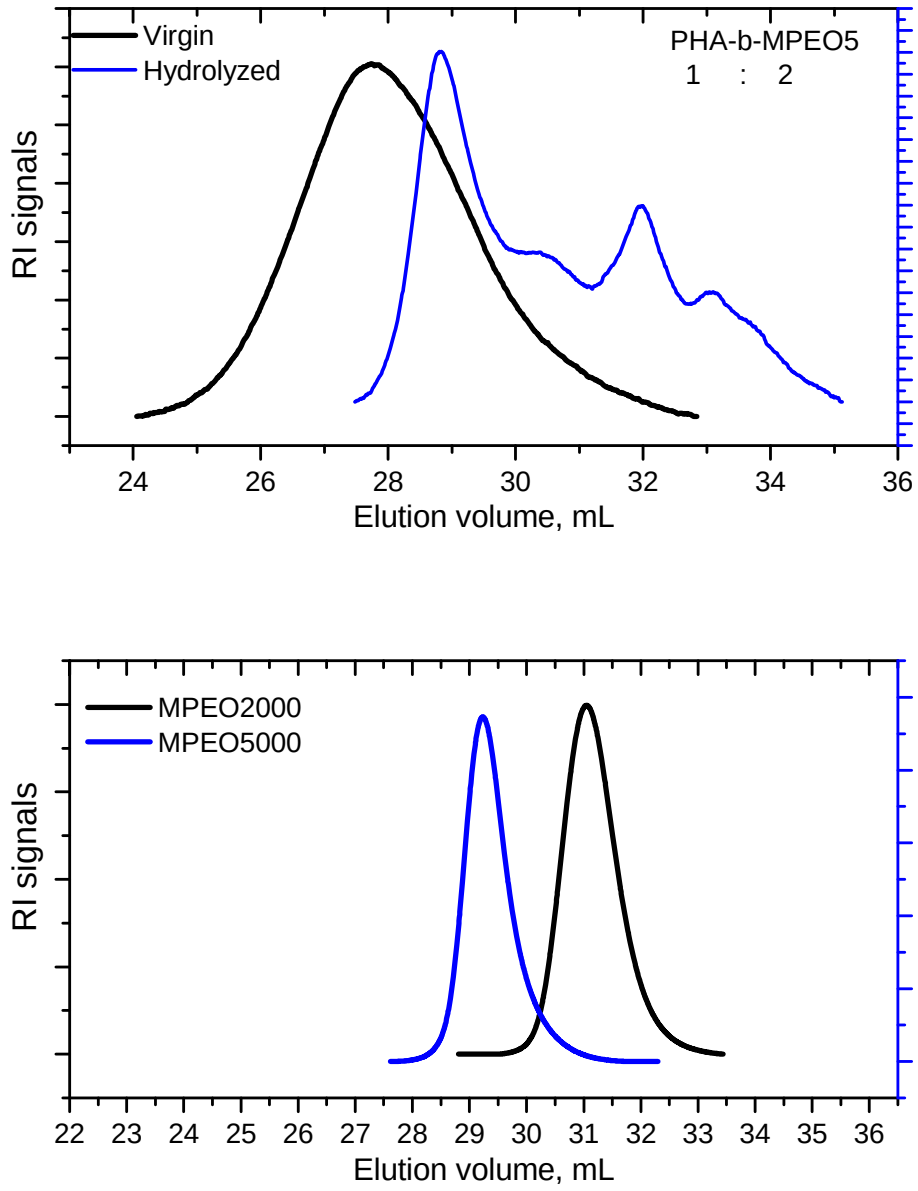

Figure 3.2 continued GPC overlays of both MPEO5 and MPEO2. They eluted at the same volume as the sharp peaks of the degraded polymers.

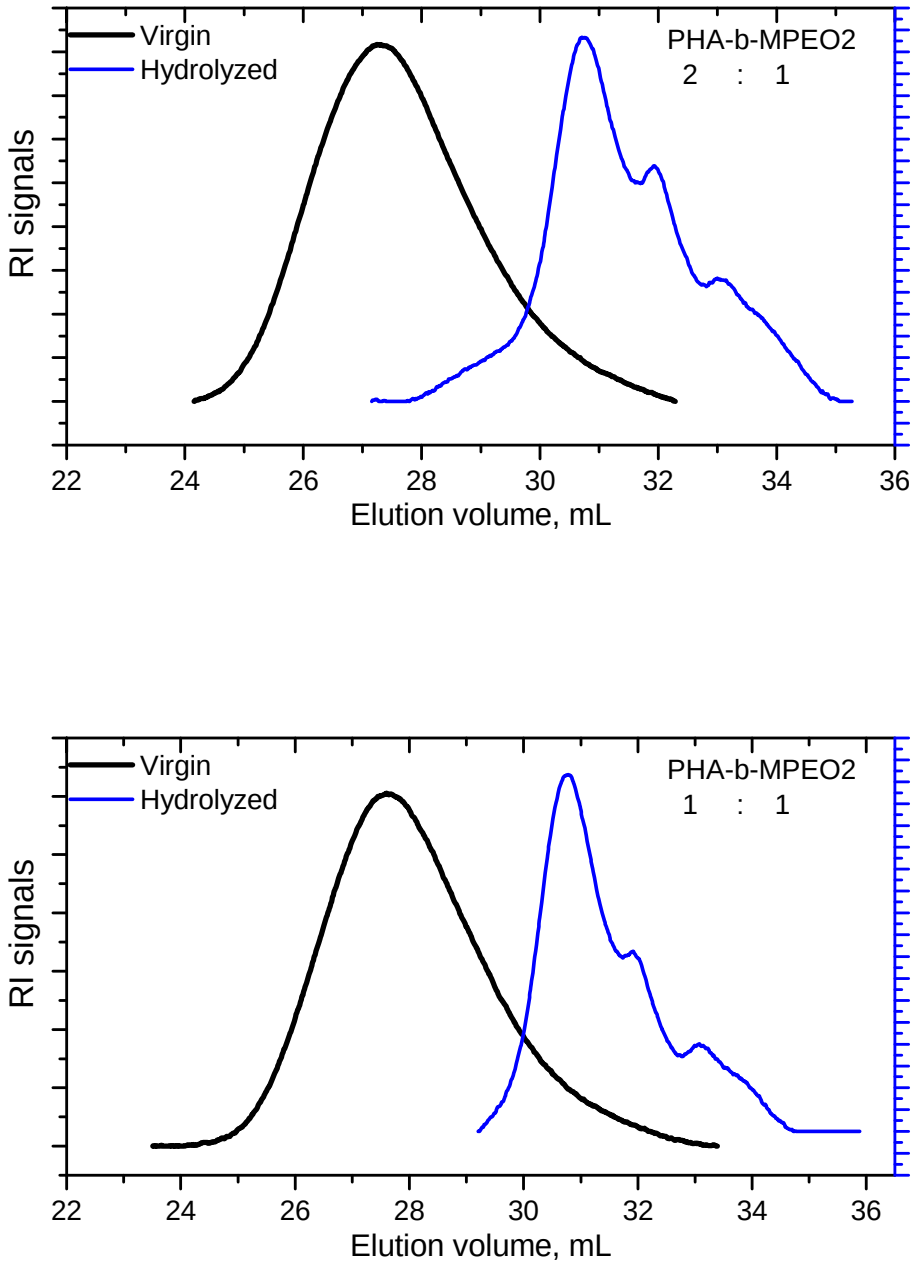

Figure 3.3. GPC overlays of both hydrolyzed and virgin PHA-b-MPEO2 (Table 3.1 runs 7-9)

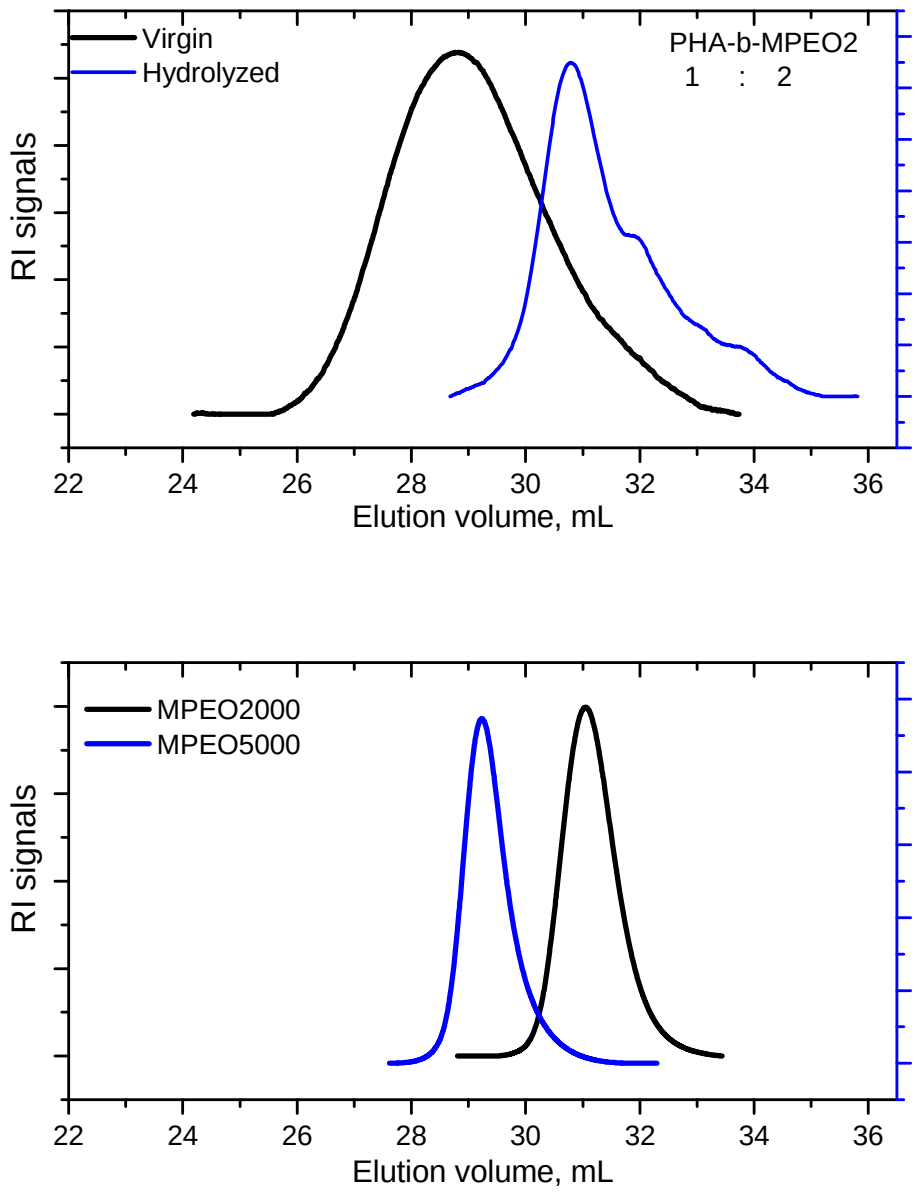

Figure 3.3 continued GPC overlays of both MPEO5 and MPEO2. They eluted at the same volume as the sharp peaks of the degraded polymers.

The kinetics of the hydrolytic degradation of the prepared block copolyesters were done for the samples PHA-b-MPEO5 with feed molar ratio 1/1 and PHA-b-MPEO2 feed molar ratio 1:1 as representative examples (Table 3.1, runs 3 and 8) using 5 and 10 % KOH aqueous solution for PHA-b-MPEO2 and PHA-b-MPEO5 respectively to see the effect of the hydrolytic solution on the degradation process as both samples have the same chemical structure and comparable molecular weight. Figures 3.4 and 3.5 show the degradation % vs. time and the weight loss vs. time respectively. As expected both degradation % as well as weight loss are increased as the degradation time increases, where after 24 h the degradation % was about 45 and 55 % for PHA-b-MPEO2 and PHA-b-MPEO5 respectively, while the weight loss was about 40 and 55 % after 18 h. Higher rate of degradation for PHA-b-MPEO5 was observed due to the usage of higher concentration of KOH solution (10%).

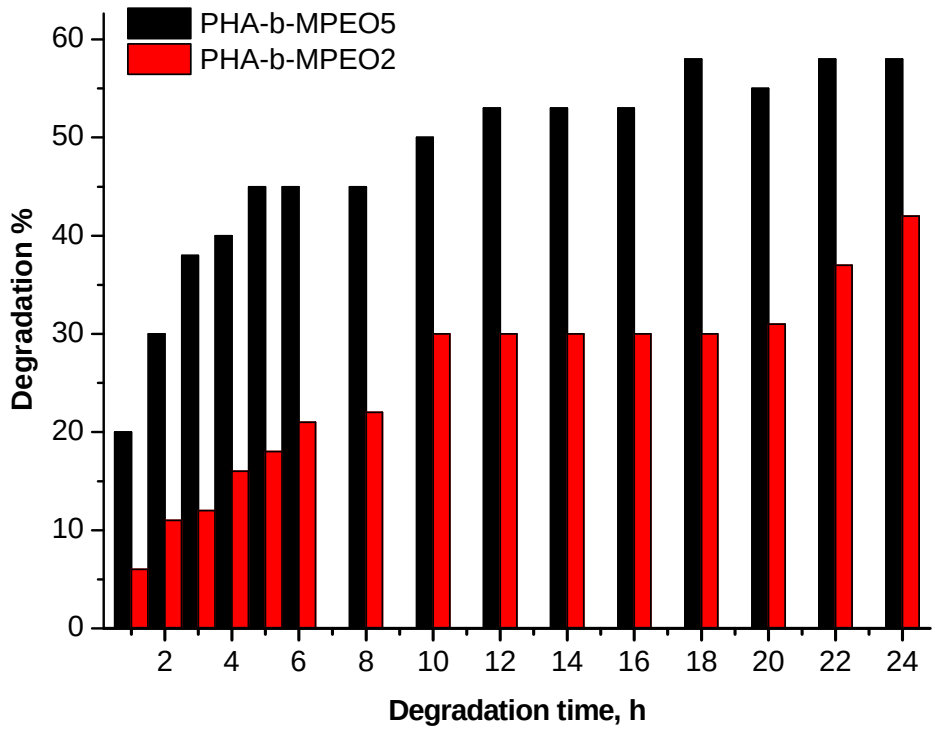

Figure 3.4. Degradation % vs. Time in the hydrolytic degradation of PHA-b-MPEO2 (molar ratio 1:1, 5% KOH solution) and PHA-b-MPEO5 (molar ratio 1:1, 10% KOH solution).

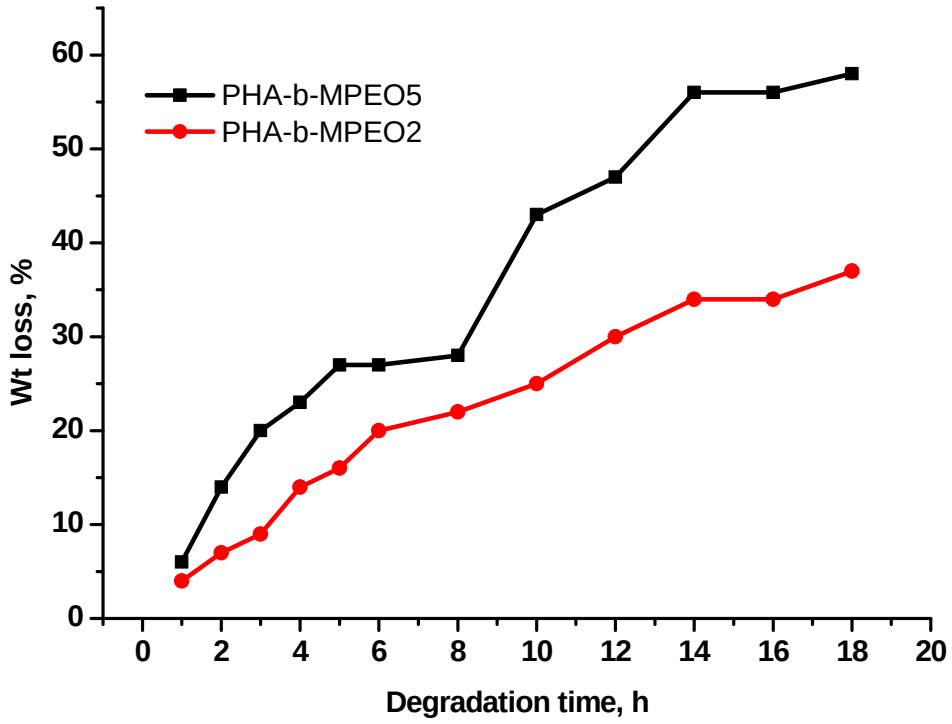

Figure 3.5. Weight loss % vs. Time in the hydrolytic degradation of PHA-b-MPEO2 (molar ratio 1:1, 5% KOH solution) and PHA-b-MPEO5 (molar ratio 1:1, 10% KOH solution)

The Molecular weights (Mn and Mw) were also decreased drastically with increasing degradation time. After only 1h the Mn of both polymers PHA-b-MPEO2 and PHA-b-MPEO5 was decreased by about 60 and 75 % respectively. No more loss in molecular weights was observed after 4 h in case of using 10 % KOH. Also the higher concentration of KOH plays a significant role for faster degradation time. Figure 3.6 shows the decrease of molecular weight with degradation time.

Table 3.2. Molecular weights of the degraded samples at different time of hydrolysis.

Degradation Time, h	PHA-b-MPEO2 5% KOH				PHA-b-MPEO5 10% KOH			
	Mn	Mw	Mp	PDI	Mn	Mw	Mp	PDI
0	14400	30000	31000	2.06	16000	36000	34000	2.20
1	5900	17000	1700	2.85	4900	12500	10000	3.04
2	4194	11300	1100	2.69	3600	12000	10000	3.38
3	2800	9000	3600	3.32	2200	5900	10000	2.63
4	3000	8000	3600	2.59	1900	5000	10000	2.85
5	2900	7600	3500	2.59	1900	5000	10000	2.78
6	2700	6900	3400	2.51	1900	5000	10000	2.76
8	2100	5800	3400	2.69	1900	5000	10600	2.67
10	2100	5100	3000	2.33	1800	4900	10000	2.74
14	1900	5500	3000	2.83	1700	4900	10000	2.91
16	1800	5000	3400	2.68	1600	4800	10000	3.07
18	1800	4900	3200	2.68	2200	5000	10000	2.36
20	1600	3500	2900	2.16	1900	5000	10000	2.86
24	1700	3500	2700	2.08	1900	5000	10000	2.76

Numerical values of Mp are not very accurate because of the multi-modal elugrams of the degraded polymers especially for PHA-b-MPO5, while in PHA-b-MPEO2 bi-modal elugrams were obtained. All the elugrams are shifted to the low molecular weight region with splitting of the original peaks into MPEO peak and other shorter oligomer chains that appear at higher elution volume as shown in figure 3.7 and 3.8 for PAH-b-MPEO5 and PHA-b-MPEO2 respectively. It is only 30 minutes and a shoulder in the GPC elugram of PHA-MPEO5 could be observed, while a clear shoulder is observed after 1 hour in PHA-b-MPEO2.

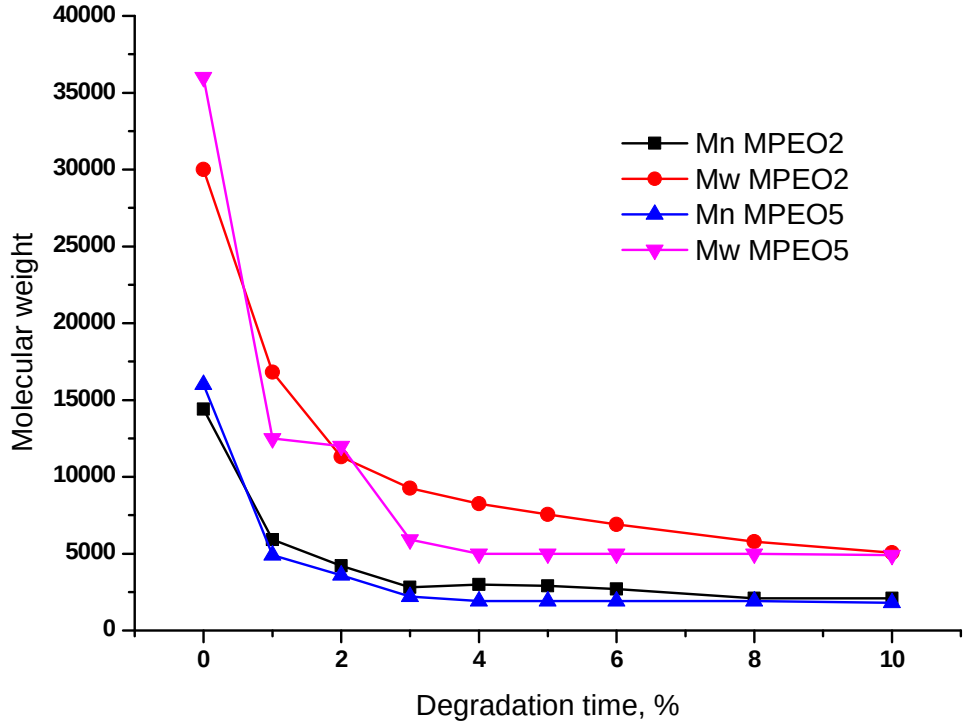

Figure 3.6. Molecular weights (Mn and Mw) % vs. Time in the hydrolytic degradation of PHA-b-MPEO2 (molar ratio 1:1, 5% KOH solution) and PHA-b-MPEO5 (molar ratio 1:1, 10% KOH solution)

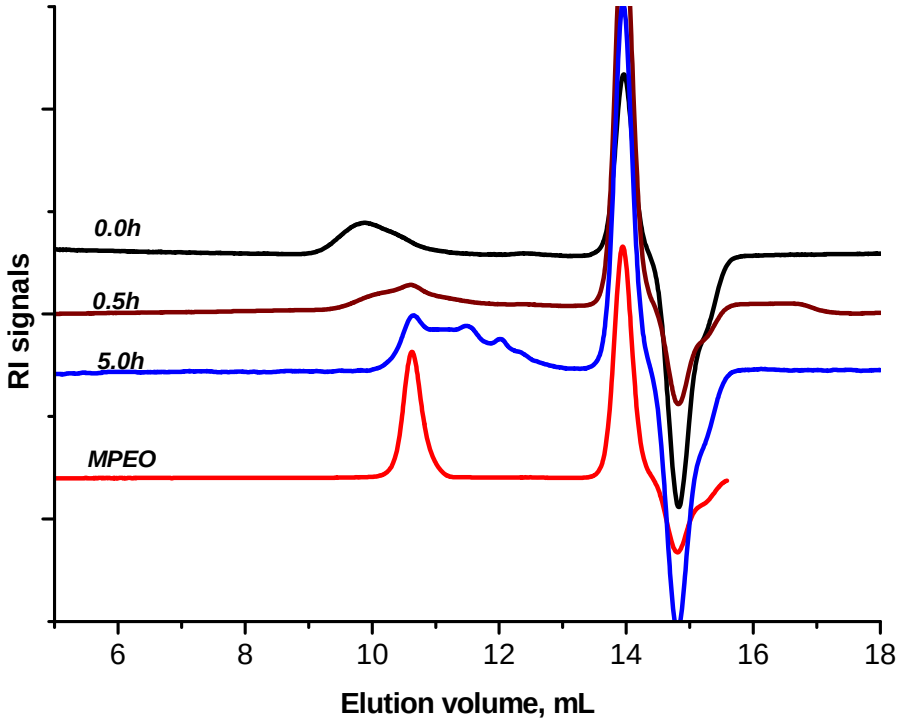

Figure 3.7 GPC Elugram of degraded PHA-b-MPEO5 with feed molar ratio 1:1 at different time (Table 3.1 run 3).

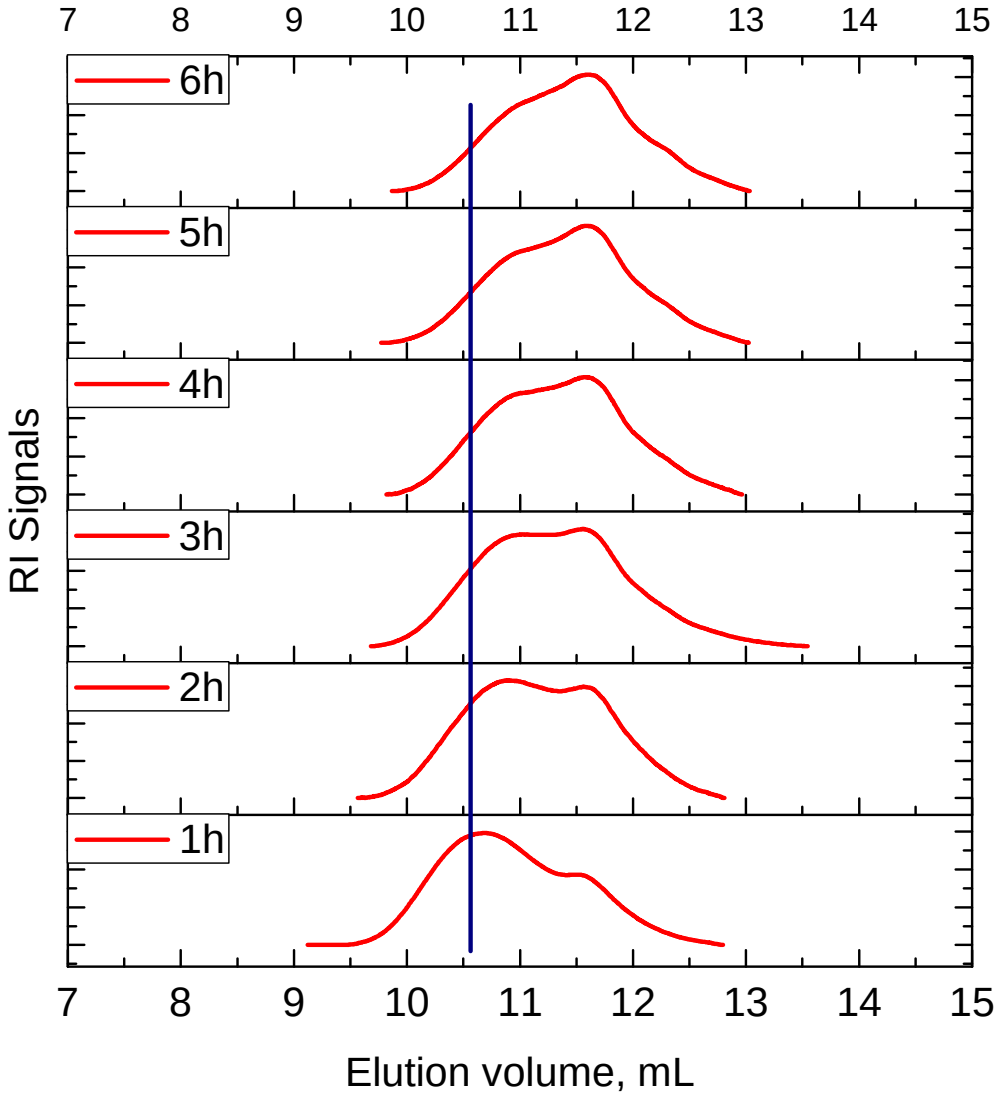

Figure 3.8. GPC Elugram of degraded PHA-b-MPEO2 at different time (Table 3.1 run 8).

3.2. Enzyme-catalyzed degradation

Degradation of the block copolymer in presence of lipase enzyme was achieved in phosphate buffer solution (pH 7). At first slabs from the polymers were cut from polymers films that made by hot press method. These slabs were immersed in the buffer solution containing the enzyme to give a final concentration of 18.5 mg enzyme / mL and 16 mg polymer / mL. In all experiments a blank sample was always accompanied. Sodium azide of concentration 18.5 mg/mL was also added to prevent fermentation/bacterial growth of the enzyme solution. Samples with 1:1 molar ratio were tested. In this process, another term is always used in such cases of enzyme catalyzed degradation and coined as erosion. Before I exhibit my data, the degradation and erosion processes are briefly discussed.

It is well established that, the degradable polymers are subjected to eroding upon degradation; therefore erosion and degradation are the critical parameters of such materials.[118] Two types of erosion are already established, namely, surface (or heterogeneous) and bulk (or homogeneous) eroding materials,[119] as sketched in figure 3.9. In surface erosion, polymers lose material from the surface only. They get smaller but keep their original geometric shape. In case of bulk eroding polymers, penetration of the bulk of the polymer by the enzymatic solution is the main degradation way.[120] Another important difference between the two mechanisms is that in case of surface erosion, molecular weight is remained constant during the erosion process. Polymer erosion is more complex than degradation, because it depends on many other processes, such as degradation, swelling, the dissolution and diffusion of oligomers and monomers, and morphological changes. The knowledge of the erosion mechanism is, therefore, important for the successful application of a degradable polymer. In tissue engineering for example, surface properties or porosity determine the performance of implantable scaffolds.[121] In drug delivery, swelling and porosity are critical to the release behavior of drugs". As with degradation, many different indicators of erosion have been proposed, such as molecular weight loss, sample weight loss and changing geometry. These latter three parameters were used to evaluate the biodegradation of the polymers under investigation as represented in table 3.3 and figures 3.9-3.18

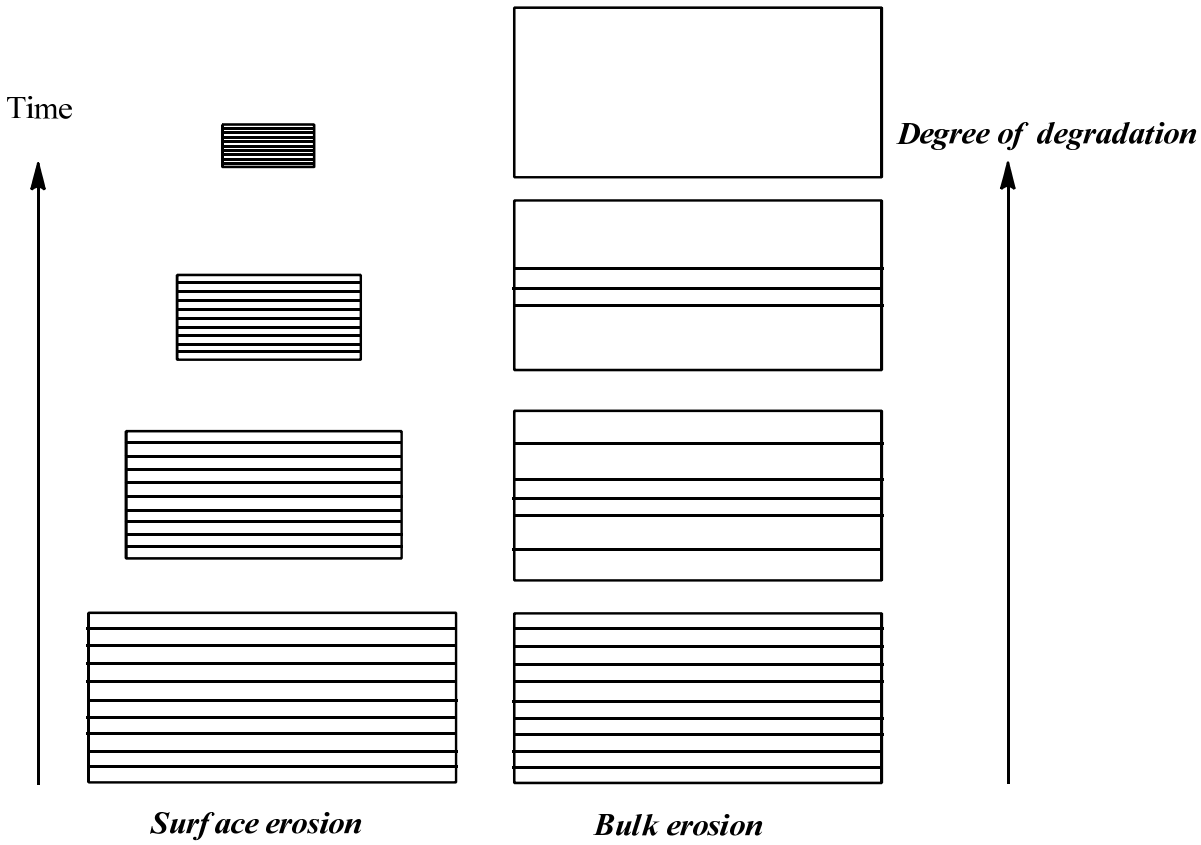

Figure 3.9 Schematic diagram illustrating surface erosion and bulk erosion in a polymer matrix.[118]

Table 3.3 Molecular weights of the block copolymers after enzyme-catalyzed degradation at different times

time days	PHA-b-MPEO5	PHA-b-MPEO2	PBS-b-MPEO5	PBA-b-MPEO5	PHS-b-MPEO5
	Molecular weight (Mn) g / mol				
0	16000	14400	18000	9000	12000
1	15000	14000	16000	2300	11000
2	15000	14500	16000	2400	10000
3	15000	14000	15000	2600	3000
4	15000	15000	16000	4100	4000
5	15000	14000	15000	---	---
8	14000	16000	17000	--	---
9	15000	15000	15000	---	--
10	14000	13000	15000	--	--
11	---	---	15000	--	---
12	---	---	15000	--	---

Molecular weights of the polymers PHA-b-MPEO5, PHA-b-MPEO2 (1:1 molar feed ratio) remain mostly constant during the degradation process until about 10 days. After that, disintegration of the polymers in the enzymatic solution took place as indicated from the GPC elugrams in figures 3.10 where the intensity of the RI detector are clearly decreased keeping in mind the concentrations of the measured samples is about 1mg/mL. In case of PBS-b- MPEO5 polymer consistency is still present in absence of reduction in molecular weights (Fig 3.11). In contrast to the previous polymers, PBA-b- MPEO5 and PHS-b- MPEO5 are fast disintegrated in a short period of erosion time with an observable reduction in molecular weights as shown in figures 3.12 and 3.13. A comparison of the molecular weights of the all kind of block copolymers polymers vs. time are plotted and represented in figure 3.14, where Mn was plotted vs. time of enzyme degradation.

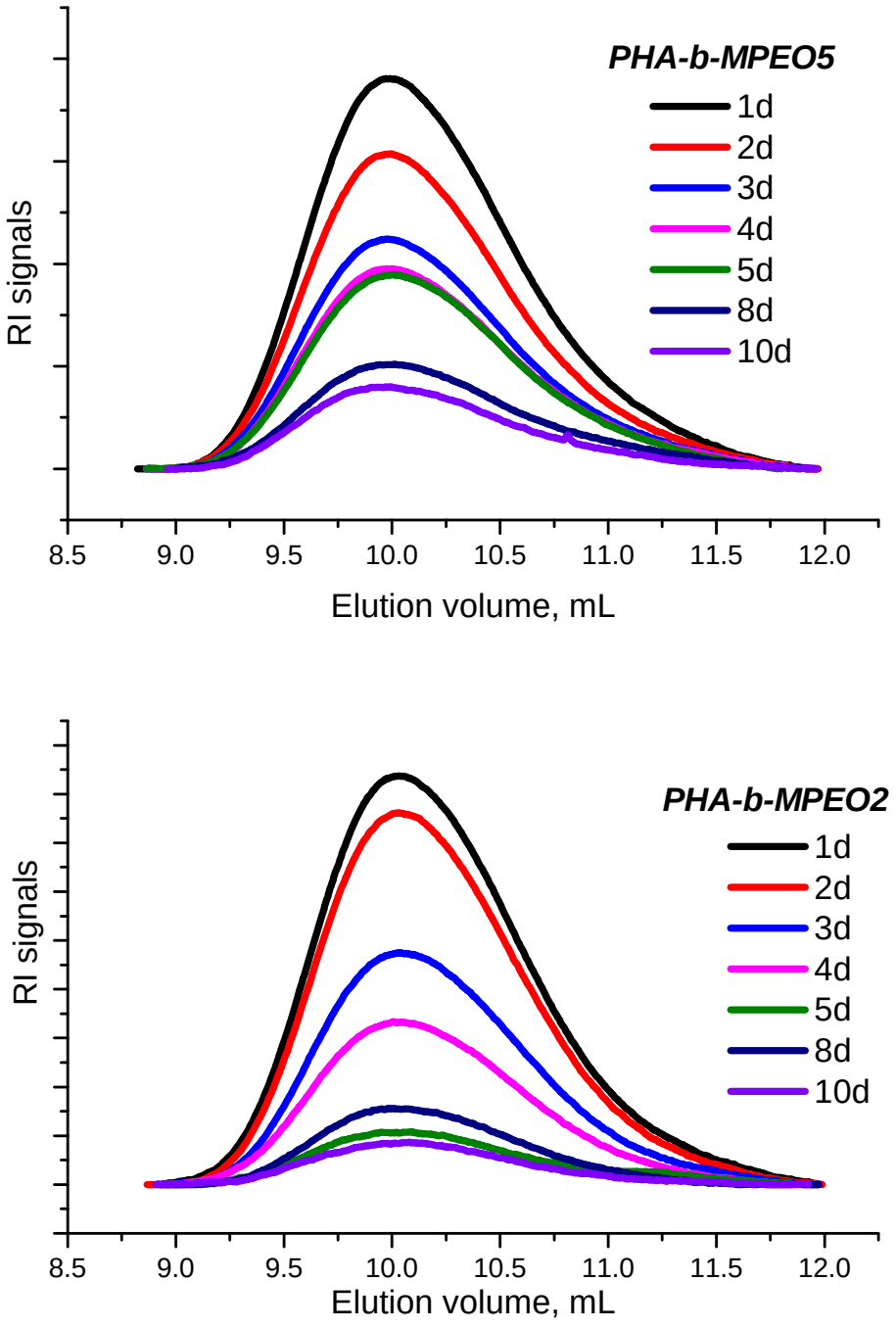

Figure 3.10 GPC elugrams of PHA-b-MPEO5 and PHA-b-MPEO5 vs. time of enzyme-catalyzed degradation.

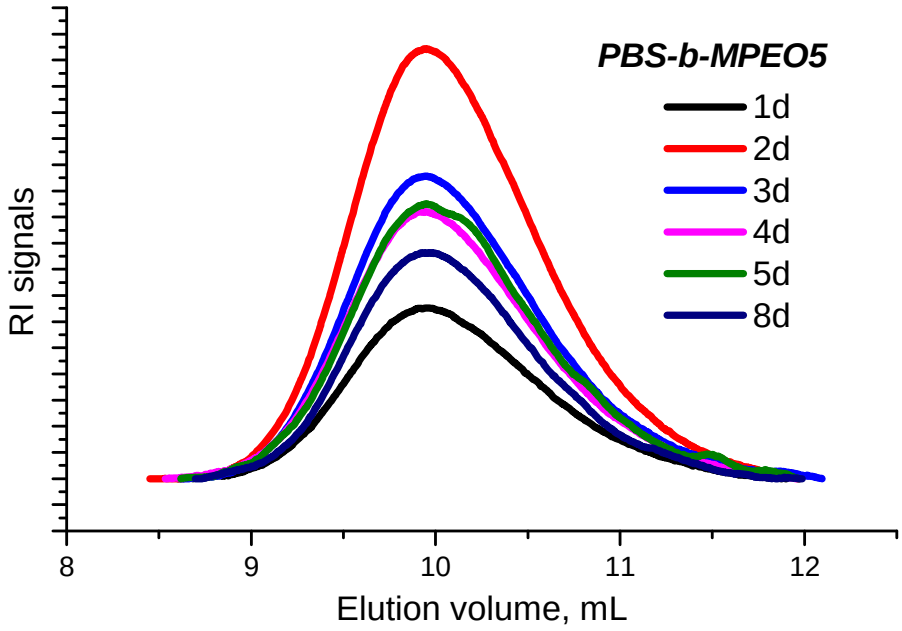

Figure 3.11 GPC elugrams of PBS-b-MPEO5 vs. time of enzyme-catalyzed degradation.

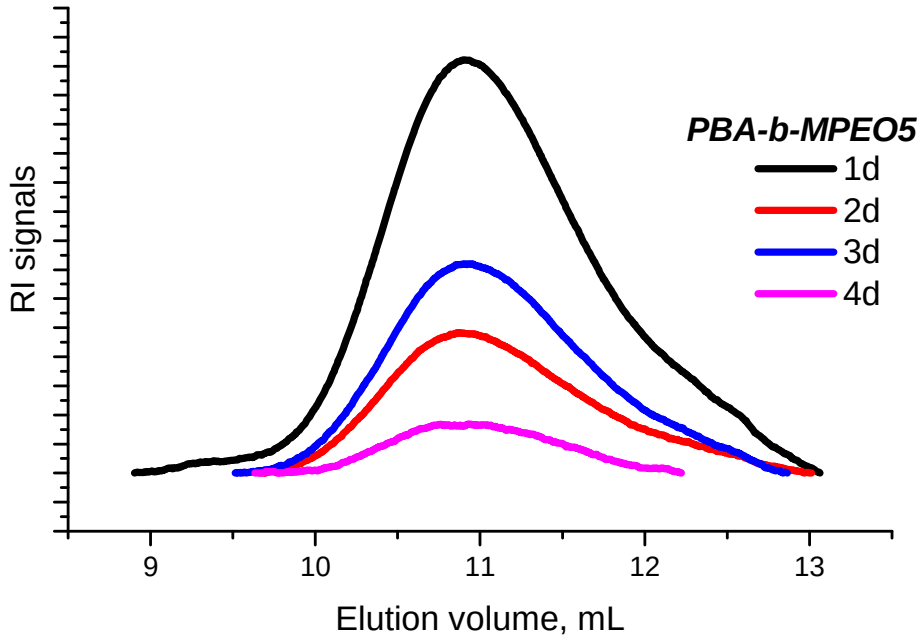

Figure 3.12 GPC elugrams of PBA-b-MPEO5 vs. time of enzyme-catalyzed degradation.

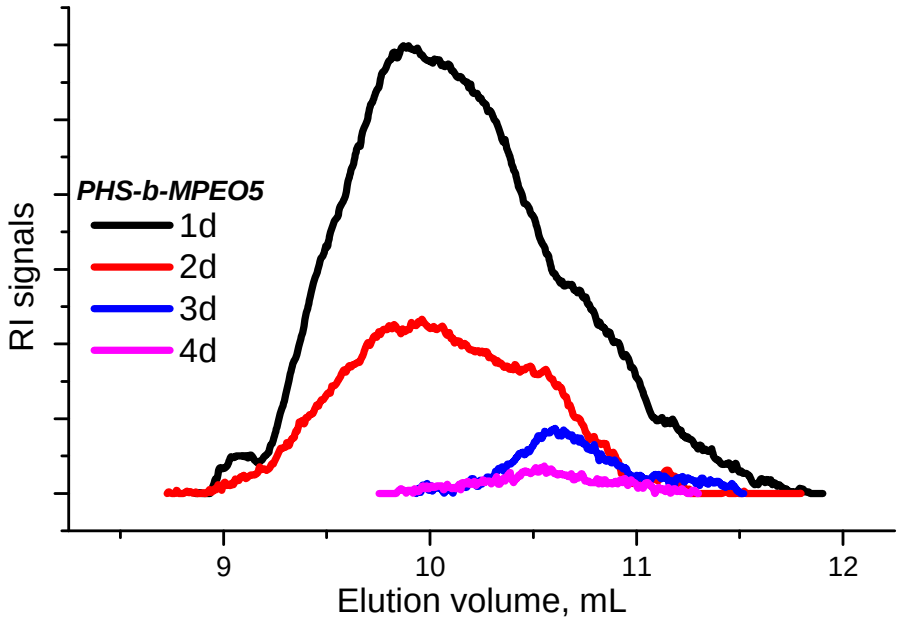

Figure 3.13 GPC elugrams of PHS-b-MPEO5 vs. time of enzyme-catalyzed degradation.

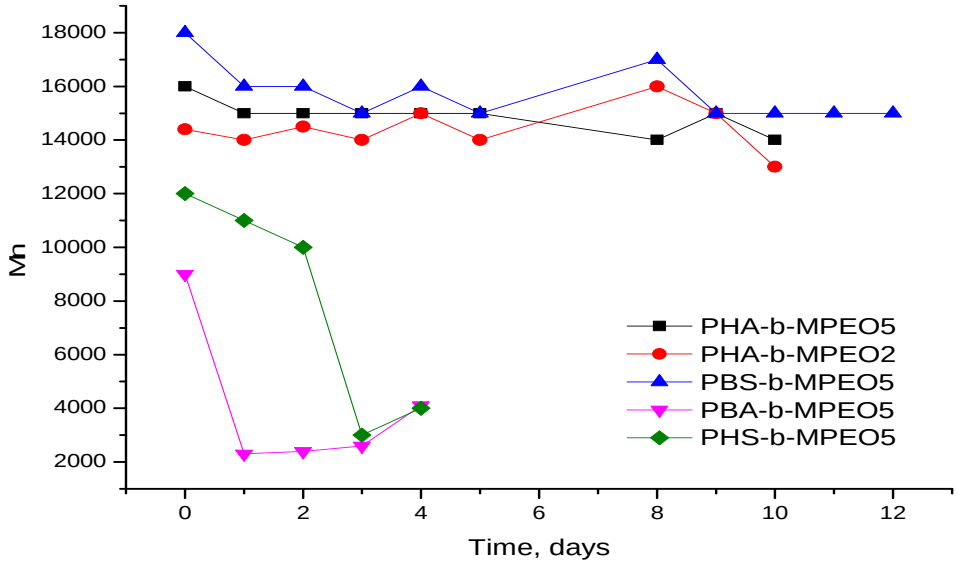

Figure 3.14 Molecular weights (Mn) vs. enzyme-catalyzed degradation time.

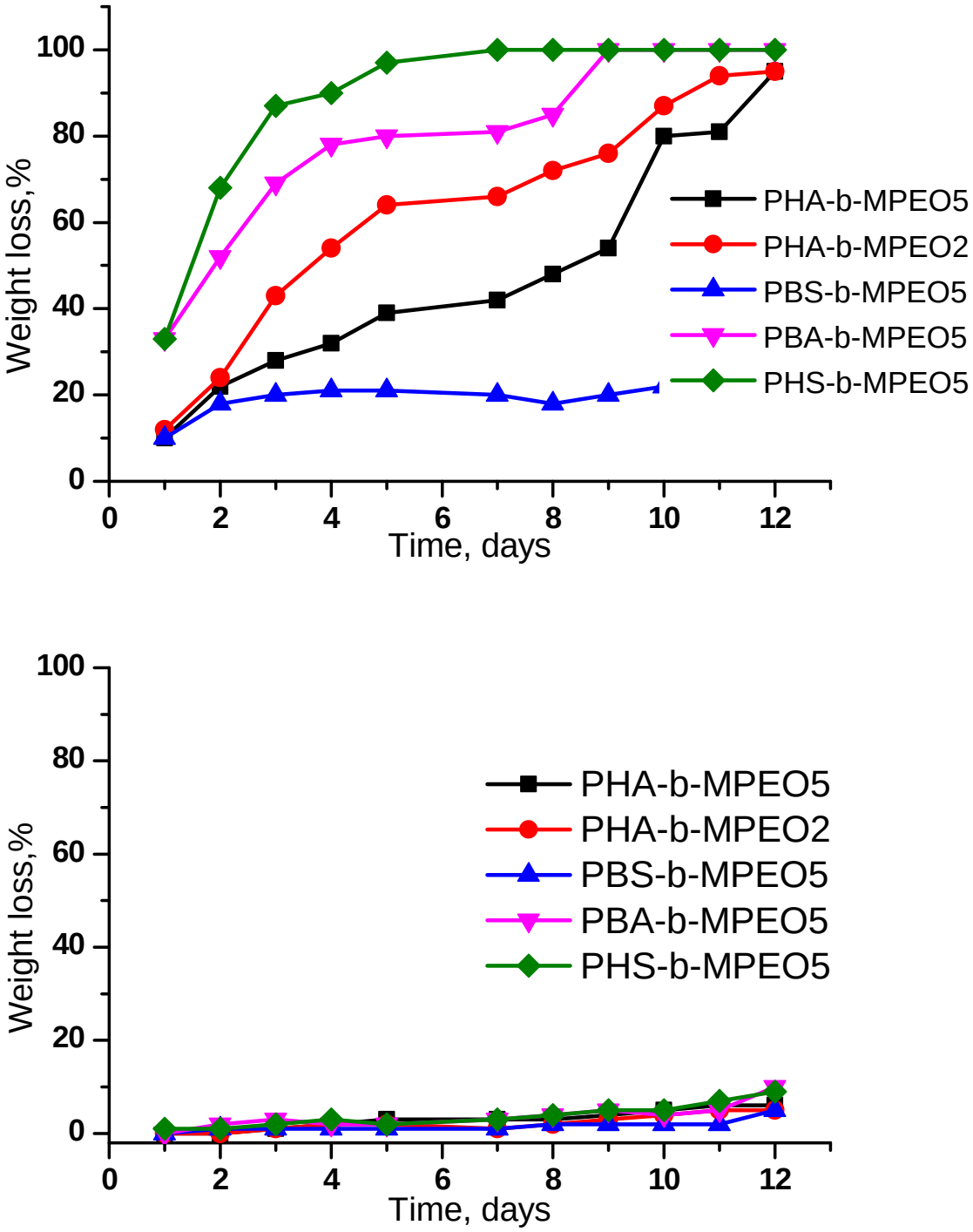

Figure 3.15 Weight losses vs. degradation time in presence (Top) and in absence (bottom) of enzyme.

Loss in weight with erosion time is shown in figure 3.15. For PHA-b-MPEO family; they have nearly the same behavior, where about 95 % of weight loss is reached in 12 days. PBS-b-MPEO5 block copolymer has very weak rate of hydrolysis, where after 12 days in the enzymatic hydrolytic solution, only about 20% weight loss is observed. By combining these results with the values of molecular weights we can conclude that for PBS based polymers, lipase cannot play the role of hero to catalyze the degradation of PBS-b-MPEO5 under the aforementioned degradation conditions (pH 7, 37 ^{o}C). According to the literature, PBS homopolymers could be degraded using (Lipase from *pseudomonas cepacia*) in slightly acidic buffer and higher temperature (pH 6, 50 ^{o}C), this only achieved using PBS films, however in case of using PBS fibers, it undergoes little enzymatic hydrolysis under the same conditions, where the molecular orientation of the polymer is crucial to determine the degradation mechanism as reported by Kimura et.al[123] and many others.[124,125] In our case we were interested to use a degradation conditions close to the physiological conditions inside the human body. This enzyme could play an essential role in the degradation of both PBA-b-MPEO5 and PHS-b-MPEO5. Only 4 days is required to degenerate 80 % of the PHS-b-MPEO5 and PBA-b-MPEO5 with drastic reduction in molecular weights. For all polymers weight loss in absence of enzyme did not exceed 10 % after immersion in enzyme-free buffer solution for 12 days.

Another point in this issue is the degraded products and mode of degradation. From NMR as in hydrolytic degradation the hydrophobic/hydrophilic ratio of the block copolymers is also disturbed under the action of the enzymatic degradation. For example an overlay of ^{1}HNMR of degraded PHA-b-MPEO5 after 1 and 12 days of enzymatic degradation in comparison with the virgin samples as well as the ^{1}HNMR of adipic acid and 1,6 hexandiol is represented in figure 3.16. This figure shows that by increasing the degradation time, the ratio of MPEO is decreased with respect to the hydrophilic segment as indicated by the integration of the MPEO protons to the terminal protons of diol moiety in the PE segments. This means the enzymatic solution attacks first the ester bond that joins the PE segments and the MPEO in contrary to what happened in case of hydrolytic degradation. Regarding to the degraded products, adipic acid moiety could be observed in the ^{1}HNMR of the degraded sample after 12 days of degradation time at 1.49 ppm that is not exist in the NMR chart after 1 day of degradation. Also hexandiol

moiety is observed at 1.35 ppm, i.e. the enzyme attacks also the hydrophobic chains of the PHA in the whole block copolymer and converts it to the individual monomers.

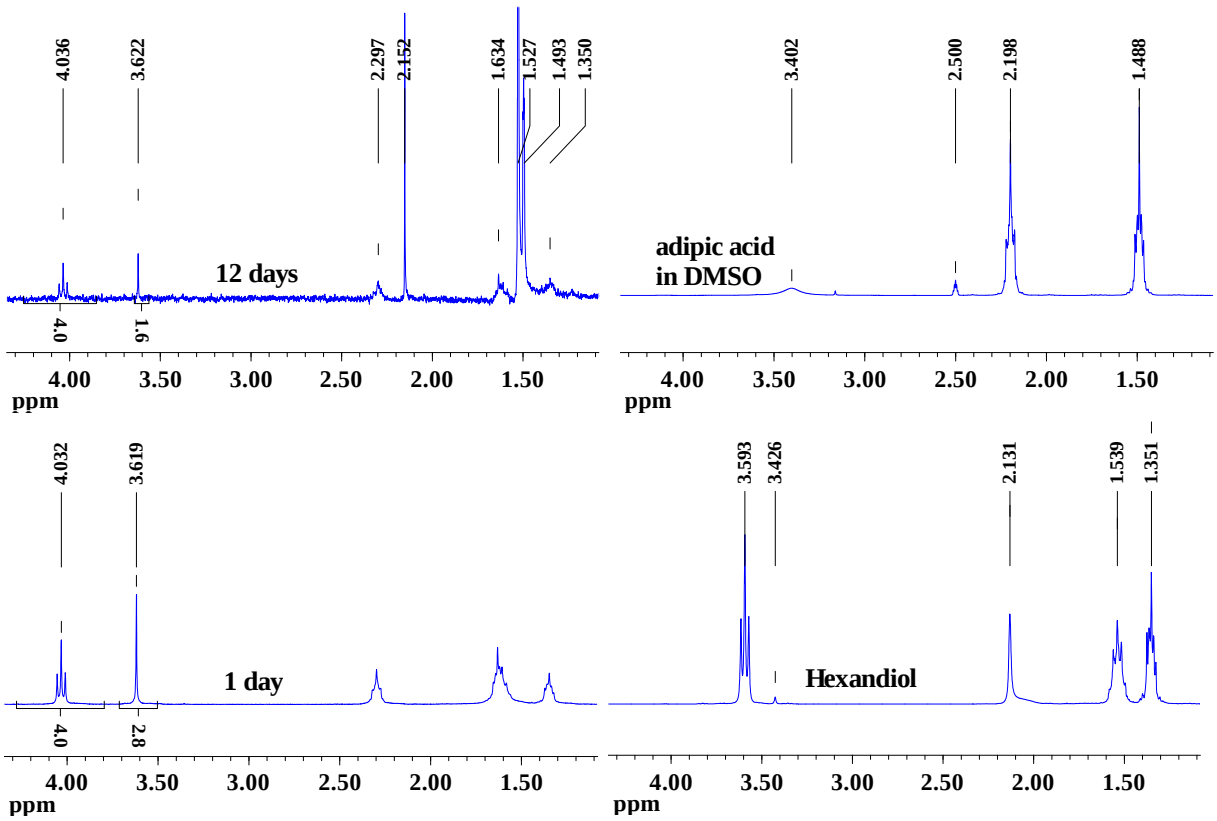

Figure 3.16.[1]H NMR overlay of PHA-b-MPO5 after 1 and 12 degradation days, adipic acid and 1,6 hexandiol. (After 12 days of degradation, a peaks of monomer are observed at 1.349 for adipic acid and 1.35 for1,6 hexandiol moiety).

3.2.2. Scanning Electron Microscope (SEM) analysis.

The morphology of degraded polymers before and after enzymatic hydrolysis was analyzed by scanning electron microscope surface (SEM). Images are shown in figures 3.17. Erosion is clearly observed on the surface of all polymers subjected to enzymatic solution in comparison with those just immersed in a buffer solution without enzyme, with appearing of many cracks and holes on the surface. The diameter of these holes is also increased with degradation times.

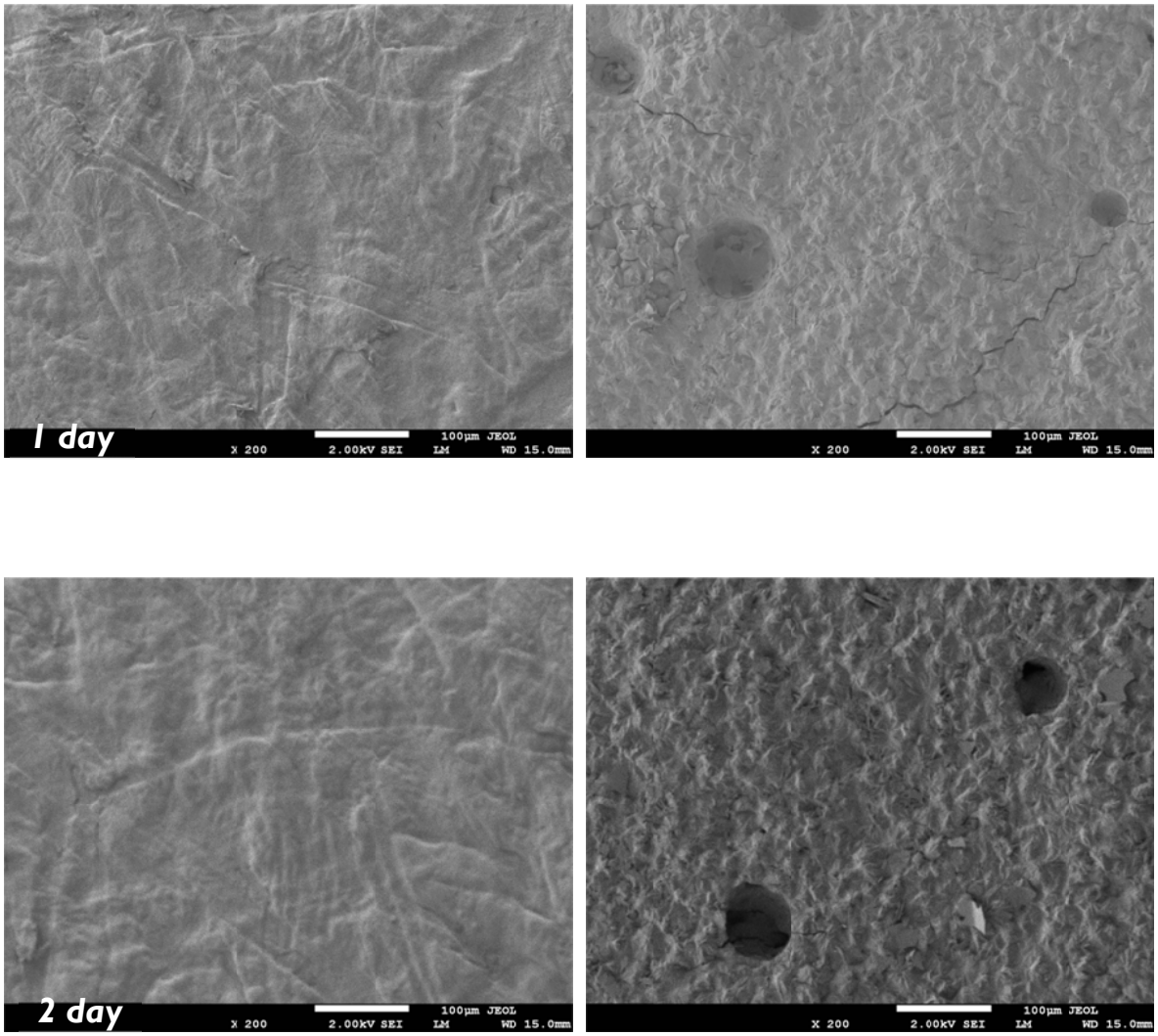

Figure 3.17 SEM images of PHA-b-MPEO5 (1:1 molar feed ratio) films subjected to enzyme degradation (right) and non-biodegraded films (left) for different degradation time.

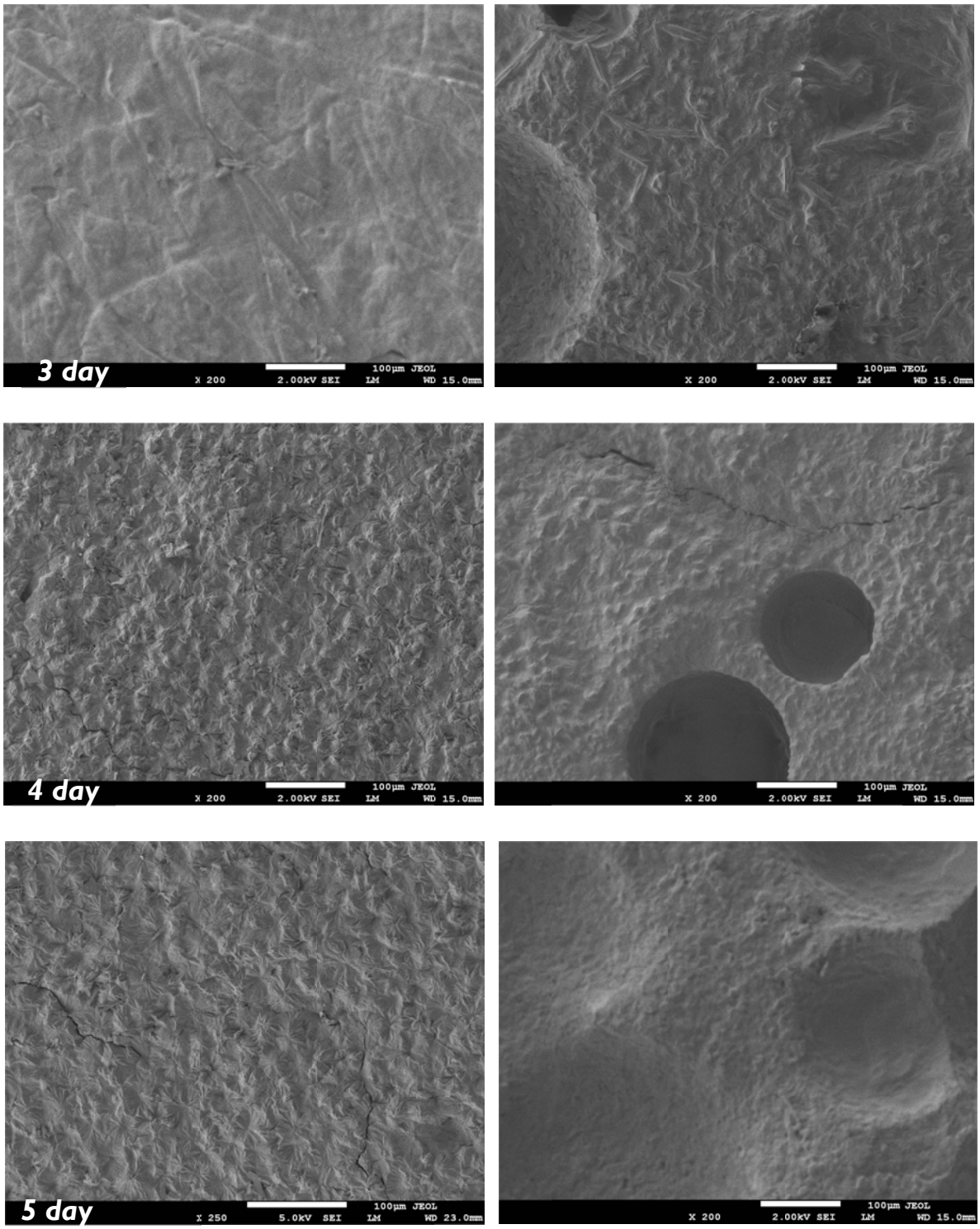

Figure 3.17 continued

3.3. Conclusion

1- Hydrolytic degradation is achieved using potassium hydroxide aqueous solution of concentration 5 % and 10%. All polymers are hydrolyzed by attacking the ester linkage of the hydrophobic segments.

2- Enzyme catalyzed degradation is also achieved using lipase from *pseudomonas cepacia* enzyme. This enzyme is suitable to degrade PHA, PBA and PHS. But it is less efficient for PBS based polymers under the stated degradation conditions.

3- Degradation mechanism was via surface erosion and the order of degradability could be arranged as follow PBA=PHS > PHA> PBS.

Chapter 4

Immobilizing of pH-dependent, bioactive ingredient on the polymer backbone

4.1. Introduction

The pH responsive polymers are those polymers that respond to small change in pH. These polymers can contribute in a wide range of application in biomedical, bioengineering and pharmaceutical areas and in particularly drug delivery systems. One of the most interesting groups that have been utilized to switch pH-inactive polymers to pH-active polymers is sulfonamide.[125-128] Sulfonamides is a common name of a large number of derivatives of 4-aminobenzene-1-sulfonamide. In 1908, 4-aminobenzene-1-sulfonamide was discovered and used in dye industry and later it gains more importance by using it as antibacterial agent. A lot of substituents have been introduced to the sulfonamide group in order to improve their antibacterial activity. Sulfonamides are considered as week acids due to the partial ionization of the hydrogen atom of the amide groups in solution. These weak acidic characters are enhanced by the electron deficiency of the nitrogen atom of the amide group that will imply to the ease of hydrogen liberation in solution. This electron deficiency is coming from the attraction of the bond electrons between sulfur and oxygen towards the more electronegative atom (oxygen). As the sulfur is more electronegative than nitrogen, it again withdraws the bond electrons of themselves i.e. sulfur and nitrogen. Then the nitrogen became less negative and week attraction with hydrogen took place thus the hydrogen is liberated easily as shown in figure 4.1

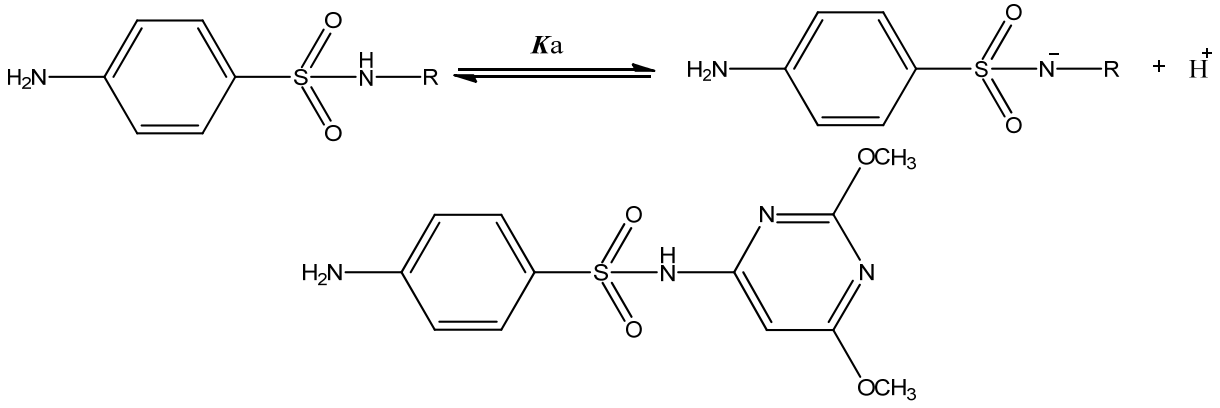

Figure 4.1 Mode of dissociation of sulfonamide group in solutions

4.2. Concept

By utilizing the benefit of the pH responsibility of the sulfonamide groups[125-128], a trial was achieved to modify our polymer by immobilizing this group onto the polymer chains. Sulfadimethoxine (SD) (4-amino-N-(2,6-dimethoxypyrimidin-4-yl) benzenesulfonamide) (Figure 4.1) and PHA-b-MPEO5 were chosen to achieve this purpose. The concept is to connect the SD at the chain end by either transamidation or direct coupling with the chain end groups as shown in figure 4.2.

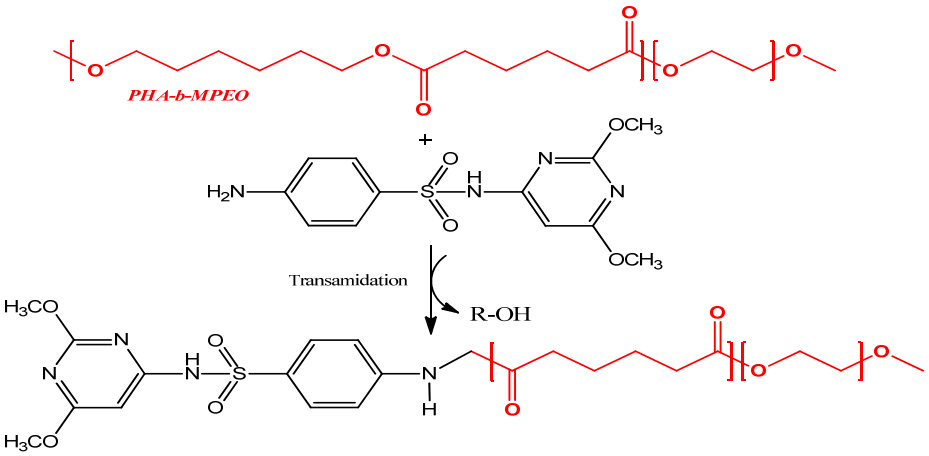

A-Transamidation mechanism

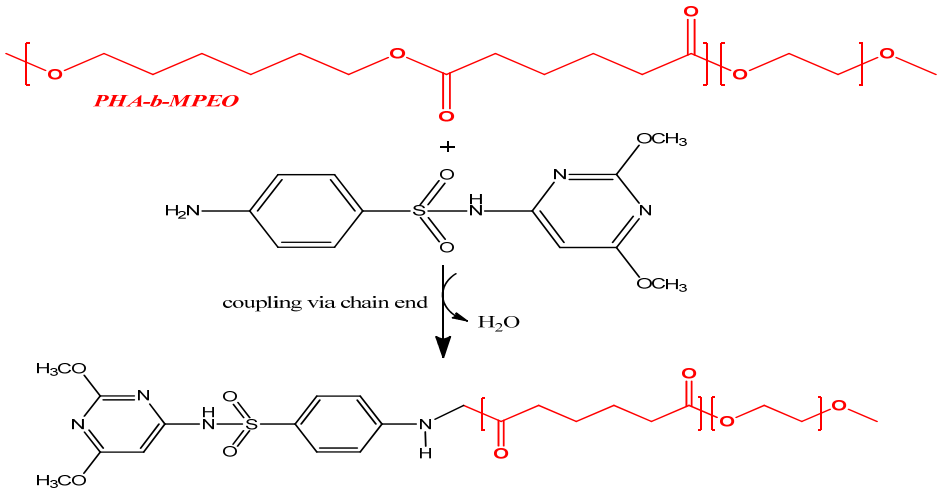

B -Coupling via chain end

Figure 4.2 Proposed mechanisms of SD immobilization onto the PHA-b-MPEO5

4.3. Experimental

Exp1. In four different experiments Sulfadimethoxine (0.0 g, 0.5 g, 1.0 g, 2.0 g) was added to 10 g of PHA-b-MPEO5 (Adipate:MPEO 1:1) and reacted together at 150 ^{o}C for 24 h, then the polymer was dissolved in chloroform and then filtered to remove the un-reacted Sulfadimethoxine as it is not soluble in Chloroform. Then the filtrate was concentrated and precipitated in n-pentane. The obtained polymer was again dissolved in Chloroform, filtered and precipitated in n-pentane again and left to dry under vacuum for 6 days at room temperature. The sample after that was analyzed by NMR and GPC.

Exp2. Another experiment is as follow. 1 g Sulfadimethoxine and 10 g of PHA-b-MPEO5 (Adipate:MPEO 1:1) were dissolved in 100 mL distilled THF in 250 mL Flask and left to reflux @ 100 ^{o}C for 4 h and 24 h.

Exp3. 1 g Sulfadimethoxine and 10 g of PHA-b-MPEO5 (Adipate:MPEO 1:1) were dissolved in 100 mL distilled THF in 250 mL Flask and left to stir @ room temperature for 5 days. Experimental conditions are summarized in Table 4.1

Table 4.1 Experimental conditions of the reaction between SD and PHA-b-MPEO5 (10g)

Run	SD Conc, g	Temperature, ^{o}C	Time	Solvent	Yield, %
YA00		Virgin sample			
YA01	---	150	24 h	---	95
YA02	0.5	150	24 h	---	95
YA03	1.0	150	24 h	---	96
YA04	2.0	150	24 h	---	94
YA05	1.0	100	24 h	100 mL THF	95
YA06	1.0	100	4 h	100 mL THF	93
YA07	1.0	r.t	5 days	100 mL THF	95

4.4. Results and discussion

At first ***Exp1*** will be discussed, where the different weights of SD were mixed directly with the solid PHA-bMPEO5 and left to react at 150°C. ^{1}HNMR of the products are shown in figure 4.3a&b. GPC elugrams are shown in figure 4.4 and the molecular weight values are represented in table 4.2.

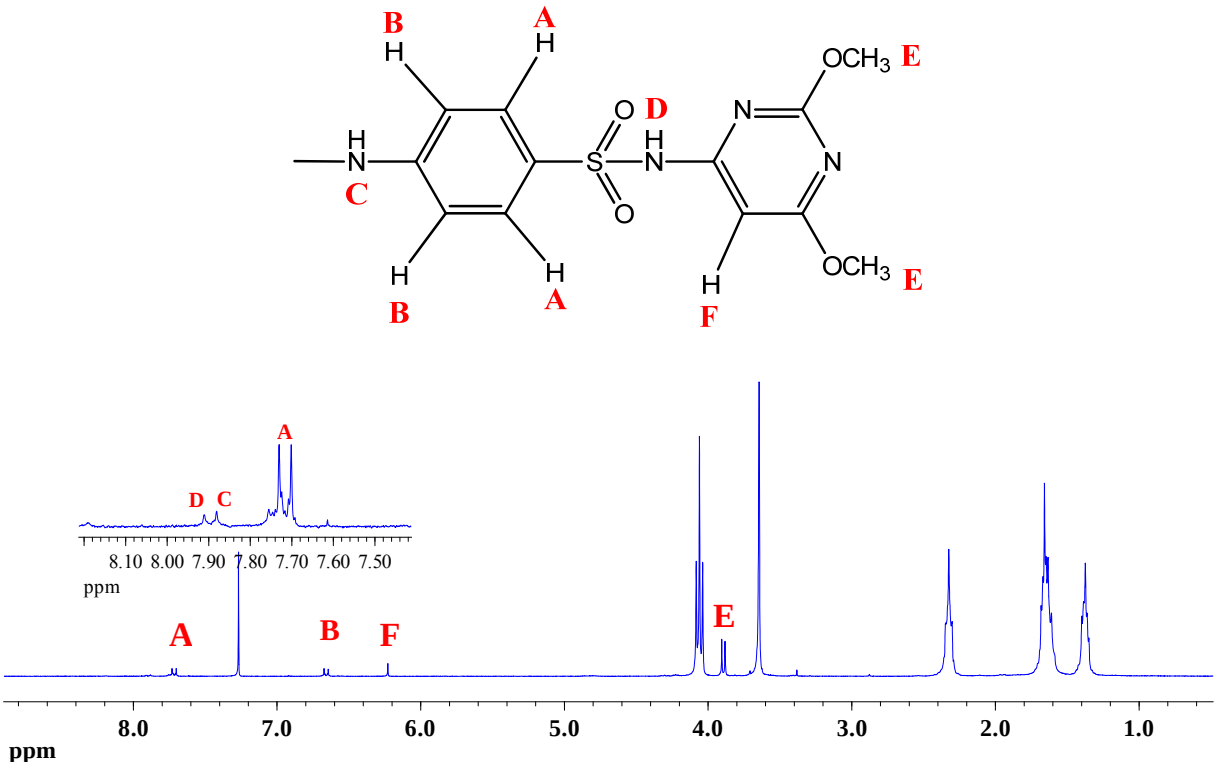

Figure 4.3a ^{1}HNMR of the SD-loaded PHA-b-MPEO5 (YA04, Table 4.1 run 3)

Peaks assignment was done with the aid of more than one reference [126,12 9] as well as the online Japanese data base (Spectral Database for Organic Compounds SDBS). From figure 4.3a,b the assignment is done without ambiguity for all protons as in SDBS, only N-H protons are shifted to less ppm depending on the surrounding environments. In the same connection and to provide full information about the mechanism of the reactions, GPC values are listed in table 4.2 including the virgin sample.

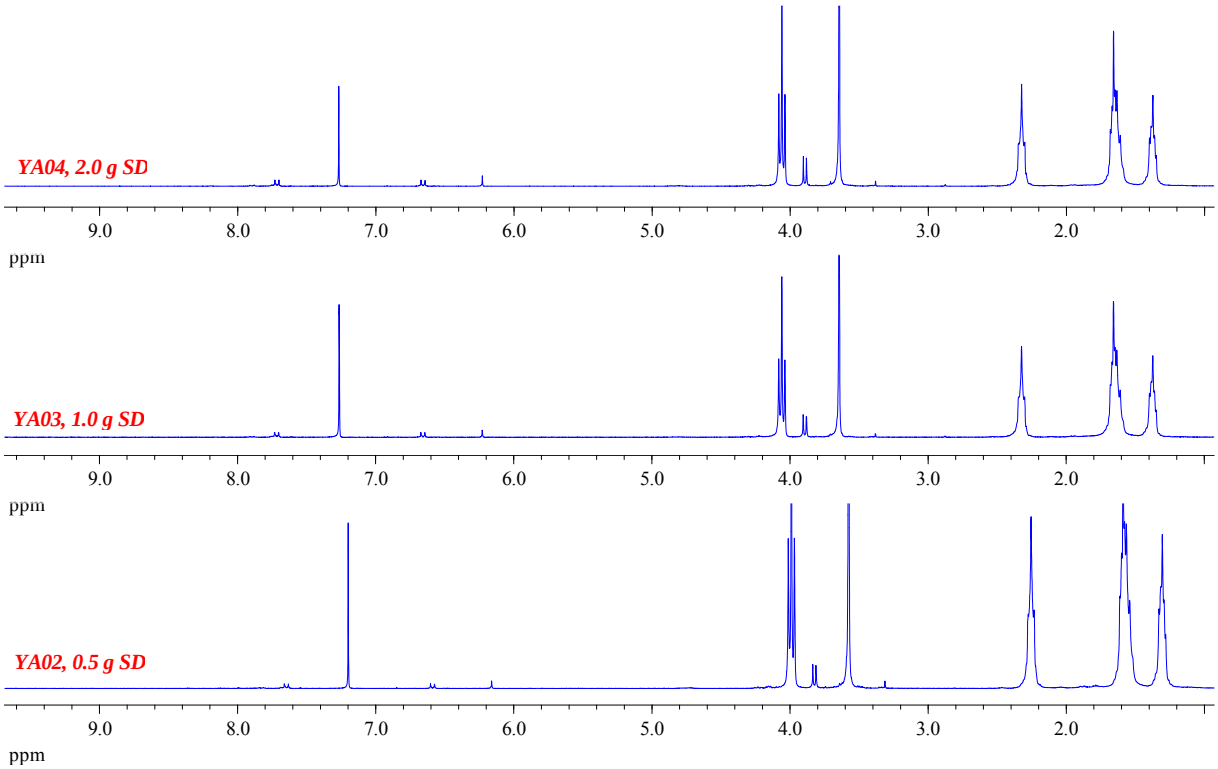

Figure 4.3b an overlay of ^{1}HNMR of the SD-loaded PHA-b-MPEO5 (YA02-YA04, Table 4.1)

Table 4.2 Molecular weights and PDI of SD-loaded PHA-b-MPEO5 as well as the virgin sample (YA00)

Run	SD conc, g	Mn	Mw	Mp	PDI
YA00	---	16000	31000	31000	1.96
YA01	---	12000	27000	15000	2.08
YA02	0.5	13000	27000	25000	2.10
YA03	1.0	11000	27000	25000	2.51
YA04	2.0	12000	26000	24000	2.12

Now I will start with NMR results. From the ^{1}HNMR, SD is actually loaded onto the polymer chains. At first I thought it is by transamidation, but as the NMR charts is exactly the same as the virgin one, and no change in the % of 1,6 hexandiol moieties or MPEO moiety, which thought to be replaced by the SD. Therefore transamidation direction is ruled out.

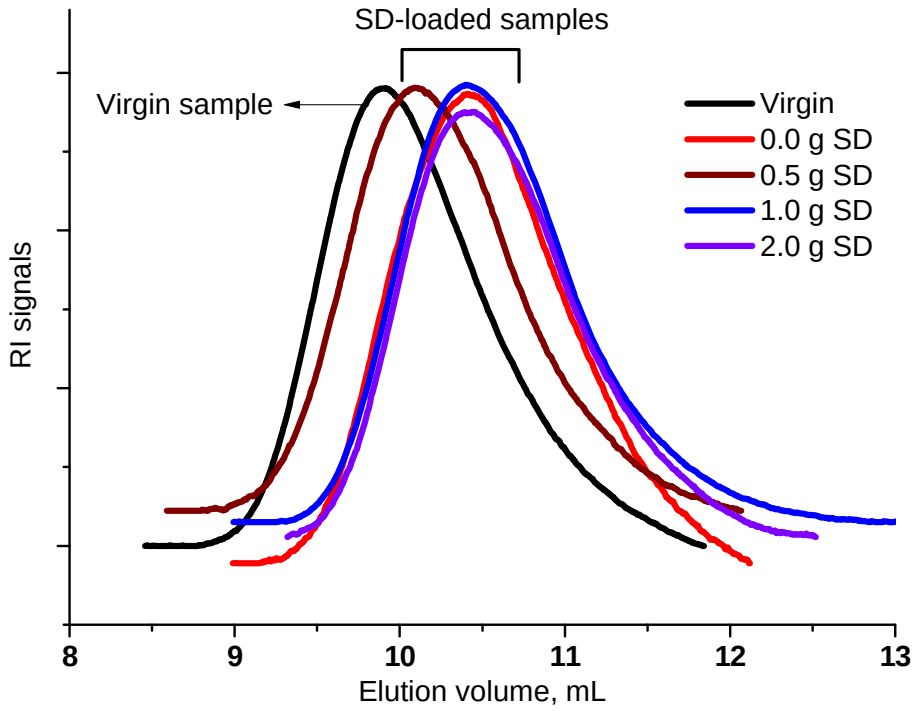

Figure 4.4 GPC elugrams of SD loaded PHA-b-MPEO5 in comparison with the virgin sample.

On the other hand the molecular weights values of the obtained products are less than the virgin sample which supports the transamidation mechanism. To see the effect of the reaction conditions on the neat polymer, one reaction is conducted under the same conditions in absence of SD (i.e. heating at 150 ^{o} C for 24h-YA01). It was found that the molecular weight of the obtained product is also reduced. This means the reaction conditions has negative impact on the polymer and a kind of degradation took place (Fig 4.4). Therefore during the heating at 150 ^{o}C, polymer starts to degrade leading to the increase in the chain end groups (OH and/or COOH) giving more chance for the coupling between these end groups and NH_2 of SD. Supporting this postulate is UV-Vis and IR analysis. The color of the SD loaded polymer is yellow and the intensity of the yellowish increased as the amount of SD used in the reaction increased (i.e. reaction of 2 g SD with 10 g polymer is more intensive yellow) because there is a large amount of SD that can react with and functionalize the OH/COOH chain end groups of the polymer (PHA-b-MPEO5). These findings are also confirmed by measuring the UV-Vis profile of the

SD-loaded polymer and compare it with the SD-free polymer as well as SD itself. A broad peak could be observed at wave length 280 nm in both SD-loaded polymer and SD itself with different intensities, while a base line of the SD-free polymer that lacks of any peak is obtained as shown in figure 4.5. This difference in yellow color could also be easily observed by human eye.

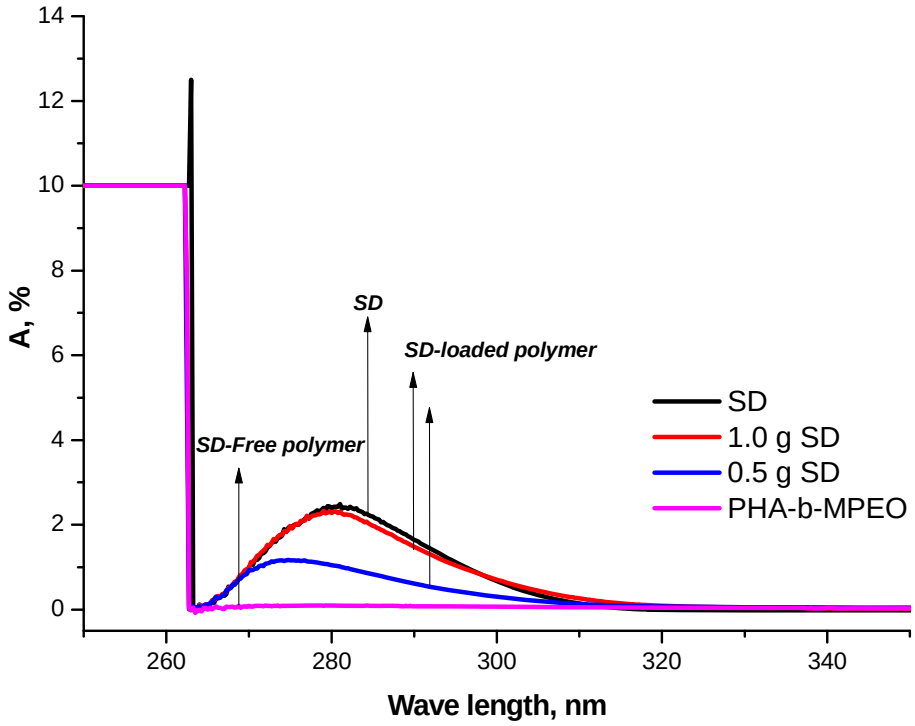

Figure 4.5 UV spectra of blank PHA-MPEO5, SD-loaded polymer and SD

IR charts of samples YA00 (virgin sample) YA01 (150°C/24h/ no SD) and YA03 (150°C/24h/ 1.0 g SD) are shown in figure 4.6. Point by point the IR charts will be analyzed. First of all a moderate to sharp peak appears at 1590 cm^{-1}. This peak does not exist in both the virgin and YA01 samples, thus it is for sure from the SD moiety in the polymer chains. By referring to an IR text book [130], this peak could be form N-H bending. In addition, at N-H and O-H stretching area (>3000 cm^{-1}), it was found that, in the virgin sample very less intensive peak is present (O-H stretch). This intensity is increased in case of YA01 sample (150°C/24h/ no SD) (O-H stretch,

more chain ends due to degradation). For the SD-loaded polymer two distinct peaks could be observed, first one is for O-H stretch in the same position as in SD-free polymer and the second is for N-H stretch, which support that the functionalization of the polymer chain end with SD is true.

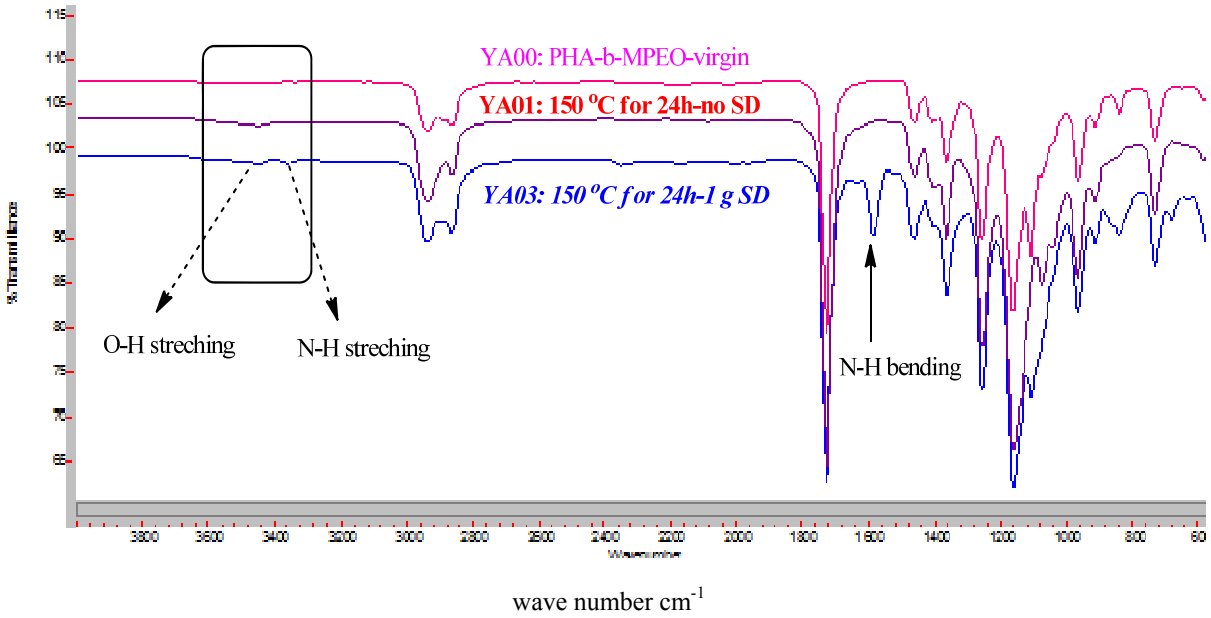

Figure 4.6 IR overlay image imported from win IR software of virgin sample YA00 (top), YA01 (middle) and (YA03, bottom). New absorbance band at 3360 cm^{-1}: N-H stretch, 1950 cm^{-1}: N-H bending could be easily observed.

In ***Exp2 and Exp3***, and in order to avoid the harsh reaction conditions in ***Exp1*** (150 °C for 24 h), the reaction was done in 100 mL THF for different time and temperatures. In ***Exp2*** the temperature was 100 °C and the reaction medium (10 g polymer, 1 g SD and 100 mL THF) was refluxed for 4 and 24 h. in ***Exp3*** the reaction was conducted at room temperature for 5 days. Molecular weights are represented in table 443, while NMR and GPC elugrams are shown in figures 4.7 and 4.8 respectively.

Table 4.3 Molecular weights and PDI of SD-loaded PHA-b-MPEO5 as well as the virgin sample

Run	SD wt.	Mn	Mw	Mp	PDI
YA00	---	16000	31000	31000	1.96
YA05	1.0	16000	32000	32000	2.25
YA06	1.0	15000	30000	31000	2.04
YA07	1.0	16000	31000	32000	1.97

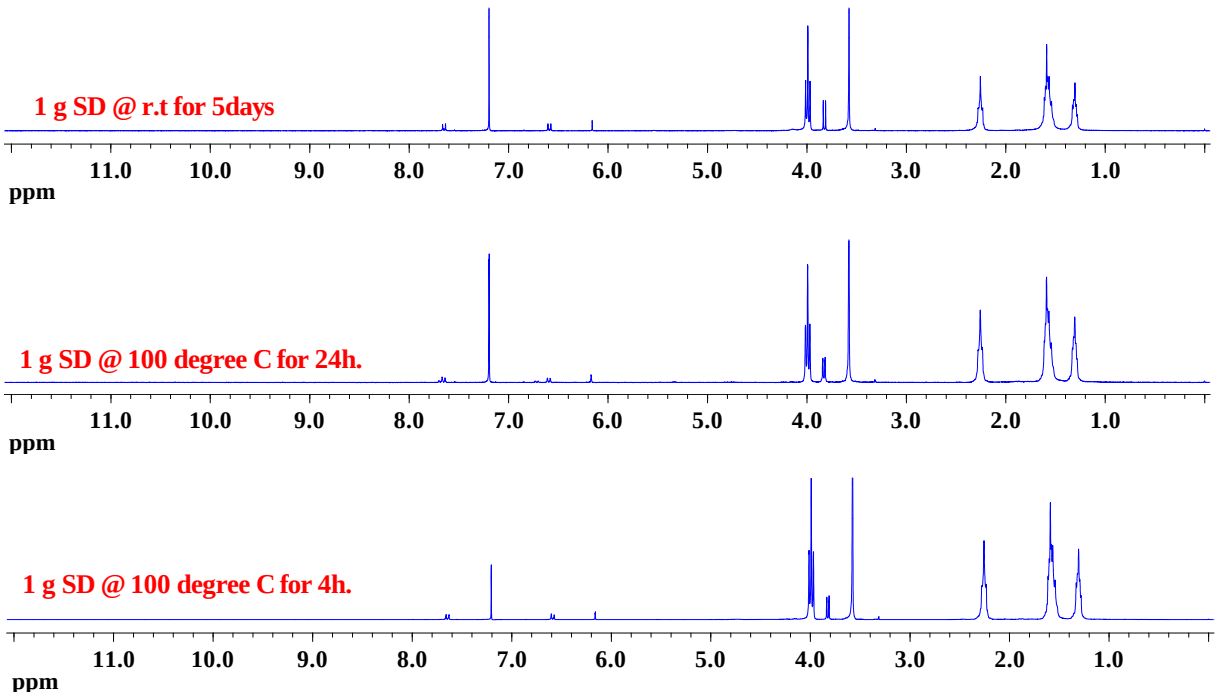

Figure 4.7 ^{1}HNMR of the SD-loaded PHA-b-MPEO5, reaction performed in THF for different times and temperatures.

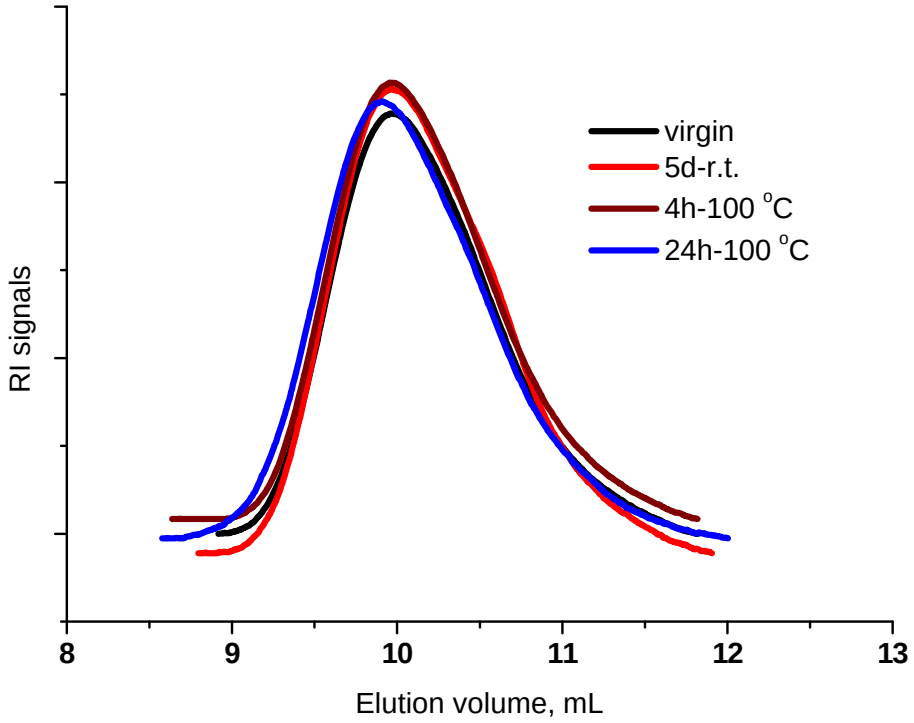

Figure 4.8 GPC elugrams of SD loaded PHA-b-MPEO in comparison with the virgin sample, prepared in THF at different times and temperatures.

In this run of experiments, the SD was successfully attached to the polymer as proven from NMR charts in figure 4.7. The produced polymers and the virgin sample both have the same molecular weight as shown in the GPC profile. All samples are eluted nearly at the same volume indicating similarities in molecular weight values as shown in figure 4.8. The degradation of the polymer during the reaction with SD was totally depressed. Therefore THF and lower temperature is more convenient to load SD onto the polymer chain.

4.5. P^H responsive polymer

pH-activity of the modified polymers was characterized by turbidity measurements. Therefore saturated polymer solution were prepared by dissolving 0.35 g of a polymer samples in phosphate buffer solution of pH 7.8 and lift to stir for 60 minutes at room temperature. The resultant turbid solution was filtered using GPC syringe filter of pore size 450 nm to remove non-soluble polymers. The resultant is a clear transparent yellowish polymer solution of pH 7.8. Transmittance was measured at different pHs, by monitoring the pH of the polymer solution by 30 %, 15 % HCl and 30 % NaOH using automatic micropipettes of size 1-10 µL. It is expected that in alkaline medium the polymer solution remains clear and the polymer is still soluble. By decreasing the pH of the solution, precipitation of the polymer starts and the solution becomes turbid leading to decrease in transmittance % as shown in figure 4.9. The turbidity of the solution is measured using PerkinElmer UV-VIS spectrophotometer at wave length 520 nm[128]. Figure 4.9 shows the solubility of the SD-loaded polymer in both alkaline and acidic medium, while figure 4.10 represents the transmittance-pH profile of different SD-loaded polymers.

Figure 4.9 Solubility of the SD-loaded polymer in both alkaline (pH 7.8, left) and acidic (pH 4.2, right) media (YA04, Table 4.2)

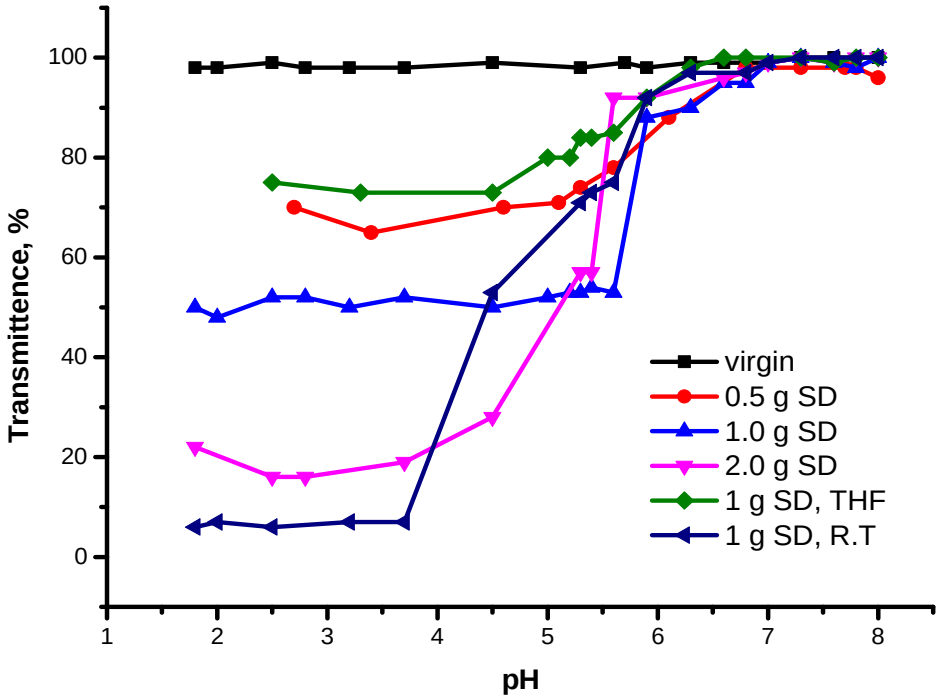

Figure 4.10 Transmittance-pH profile of SD-loaded PHA-b-MPEO5 under different conditions.

All loaded polymer show soluble-insoluble transition within pH range from 6.0 to 5.6 within narrow range of pH (0.4), which is close to the dissociation constant of pure SD (pKa 5.9, Clarke's Analysis of Drugs and Poisons). This little difference might be due to the presence of any free COOH that can contribute in the transition process. In contrast the blank sample (SD free) show stationary transmittance trend. Polymer sample that reacted at room temperature over a long time show the best transition. This means the saturated solution at pH 7.8 of this sample has larger amount of the polymer than the others, which upon precipitation in acidic pH range, it gives lower transmittance value, i.e. higher absorbance, which reflect a higher concentration. Therefore longer reaction time between SD and PHA-b-MPEO5 is required to functionalize most of the chain ends of the polymer. Also low temperature is preferred to avoid the degradation of the polymer.

4.5. Conclusion

1- Synthesis of pH responsive polymer form the prepared block copolymers was achieved by immobilizing a pH-responsive (Sulfadimethoxine, SD) moiety on the chain end of the PHA-b-MPEO5 of feed molar ratio 1:1. the structure was proven using NMR, IR and UV spectroscopy

2- Low temperature, longer reaction time and using proper solvent (THF) are required to obtain well-functionalized chain ends without sacrificing the polymer properties especially molecular weight.

3- High temperature in absence of solvents lead to polymer degradation

4- The SD-loaded polymer exhibit pH transition as proven by turbidity measurements and the pKa of the loaded polymers ranged from 5.6 to 6, which is close to the pKa of the SD itself (5.9).

Chapter 5

Amphiphilic properties

Determination of critical micelle concentration (cmc)

5.1. Introduction

The amphiphilic nature of the prepared polymers makes these polymers acting as a surfactant. Surfactants have a characteristic molecular structure having a group that has very little attraction for the solvent called the lyophobic group and another group which has a strong attraction for the solvent known as the lyophilic group. Thus a surfactants are amphiphilic in nature and when they present at low concentrations in a system, they have the ability of a) adsorbing onto the surface or interfaces of the system, b) altering the surface or interfacial free energy to a large extent. The term interface means the boundary between any two immiscible liquid phases. For example, when a surfactant is dissolved in an aqueous medium, the lyophobic group (hydrophobic group) breaks the hydrogen bonds between the water molecules and structures the water lying in the vicinity of the hydrophobic groups. As a result of this distortion, some of the surfactant molecules are expelled to the interface of the system with the hydrophobic groups oriented in such a way that they are away from the water molecules i.e. towards the air. Since the air molecules are non-polar in nature just like the hydrophobic groups, this decrease in the dissimilarity between two phases in contact with each other at the surface resulting in disruption of the cohesive energy at the surface and thus lower the surface tension. Hence, they are also known as surface active molecules. Surfactant molecules can arrange in the form of aggregates, in which the hydrophobic parts are oriented within clusters and the hydrophilic parts are exposed to the solvent. Such aggregates are called micelles. The amount of the surfactant molecules present at the surface or as micelles in the bulk of the liquid depends on the concentration of the surfactant. At low concentrations, the surfactant molecules prefer to arrange on the surface. As the concentration of the surfactant increases and the surface becomes loaded with the surfactant, more molecules will arrange as micelles. At a specific concentration, the surface becomes completely loaded and further addition of the surfactant molecules must arrange as micelles. This concentration is known as the ***critical micelle concentration (cmc)*** which can be determined

using surface tension measurements. Fluorescence measurement using a hydrophobic probe as Pyrene is also well established method for cmc determination as reported in the literatures since long time [131,132] as shown in figure 5.1.

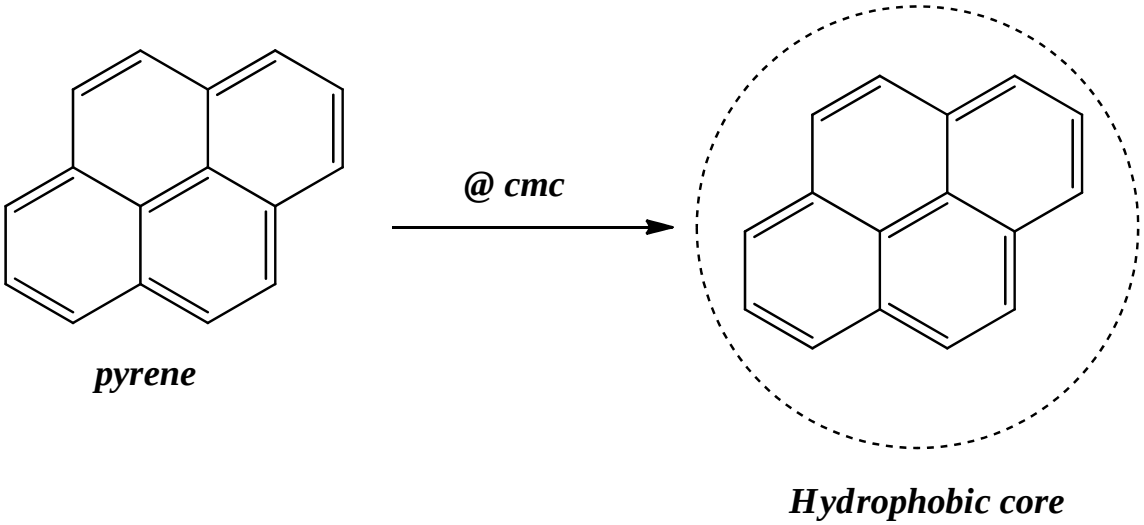

Figure 5.1 Representative diagram of trapped pyrene inside the formed micelles @ cmc

5.2. Concept

Determination of cmc using fluorescence depends upon the response of a probe or dye to the hydrophobicity and hydrophilicity of the medium. At cmc of a surfactant, the formed micelles having hydrophobic core can trap the hydrophobic probe, and then disturbing its fluorescence emission spectra. The most utilized probe is pyrene. Pyrene has five characteristics vibronic peaks in florescence emission spectra, taking the numbers I_1 to I_5 at wave lengths (373, 380, 383, 390, 396 nm respectively).[131] The intensity of these peaks in the florescence emission spectra is highly influenced by the type of the medium. The I_1/I_3 ratio is considered as an indicator of the hydrophobicity of the environment of pyrene and utilized generally to determine the cmc of an amphiphilic material.[131-136] A series of different concentration of a surfactant for example is prepared then plotted against I_1/I_3. This ratio always gives a stationary behavior before cmc and this behavior is revised after cmc. The concentration at the onset point of reversion is considered to be the cmc of the material. Therefore this chapter aimed to establish and reproduce the validity of this method for cmc determination of our polymers.

5.3. Experimental

Exp1. To see the behavior of pyrene in different polar solvents, 10^{-6} M of pyrene was prepared in solvents having different polarities then the Florescence emission spectra were recorded on Florescence spectrophotometer at excitation wave length of 225 nm as shown in figure 5.2.

Exp2. To evaluate the reliability of this method, it was tried with two common surfactants. One is non-ionic surfactants, namely, Polyethylene glycol hexadecyl ether, ***(Polyoxyethylene (10) cetyl ether) (new commercial name is Brij C10) and old commercial name is (Brij 56, the sample which I have in the Lab)***, with cmc value of 0.002 mM. The second one is the well-known anionic surfactant sodium dodecyl sulfate SDS (cmc = 8.27 mM). Therefore series of different concentrations before and after cmc were prepared from 10^{-6} pyrene solution and the fluorescence emission spectra were recorded at excitation wave length 330 nm. The stock solution of 10^{-06} M of pyrene was prepared, by first dissolving pyrene in DMSO to get 0.1 M solution, and then from this solution 10^{-06} M in water was papered by dilution as expressed in the literature.[135]

Exp3. For our polymers, sample PHA-b-MPEO5 with feed molar ratio 1:1 as well as samples of SD loaded polymers is also subjected to the fluorescence measurements. At first, different concentrations of these polymers were prepared in phosphate buffer (pH 7) containing 10^{-6} M pyrene, then the samples were excited at wave length 330 nm and the emission spectra was recorded then the I_1/I_3 ratio was plotted against the concentration.

5.4. Results and discussion

5.4.1. Fluorescence emission of Pyrene only

At first pyrene fluorescence was measured in different solvents, to see the effect of the hydrophobicity on the peak intensity of the pyrene. Figure 5.2 shows the emission spectra in water, methanol, ethanol, acetonitrile and hexane. It is clearly seen that the vibronic peak at 373 or 374 I_1 (both positions are used as stated in the literature) [131-136] is decreased as the solvent become more hydrophobic.

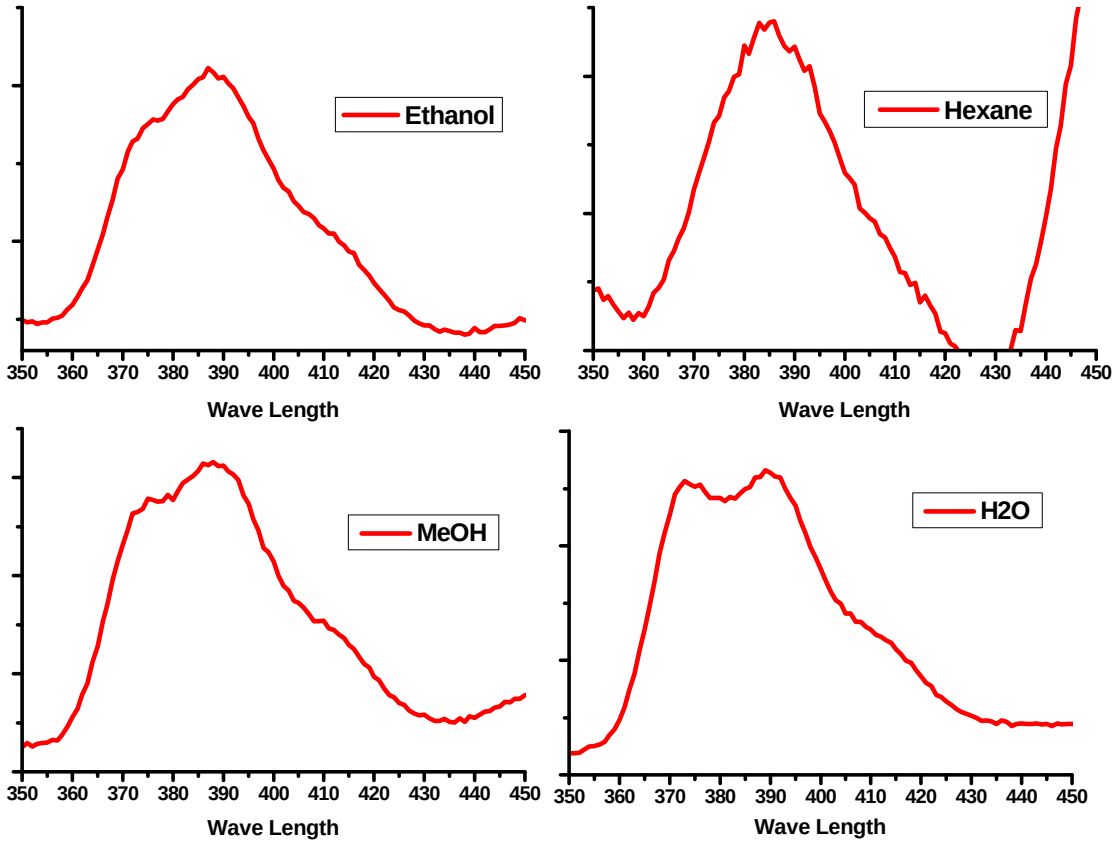

Figure 5.2 Fluorescence spectra of pyrene in different solvents, excitation wave length 225 nm; pyrene concentration is 10^{-6} M, Intensity of pyrene peaks are clearly influenced by the polarity of the solvents.

5.4.2. Fluorescence emission of Brij 56 and SDS

Figure 5.3 shows the whole fluorescence spectral profile of both Brij 56 and SDS of different concentrations, while figure 5.4 represents the plot of I_1/I_3 vs. concentration.

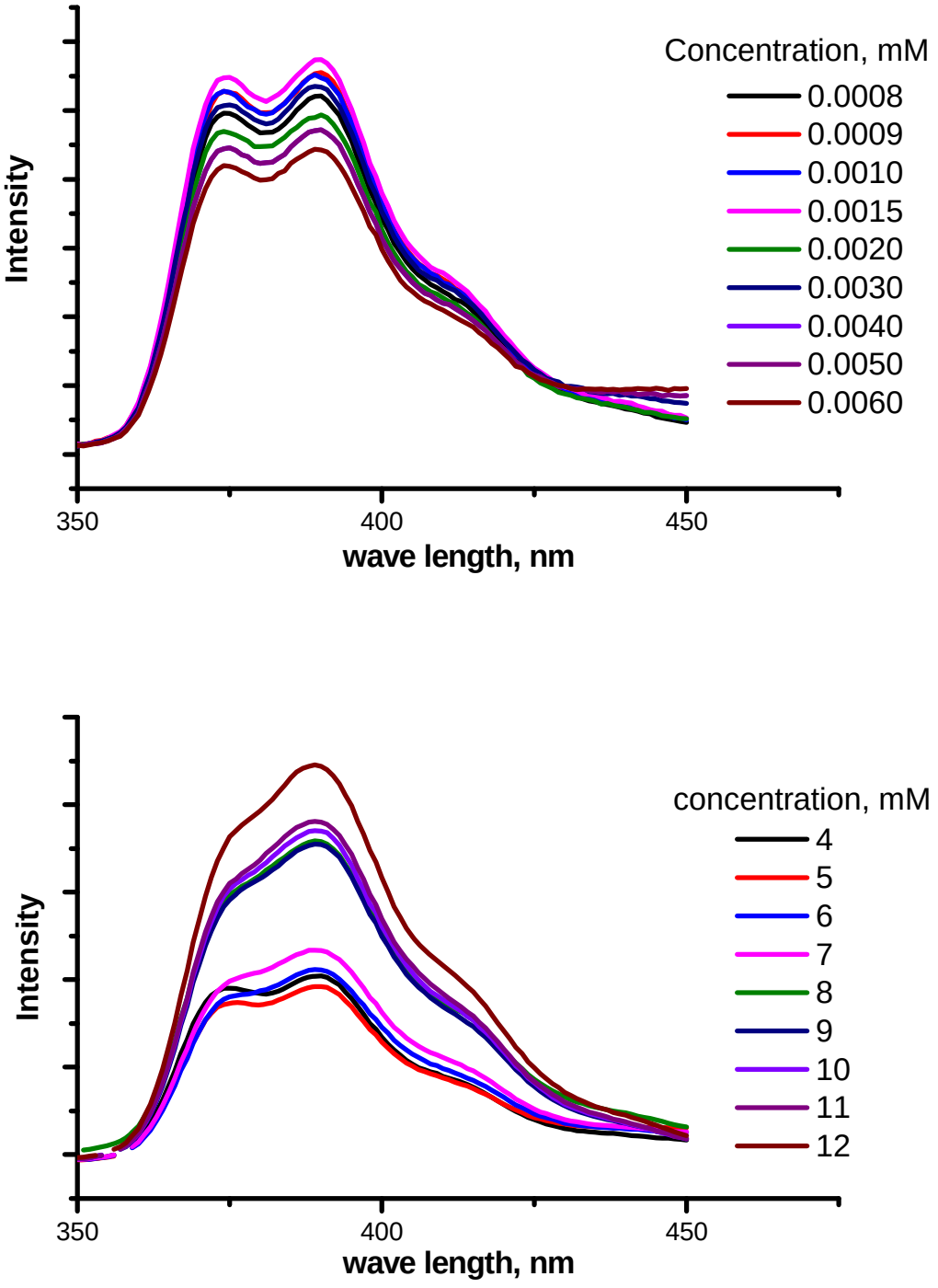

Figures 5.3 Whole fluorescence spectral profile of both Brij 56 (Top) and SDS (Bottom) of different concentrations.

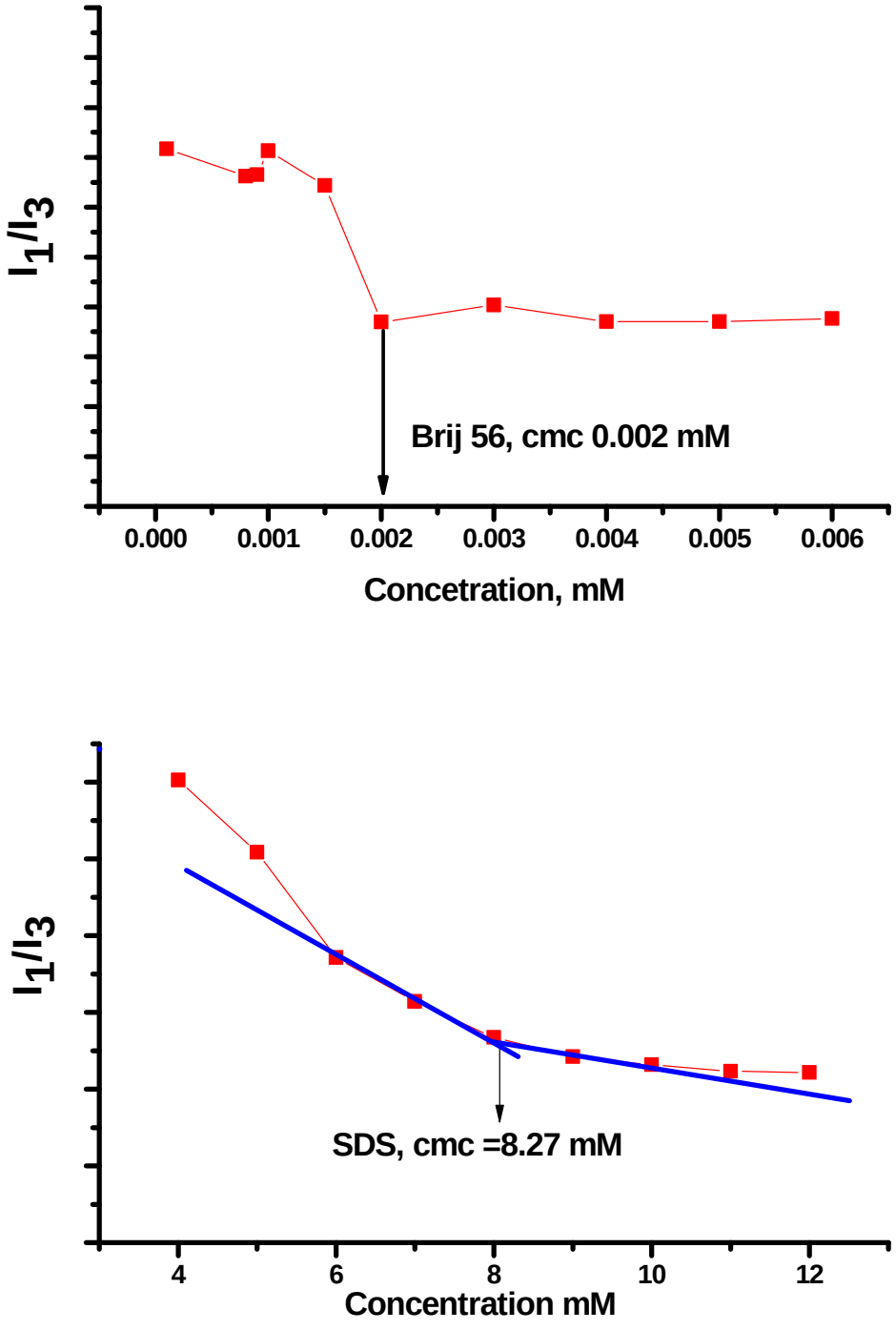

Figure 5.4. I_1/I_3 vs. concentration of Brij 56 (Top) and SDS (bottom).

The process of cmc determination using fluorescence-pyrene methods is very useful for low molecular weight surfactants. Values of the obtained cmc of both Brij 56 and SDS are exactly as mentioned in the literatures.[135,137]

5.4.3 Fluorescence emission of PHA-b-MPEO5

The nice results obtained in Brij and SDS fluorescence measurements encouraged me to investigate the PHA-b-MPEO5 drug free and drug loaded samples. Of course the process here will not be easy like the previous section, because, in case of Brij 56 and SDS, I already knew the cmc values and only accurate preparation of 4 concentrations before and after cmc, you will reach your target, but here in this case, of course it will not be ideal. To achieve this target two samples are chosen to undergo this investigation. These samples are PHA-b-MPEO5 (feed ratio 1:1) and the SD-loaded polymer that have been reacted with 0.5 g SD (YA02-Table 4.1). At first a long series of different concentrations of PHA-b-MPEO5 were prepared using the same procedures described previously. Pyrene concentration is also 10^{-6} M. Fluorescence spectra are shown in figure 5.5, while the I_1/I_3-concentration plot is shown in figure 5.6.

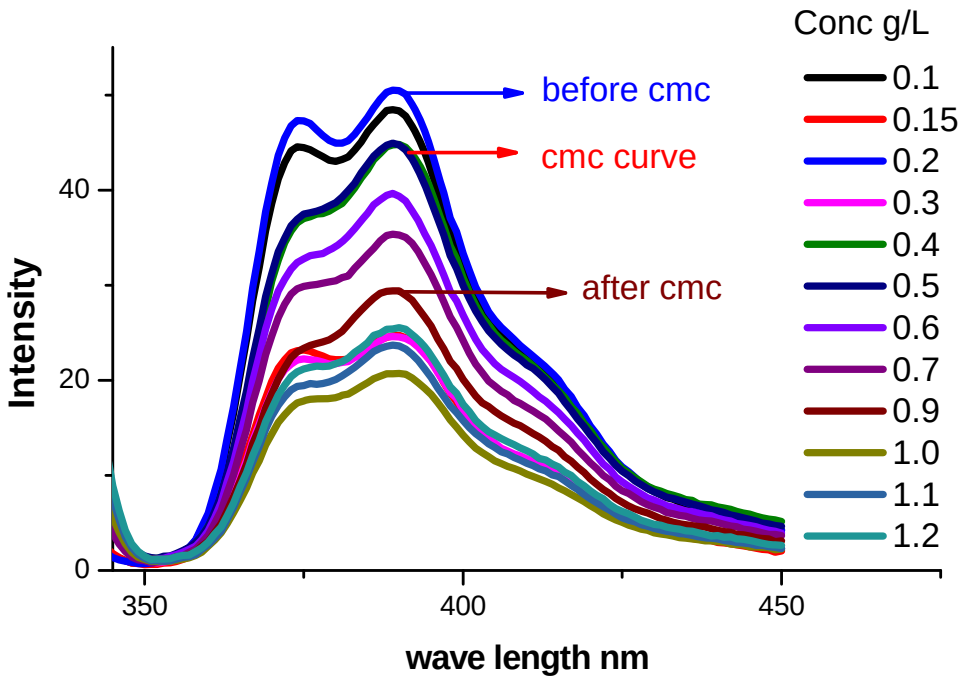

Figures 5.5 Fluorescence spectral profile of PHA-b-MPEO5 (1:1).

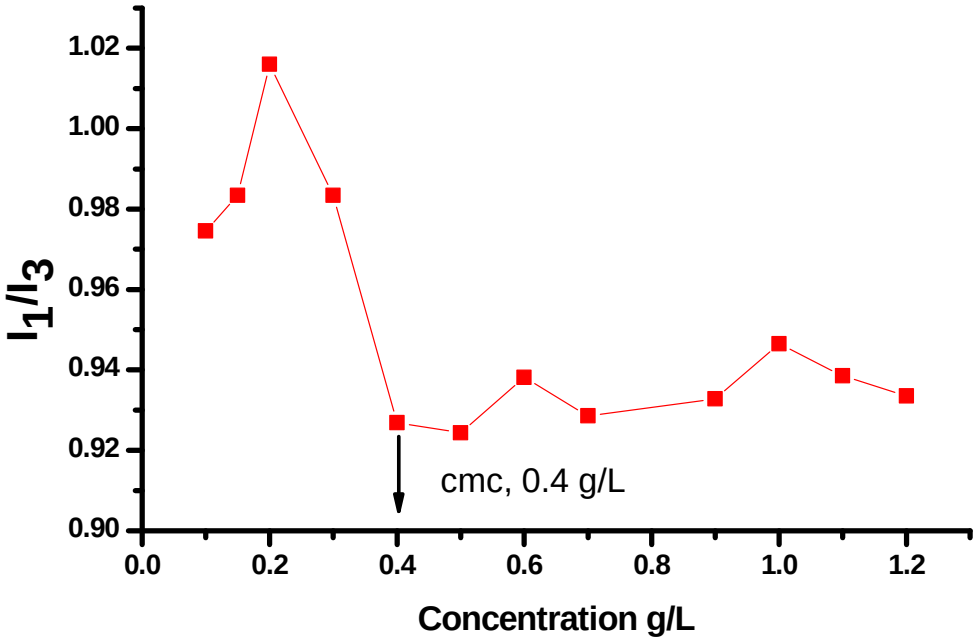

Figure 5.6. I_1/I_3 vs. concentration of PHA-b-MEO5 with feed ratio 1:1(Mn 16000)

From figure 5.6, it is clearly seen that concentration at 0.4 g/L has the dropping point after that the I_1/I_3 remains nearly unchanged as the concentration increased which represents the cmc of the PHA-b-MPEO, as also shown in figure 5.5 of the fluorescence curve, where the beginning of the steep of the curve occurs at the same concentration. For the drug loaded polymer the results are shown in figure 5.7, where the I_1/I_3 – concentration plot shows also the same trend that observed in the PHA-b-MPEO5. The dropping point occurs at concentration of 0.75g/L that represents the cmc value of this polymer, which differ from the value of SD-free polymer because both polymers have different molecular weights.

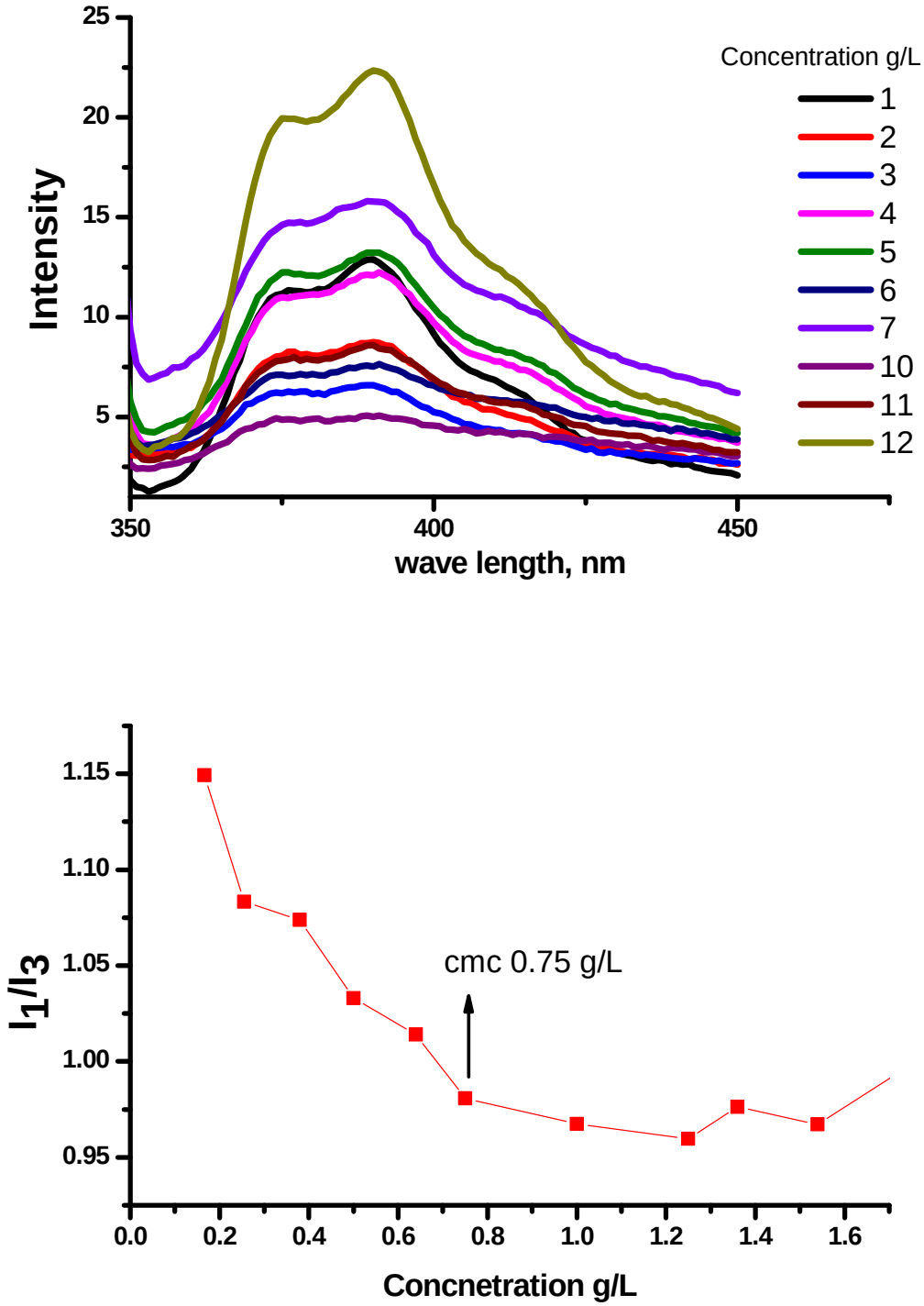

Figures 5.7 Fluorescence spectral profile of SD-loaded PHA-b-MPEO5 (Top) and I_1/I_3 vs. concentration plot (bottom).

5.5. Conclusion

1- Fluorescence spectroscopy using pyrene as a probe is an efficient method for the determination of cmc of different surfactants.

2- The obtained values of cmc of the commercial surfactants SDS and Brij 56 by Fluorescence techniques are matching with the values reported in the literatures obtained by other methods such as surface tension measurements.

3- Values of cmc of PHA-b-MPEO5, SD-free and SD-loaded polymer could also obtained by the same method and the cmc values of SD-free polymer and SD-loaded polymer are 0.4 and 0.75 g/L respectively. The difference in these values is because both polymers have different molecular weights.

Chapter 6

Experimental Part

6.1. Materials

1,4 butandiol	Merck , Distilled before use (160^{o}C-under vacuum)
1,6 hexandiol	Merck , Distilled before use (160^{o}C-under vacuum)
Adipic acid	Merck, used as received
Succinic acid	Merck, used as received
Methoxypolyethylene oxide (Mn 5000)	Sigma-Aldrich, used as received
Methoxypolyethylene oxide (Mn 2000)	Sigma-Aldrich, used as received
Titanium IV-Butoxide	Sigma-Aldrich, used as received
Polyphosphoric acid	Sigma-Aldrich, used as received
Sulfadimethoxine (4-amino-N-(2,6-dimethoxypyrimidin-4-yl) benzenesulfonamide)	Sigma-Aldrich, used as received
Pyrene	Sigma-Aldrich, used as received
Sodium hydroxide	Grüssing – Germany, Local Market
Potassium hydroxide	Grüssing – Germany, Local Market
HCl, 37 %	Grüssing – Germany, Local Market
Organic solvents (Acetone, THF, Choroform,..	BASF, distilled before use
Lipase from pseudomonas cepacia Enzyme	Sigma-Aldrich
SDS	Sigma-Aldrich
Brij 56	Sigma-Aldrich

6.2. Instrumentation and characterization

6.2.1. Gel permeation chromatography (GPC)

The molecular weights of all polymers were measured by Chloroform GPC at 25°C. Sample concentration was 1 g L^{-1}. The apparatus consists of a Gynkotek HPLC pump, a Agilent Autosampler 1200, linear columns (PSS, polystyrene) consisting of a pre-column 10 µ, 8 x 50 mm, a column 10 Å, 8 x 300 mm and two columns 3000 Å, 8 x 300 mm. As detector, RI detector of Knauer Company was used. As calibration, linear PMMA with a narrow mass distribution and molecular weight between 500 and 1,000,000 was used. Toluene was used as an internal standard. The elugram was evaluated with PSS WinGPC Unity program.

6.2.2. Nuclear magnetic resonance spectroscopy (NMR)

1D and 2D NMR measurements were done in the NMR Department at the Philipps Universität Marburg. ^{1}H (400.13 MHz) and ^{13}C (100.21 MHz)-NMR spectra were recorded on a Bruker DRX-300 spectrometer using Tetramethylsilane (TMS) as an internal standard. ^{1}H-^{13}C NMR correlation experiments were performed on a Bruker DRX-500 spectrometer, with typical experiment time was about 1.5 and 3.0 h for HMQC and HMBC, respectively.

6.2.3. Infrared spectroscopy (FTIR)

The IR spectra were measured on a FT-IR spectrometer of type Excalibur Series with an attached IR microscope of the type UMA 600 from Digilab. Infrared spectroscopy (IR) was performed by means of Digilab (Excalibur series) instrument with ATR crystal ZnSe and WinIRPro software version 3.3.

6.2.4. UV-Vis spectroscopy

All UV-Vis spectra of the SD-loaded polymers were measured by UV-Vis spectrometer of the type Lambda 9 of the company Perkin Elmer, which was operated by the software Lambda SPX. For the measurement, two quartz cuvettes (Perkin Elmer) were used with 2 mL capacity. The spectra were evaluated and analyzed by the software Lambda SPX. The scan range is from 400 to 200 nm with scanning rate 420nm/min using the scan mode of the instrument.

6.2.5. Turbidity measurement

The same UV-Vis spectrometer was used to evaluate the pH-dependence of the SD-loaded polymer by measuring the transmittance at different pHs at wave length 520 nm using fixed mode of the instrument.

6.2.6. Fluorescence measurement

Fluorescence emission spectra were measured using spectrophotometer xxx. Excitation wave length is 330 nm and scanning range was from 200 to 450 nm using low sensitivity low with super scan velocity.

6.2.7. Wide Angle X-ray Diffraction (WAXD)

The materials were examined by X-ray powder diffraction (X'Pert MPD x-ray powder diffractometer (Philips)) operating in Bragg–Brentano geometry with Cu-Ka radiation. The diffractometer was equipped with a graphite monochromator at the detector side. The sample holder was a single-crystal silicon plate. The patterns were collected in a continuous scan mode in the range $10^{o} \leq 15$ min. $\leq 100^{o}$.

6.2.8. Thermal Gravimetric Analysis (TGA)

Thermal gravimetric analysis was done by using Mettler thermal analyzers having 851 thermogravimetric modules. Thermal stability was determined by recording TGA traces in nitrogen atmosphere (flow rate = 50 mL min^{-1}). A heating rate of 10°C min-1 and a sample size of 10-12 mg was used in each experiment. The samples were heated from room temperature to 800 °C at a heating rate of 10 °C/min.

6.2.9 Differential scanning calorimetry (DSC)

Mettler Thermal Analyzer having 821 DSC module was used for thermal analysis of the polymers. DSC scans were recorded in nitrogen atmosphere (flow rate = 80 ml min^{-1}). DSC measurement conditions were varied depending on the type of the polymers. For PHA-b-MPEO5/2 i.e. adipate based polymers the endothermic/exothermic cycles were as follow, the

samples were heated in the first heating cycle from –100 ^{o}C to 100 ^{o}C at a heating rate 20 ^{o}C/min. The samples were cooled again to –100 ^{o}C with cooling rate -20 ^{o}C/min and again heated in the second heating cycle till 100 ^{o}C. In case of remaining polymers the heating cycles were as follow; the first heating cycle from –150 ^{o}C to 150 ^{o}C at a heating rate 20 ^{o}C/min. The samples were cooled again to –150 ^{o}C with a cooling rate -20 ^{o}C/min and again heated in the second heating cycle till 150 ^{o}C.

6.2.10. Film and Slab formation

Films and slabs of polymer samples were prepared using a compression molding machine. About 20 g of polymer were spread on a steel sheet, and then heated under compressing form 5 min., then left to cool down using inlet-outlet water circle. Compressing temperature for succinate based polymers was 150 ^{o}C, for remaining polymers, was 80 ^{o}C

6.2.11. Mechanical properties

The tensile strength of the samples was measured using Zwick/Roell Materials Testing machine (Type: KAF-TC). The samples were cut in the shape of a bone with a total length of 20 mm. It was then mounted directly onto the clamps having a grip to grip separation of 16 mm at the start position. The software used was testXpert II. The values for the diameter of each sample were fed before the measurement began. The curves for stress versus strain were recorded. Each measurement was repeated 5 times and an average value was calculated automatically by the software.

6.2.12. Electron microscopy

The SEM images were obtained using Scanning electron microscopy (SEM) (CamScan Series 4, Cambridge Scanning Company Limited). The films were coated with gold in an Edwards Auto 306 sputter-coater at $< 5 \times 10^{-5}$ mbars.

6.3. Methodology

6.3.1. Polymer synthesis

A typical experiment of synthesis of PHA-b-MPEO5 1:1 molar ratio is as follow: 249 g (1.7 mol), of Adipic acid, 201 g (1.7 mol) of 1,6 hexandiol and 75 g (1.7 mol) of MPEO5 were mixed together in a pre-evacuated 1 L N_2-Flask under argon, then 0.05 mol % of titanium IV-butoxide was added via 1mL syringe. Under N_2 the system was connected to condenser that ended with graduated schlenk tube and placed in oil bath at 190 ^oC. Reaction continued under N_2 until no more water was repelled out. At this point 0.1g % of Polyphosphoric acid was added via 1 mL syringe. After one hour the temperature was increased to 210 ^oC, then one hour later it was increased to 230 ^oC. Another hour later, N_2 was removed and vacuum (0.4 mbar) was applied and the reaction left to run for 35 hours. After that the obtained viscous polymer is left to cool down (better not to wait until solidification, otherwise it takes longer time and more solvent to be dissolved again). The collected polymer was dissolved in THF or chloroform and precipitated in n-Hexane or n-pentane. Pentane is preferred for best and fast drying. Figure 6.1 represents a sketch of the polycondensation system. Table 6.1 shows the data of synthesis of the all polymers using the same procedures.

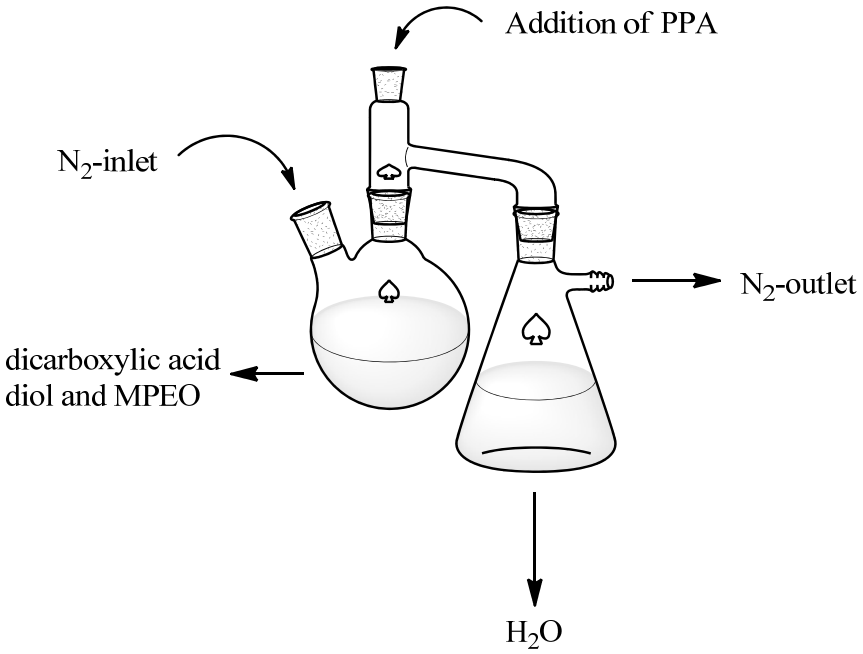

Figure 6.1 a sketch of the polycondensation system

Feed molar of, diol and dicarboxylic acid was kept always 1:1 in all experiments. Catalyst concentration was kept 0.05 mol % with respect to the molar concentration of used dicarboxylic. PPA is also kept constant and represented by weight. It is used in 0.1 % with respect to the used dicarboxylic.

Table 6.1 Feed amounts, yield and conversions of the prepared block copolymers and the sample numbers as expressed in the lab Journal.

Sample	MPEO, g	Adipic acid, g	1,6 Hexandiol, g	MPEO/Adipate	Yield g	Conv. %
			PHA-b-MPEO5			
20100802YA1	68.4	57.0	46.0	¼:1	143	83
20100806YA1	34.2	57.0	46.0	½:1	120	87
20100901YA1	75.0	249	201	1:1	446	85
20100811YA1	8.6	57.0	46.0	2:1	115	88
20100825YA1	8.6	114	92.0	4:1	185	86
			PHA-b-MPEO2			
20100906YA1	101.6	84.5	68.4	¼:1	210	83
20100804YA1	34.2	57	46.0	½:1	116	85
20100729YA1	34.2	114	92.0	1:1	217	90
20100813YA1	13.84	92.1	74.5	2:1	160	88
20100827YA1	8.60	114	92.0	4:1	200	93
	---	100	81.0	PHA-Homo	155	86

Table 6.1 continued

Sample	MPEO, g	Succinic acid, g	Butandiol, g	MPEO/Suc	Yield g	Conv. %
PBS-b-MPEO5						
20101119YA1	18.9	201	153.9	¼:1	340	90
20101111YA1	37.2	200	152.6	½:1	350	90
20101025YA1	37.2	100	76.3	1:1	190	89
20101122YA1	141	190	145	2:1	390	82
20101123YA1	149	100	76.3	4:1	260	80
20101117YA1	---	119.3	90.1	PBS-Homo	170	81
Sample	MPEO, g	Adipic acid, g	Butandiol, g	MPEO/Suc	Yield g	Conv. %
PBA-b-MPEO5						
20110524YA1	19	63.5	40	1:1	98	80
Sample	MPEO, g	Succinic acid, g	Hexandiol, g	MPEO/Suc	Yield g	Conv. %
PHS-b-MPEO5						
20110302YA2	19	50	50	1:1	100	85

6.3.2. Hydrolytic degradation

Hydrolytic degradability was tested in extreme basic conditions. Generally, 200 mg of the copolymer was dissolved in a bottle containing 20 ml of 5% or 10% KOH aqueous solution and was stirred for different times at room temperature. After this, solution was neutralized using 10% HCl. The mixture was extracted with chloroform, washed with water, and dried over sodium sulfate. After filtration, the solvent was evaporated under reduced pressure. The remaining solid was dried in a vacuum oven at 40 ^{o}C and analyzed by NMR and GPC.

6.3.3. Enzymatic degradation

Enzyme-catalyzed degradation of the block copolymers was performed using lipase from *pseudomonas cepacia* enzyme (Sigma). At first slabs with dimension 5 x 5 x 0.5 mm from the polymers were cut from polymers films that made by hot compression method. These slabs were immersed in phosphate buffer solution (pH 7) containing the enzyme to give a final concentration of 18.5 mg enzyme/ mL and 16 mg polymer / mL in 10 mL vials. In all experiment a blank sample was always accompanied. Sodium azide of concentration 18.5 mg/mL was also added to prevent fermentation/bacterial growth of the enzyme solution. Samples with 1:1 molar ration were tested. The vials containing buffer solutions, polymers and enzyme was incubated at 37 ^{o}C with shaking speed 50 RPM. At pre-determined times, vials were removed from the incubator, and then filtered and the residual films were dried at 30 ^{o}C for 4 days, and then subjected to NMR, GPC and SEM analysis.

References

1. Coulembier, O.; Degee, P.; Hedrick, J. L.; Dubois, P. From controlled ring-opening polymerization to biodegradable aliphatic polyester: Especially poly([beta]-malic acid) derivatives. *Progress in Polymer Science* **2006,** *31* (8), 723-747.

2. Bastioli, C. *Handbook of biodegradable polymers;* **Rapra Technology Limited**: 2005.

3. Kashiwagi, T.; Hirata, T.; Brown, J. E. Thermal and oxidative degradation of poly-(methyl methacrylate) molecular weight. *Macromolecules* **1985,** *18* (2), 131-138.

4. Peterson, J. D.; Vyazovkin, S.; Wight, C. A. Kinetic Study of Stabilizing Effect of Oxygen on Thermal Degradation of Poly(methyl methacrylate). *The Journal of Physical Chemistry B* **1999,** *103* (38), 8087-8092.

5. Booth, C. The mechanical degradation of polymers. *Polymer* **1963,** *4*, 471-478.

6. GUILLET, J. E.; DHANRAJ, J.; GOLEMBA, F. J.; HARTLEY, G. H. Fundamental Processes in the Photodegradation of Polymers. In *Stabilization of Polymers and Stabilizer Processes*, 85 ed.; AMERICAN CHEMICAL SOCIETY: 1968; pp 272-286.

7. Chalmers, J. M.; Meier, R. J. Polymer Degradation and Oxidation: An Introduction. In *Comprehensive Analytical Chemistry; Molecular Characterization and Analysis of Polymers*, Volume 53 ed.; John, M. C. a. R., Ed.; Elsevier: 2008; pp 387-450.

8. Rychl, J.; Matisovβ-Rychlβ, L. The Role of Oxidation in Degradation of Polymers: The Relation of Oxidation to the Light Emission from Oxidized Polymers. In *Comprehensive Analytical Chemistry; Molecular Characterization and Analysis of Polymers*, Volume 53 ed.; John, M. C. a. R., Ed.; Elsevier: 2008; pp 451-498.

9. Schlick, S.; Kruczala, K. Chapter 12 ESR and ESR Imaging Methods for the Study of Oxidative Polymer Degradation. In *Comprehensive Analytical Chemistry Molecular Characterization and Analysis of Polymers*, Volume 53 ed.; John, M. C. a. R., Ed.; Elsevier: 2008; pp 499-524.

10. Konaganti, V. K.; Madras, G. Ultrasonic degradation of poly(methyl methacrylate-co-alkyl acrylate) copolymers. *Ultrasonics Sonochemistry* **2010,** *17* (2), 403-408.

11. HILL, D. J. T.; O'DONNELL, J. H.; POMERY, P. J. Fundamental Aspects of Polymer Degradation by High-Energy Radiation. In *Materials for Microlithography*, 266 ed.; American Chemical Society: 1985; pp 125-149.

12. Sabino, M. A.; Sabater, L.; Ronca, G.; Müller, A. J. The effect of hydrolytic degradation on the tensile properties of neat and reinforced Poly(p-dioxanone). *Polymer Bulletin* **2002,** *48* (3), 291-298.

13. Nagata, M.; Kiyotsukuri, T.; Ibuki, H.; Tsutsumi, N.; Sakai, W. Synthesis and enzymatic degradation of regular network aliphatic polyesters. *Reactive and Functional Polymers* **1996,** *30* (1-3), 165-171.

14. Edlund, U.; Albertsson, A. Degradable Polymer Microspheres for Controlled Drug Delivery. In *Degradable Aliphatic Polyesters*, 157 ed.; Springer Berlin / Heidelberg: 2002; pp 67-112.

15. Watanabe, J.; Kotera, H.; Akashi, M. Reflexive Interfaces of Poly(trimethylene carbonate)-Based Polymers:Γ_ë Enzymatic Degradation and Selective Adsorption. *Macromolecules* **2007,** *40* (24), 8731-8736.

16. Erdmann, L.; Macedo, B.; Uhrich, K. E. Degradable poly(anhydride ester) implants: effects of localized salicylic acid release on bone. *Biomaterials* **2000,** *21* (24), 2507-2512.

17. Erdmann, L.; Uhrich, K. E. Synthesis and degradation characteristics of salicylic acid-derived poly(anhydride-esters). *Biomaterials* **2000,** *21* (19), 1941-1946.

18. Witt, U.; Einig, T.; Yamamoto, M.; Kleeberg, I.; Deckwer, W.-D.; Müller, R.-J. Biodegradation of aliphatic-aromatic copolyesters: evaluation of the final biodegradability and ecotoxicological impact of degradation intermediates. *Chemosphere* **2001,** *44* (2), 289-299.

19. Müller, R. J. Biodegradability of Polymers: Regulations and Methods for Testing. In *Biopolymers Online*, Wiley-VCH Verlag GmbH & Co. KGaA: 2005.

20. Amass, W.; Amass, A.; Tighe, B. A review of biodegradable polymers: uses, current developments in the synthesis and characterization of biodegradable polyesters, blends of biodegradable polymers and recent advances in biodegradation studies. *Polym. Int.* **1998,** *47* (2), 89-144.

21. Zhang, S. J.; Yu, H. Q.; Ge, X. W.; Zhu, R. F. Optimization of Radiolytic Degradation of Poly(vinyl alcohol). *Industrial & Engineering Chemistry Research* **2005,** *44* (7), 1995-2001.

22. Watanabe, M.; Kawai, F. Numerical simulation for enzymatic degradation of poly(vinyl alcohol). *Polymer Degradation and Stability* **2003,** *81* (3), 393-399.

23. Baimuratov, E.; Saidov, D. S.; Kalontarov, I. Y. Thermal, photo and [gamma]-radiation degradation of mechanically loaded poly(vinyl alcohol) (PVA). *Polymer Degradation and Stability* **1993,** *39* (1), 35-39.

24. Park, H.; Pearce, E. M.; Kwei, T. K. Thermal oxidation of blends of polystyrene and poly(vinyl methyl ether). *Macromolecules* **1990,** *23* (2), 434-441.

25. Chien, Y. Y.; Pearce, E. M.; Kwei, T. K. Photooxidation of blends of polystyrene and poly (vinyl methyl ether). *J. Polym. Sci. A Polym. Chem.* **1991,** *29* (6), 849-856.

26. Mailhot, B.; Morel, S.; Gardette, J. L. Photochemical behaviour of poly(vinylmethylether). *Polymer Degradation and Stability* **1998,** *62* (1), 117-126.

27. Burkersroda, F. v.; Schedl, L.; Göpferich, A. Why degradable polymers undergo surface erosion or bulk erosion. *Biomaterials* **2002,** *23* (21), 4221-4231.

28. A-N Clarinval Classification of biodegradable polymers. In *Biodegradable polymers for industrial applications*, Woodhead Publishing Limited: 2005; p 3.

29. Ikada, Y.; Tsuji, H. Biodegradable polyesters for medical and ecological applications. *Macromol. Rapid Commun.* **2000,** *21* (3), 117-132.

30. Mochizuki, M.; Hirami, M. Structural Effects on the Biodegradation of Aliphatic Polyesters. *Polym. Adv. Technol.* **1997,** *8* (4), 203-209.

31. Edlund, U.; Albertsson, A.-C. Polyesters based on diacid monomers. *Advanced Drug Delivery Reviews* **2003,** *55* (4), 585-609.

32. Löfgren, A.; Albertsson, A. C.; Dubois, P.; Jerome, R. Recent Advances in Ring-Opening Polymerization of Lactones and Related Compounds. *Journal of Macromolecular Science, Part C: Polymer Reviews* **1995,** *35* (3), 379-418.

33. Endo, T. General Mechanisms in Ring-Opening Polymerization. In *Handbook of Ring-Opening Polymerization*, Wiley-VCH Verlag GmbH & Co. KGaA: 2009; pp 53-63.

34. Buchmeiser, M. R. Ring-Opening Metathesis Polymerization. In *Handbook of Ring-Opening Polymerization*, Wiley-VCH Verlag GmbH & Co. KGaA: 2009; pp 197-225.

35. Coulembier, O.; Dubois, P. Polyesters from Β-Lactones. In *Handbook of Ring-Opening Polymerization*, Wiley-VCH Verlag GmbH & Co. KGaA: 2009; pp 227-254.

36. Dechy-Cabaret, O.; Martin-Vaca, B.; Bourissou, D. Polyesters from Dilactones. In *Handbook of Ring-Opening Polymerization*, Wiley-VCH Verlag GmbH & Co. KGaA: 2009; pp 255-286.

37. Albertsson, A. C.; Varma, I. K.; Srivastava, R. K. Polyesters from Large Lactones. In *Handbook of Ring-Opening Polymerization*, Wiley-VCH Verlag GmbH & Co. KGaA: 2009; pp 287-306.

38. Kobayashi, S.; Uyama, H.; Kimura, S. Enzymatic Polymerization. *Chemical Reviews* **2001,** *101* (12), 3793-3818.

39. Gross, R. A.; Kumar, A.; Kalra, B. Polymer Synthesis by In Vitro Enzyme Catalysis. *Chemical Reviews* **2001,** *101* (7), 2097-2124.

40. Kobayashi, S.; Makino, A. Enzymatic Polymer Synthesis: An Opportunity for Green Polymer Chemistry. *Chemical Reviews* **2009,** *109* (11), 5288-5353.

41. Srivastava, R. K.; Albertsson, A. C. Porous Scaffolds from High Molecular Weight Polyesters Synthesized via Enzyme-Catalyzed Ring-Opening Polymerization. *Biomacromolecules* **2006,** *7* (9), 2531-2538.

42. Jiang, Z.; Azim, H.; Gross, R. A.; Focarete, M. L.; Scandola, M. Lipase-Catalyzed Copolymerization of ω-Pentadecalactone with p-Dioxanone and Characterization of Copolymer Thermal and Crystalline Properties. *Biomacromolecules* **2007,** *8* (7), 2262-2269.

43. Srivastava, R. K.; Albertsson, A. C. Microblock Copolymers as a Result of Transesterification Catalyzing Behavior of Lipase CA in Sequential ROP. *Macromolecules* **2007,** *40* (13), 4464-4469.

44. Naolou, T.; Busse, K.; Kressler, J. ê. Synthesis of Well-Defined Graft Copolymers by Combination of Enzymatic Polycondensation and Γ_£ClickΓ_¦ Chemistry. *Biomacromolecules* **2010,** *11* (12), 3660-3667.

45. Dai, S.; Xue, L.; Zinn, M.; Li, Z. Enzyme-Catalyzed Polycondensation of Polyester Macrodiols with Divinyl Adipate: A Green Method for the Preparation of Thermoplastic Block Copolyesters. *Biomacromolecules* **2009,** *10* (12), 3176-3181.

46. Heise, A.; Duxbury, C. J.; Palmans, A. R. A. Enzyme-Mediated Ring-Opening Polymerization. In *Handbook of Ring-Opening Polymerization*, Wiley-VCH Verlag GmbH & Co. KGaA: 2009; pp 379-397.

47. Hofmann, G. O. Biodegradable implants in traumatology: a review on the state-of-the-art. *Archives of Orthopaedic and Trauma Surgery* **1995,** *114* (3), 123-132.

48. Bstman, O.; PihlajamΣki, H. Clinical biocompatibility of biodegradable orthopaedic implants for internal fixation: a review. *Biomaterials* **2000,** *21* (24), 2615-2621.

49. Pool, R. In Search of the Plastic Potato. *Science* **1989,** *245* (4923), 1187-1189.

50. Auras, R.; Harte, B.; Selke, S. An Overview of Polylactides as Packaging Materials. *Macromol. Biosci.* **2004,** *4* (9), 835-864.

51. Czajka, D. R.; Lion, L. W.; Shuler, M. L.; Ghiorse, W. C. Evaluation of the utility of bacterial extracellular polymers for treatment of metal-contaminated soils: Polymer persistence, mobility, and the influence of lead. *Water Research* **1997,** *31* (11), 2827-2839.

52. Rogers, M. E.; Long, T. E.; Turner, S. R. Introduction to Synthetic Methods in Step-Growth Polymers. In *Synthetic Methods in Step-Growth Polymers*, John Wiley & Sons, Inc.: 2003; pp 1-16.

53. Hadjichristidis, N.; Pispas, S.; Floudas, G. Block Copolymers by Anionic Polymerization. In *Block Copolymers*, John Wiley & Sons, Inc.: 2002; pp 1-27.

54. Hadjichristidis, N.; Pispas, S.; Floudas, G. Block Copolymers by Cationic Polymerization. In *Block Copolymers*, John Wiley & Sons, Inc.: 2002; pp 28-46.

55. Hadjichristidis, N.; Pispas, S.; Floudas, G. Block Copolymers by Living Free Radical Polymerization. In *Block Copolymers*, John Wiley & Sons, Inc.: 2002; pp 47-64.

56. Hawker, C. J. Nitroxide-Mediated Living Radical Polymerizations. In *Handbook of Radical Polymerization*, John Wiley & Sons, Inc.: 2002; pp 463-521.

57. Matyjaszewski, K.; Xia, J. Fundamentals of Atom Transfer Radical Polymerization. In *Handbook of Radical Polymerization*, John Wiley & Sons, Inc.: 2002; pp 523-628.

58. Junkers, T.; Lovestead, T. M.; Barner-Kowollik, C. The RAFT Process as a Kinetic Tool: Accessing Fundamental Parameters of Free Radical Polymerization. In *Handbook of RAFT Polymerization*, Wiley-VCH Verlag GmbH & Co. KGaA: 2008; pp 105-149.

59. Hadjichristidis, N.; Pispas, S.; Floudas, G. Synthesis of Block Copolymers by a Combination of Different Polymerization Methods. In *Block Copolymers*, John Wiley & Sons, Inc.: 2002; pp 91-113.

60. Osada, K.; Kataoka, K. Drug and Gene Delivery Based on Supramolecular Assembly of PEG-Polypeptide Hybrid Block Copolymers. In *Peptide Hybrid Polymers*, 202 ed.; Klok, H. A., Schlaad, H., Eds.; Springer Berlin / Heidelberg: 2006; pp 113-153.

61. Winzenburg, G.; Schmidt, C.; Fuchs, S.; Kissel, T. Biodegradable polymers and their potential use in parenteral veterinary drug delivery systems. *Advanced Drug Delivery Reviews* **2004,** *56* (10), 1453-1466.

62. Voronov, A.; Vasylyev, S.; Kohut, A.; Peukert, W. Surface activity of new invertible amphiphilic polyesters based on poly(ethylene glycol) and aliphatic dicarboxylic acids. *Journal of Colloid and Interface Science* **2008,** *323* (2), 379-385.

63. Yang, A.; Yang, L.; Liu, W.; Li, Z.; Xu, H.; Yang, X. Tumor necrosis factor alpha blocking peptide loaded PEG-PLGA nanoparticles: Preparation and in vitro evaluation. *International Journal of Pharmaceutics* **2007,** *331* (1), 123-132.

64. Yang, L.; El Ghzaoui, A.; Li, S. In vitro degradation behavior of poly(lactide)-poly(ethylene glycol) block copolymer micelles in aqueous solution. *International Journal of Pharmaceutics* **2010,** *400* (1-2), 96-103.

65. Younes, H.; Cohn, D. Morphological study of biodegradable PEO/PLA block copolymers. *Journal of Biomedical Materials Research* **1987,** *21* (11), 1301-1316.

66. Kimura, Y.; Matsuzaki, Y.; Yamane, H.; Kitao, T. Preparation of block copoly(ester-ether) comprising poly(l-lactide) and poly(oxypropylene) and degradation of its fibre in vitro and in vivo. *Polymer* **1989,** *30* (7), 1342-1349.

67. Xiong, C. D.; Cheng, L. M.; Xu, R. P.; Deng, X. M. Synthesis and characterization of block copolymers from D,L-lactide and poly(tetramethylene ether glycol). *J. Appl. Polym. Sci.* **1995,** *55* (6), 865-869.

68. Zhang, J.; Luo, L.; Lyu, S.; Schley, J.; Pudil, B.; Benz, M.; Buckalew, A.; Chaffin, K.; Hobot, C.; Sparer, R. Spontaneous transesterification reactions between poly(lactide-co-glycolide) and poly(trimethylene carbonate) at the interface. *J. Appl. Polym. Sci.* **2010,** *117* (4), 2153-2158.

69. Dobrzynski, P. Synthesis of biodegradable copolymers with low-toxicity zirconium compounds. III. Synthesis and chain-microstructure analysis of terpolymer obtained from L-lactide, glycolide, and ε-caprolactone initiated by zirconium (IV) acetylacetonate. *J. Polym. Sci. A Polym. Chem.* **2002,** *40* (18), 3129-3143.

70. Mazarro, R.; de Lucas, A.; Gracia, I.; Rodriguez, J. F. Copolymerization of D,L-lactide and glycolide in supercritical carbon dioxide with zinc octoate as catalyst. *J. Biomed. Mater. Res.* **2008,** *85B* (1), 196-203.

71. Ferruti, P.; Penco, M.; D'Addato, P.; Ranucci, E.; Deghenghi, R. Synthesis and properties of novel block copolymers containing poly(lactic-glycolic acid) and poly(ethyleneglycol) segments. *Biomaterials* **1995,** *16* (18), 1423-1428.

72. Penco, M.; Marcioni, S.; Ferruti, P.; D'Antone, S.; Deghenghi, R. Degradation behaviour of block copolymers containing poly(lactic-glycolic acid) and poly(ethylene glycol) segments. *Biomaterials* **1996,** *17* (16), 1583-1590.

73. Deng, X. M.; Xiong, C. D.; Cheng, L. M.; Xu, R. P. Synthesis and characterization of block copolymers from D, L-lactide and poly(ethylene glycol) with stannous chloride. *J. Polym. Sci. C Polym. Lett.* **1990,** *28* (13), 411-416.

74. Kricheldorf, H. R.; Meier-Haack, J. Polylactones, 22 ABA triblock copolymers of L-lactide and poly(ethylene glycol). *Makromol. Chem.* **1993,** *194* (2), 715-725.

75. Kricheldorf, H. R.; Boettcher, C. Polylactones 27. Anionic polymerization of L-lactide. Variation of endgroups and synthesis of block copolymers with poly(ethylene oxide). *Makromolekulare Chemie. Macromolecular Symposia* **1993,** *73* (1), 47-64.

76. Youxin, L.; Kissel, T. Synthesis and properties of biodegradable ABA triblock copolymers consisting of poly(l-lactic acid) or poly (l-lactic-co-glycolic acid) A-blocks attached to central poly (oxyethylene) B-blocks. *Journal of Controlled Release* **1993,** *27* (3), 247-257.

77. Youxin, L.; Volland, C.; Kissel, T. In-vitro degradation and bovine serum albumin release of the ABA triblock copolymers consisting of poly (L(+) lactic acid), or poly(L(+) lactic acid-co-glycolic acid) A-blocks attached to central polyoxyethylene B-blocks. *Journal of Controlled Release* **1994,** *32* (2), 121-128.

78. Ma, J.; Feng, P.; Ye, C.; Wang, Y.; Fan, Y. An improved interfacial coacervation technique to fabricate biodegradable nanocapsules of an aqueous peptide solution from polylactide and its block copolymers with poly(ethylene glycol). *Colloid and Polymer Science* **2001,** *279* (4), 387-392.

79. Zhu, Z.; Xiong, C.; Zhang, L.; Yuan, M.; Deng, X. Preparation of biodegradable polylactide-co-poly(ethylene glycol) copolymer by lactide reacted poly(ethylene glycol). *European Polymer Journal* **1999,** *35* (10), 1821-1828.

80. Hu, D. S.-G.; Liu, H. J.; Pan, I. L. Inhibition of bovine serum albumin adsorption by poly(ethylene glycol) soft segment in biodegradable poly(ethylene glycol)/poly(L-lactide) copolymers. *J. Appl. Polym. Sci.* **1993,** *50* (8), 1391-1396.

81. Hagan, S. A.; Davis, S. S.; Illum, L.; Davies, M. C.; Garnett, M. C.; Taylor, D. C.; Irving, M. P.; Tadros, T. F. Estimation of the Poly(ethylene glycol) Chain Length of L-Polylactide-Polyethylene Glycol in Aqueous Dispersions Using Viscoelastic Measurements. *Langmuir* **1995,** *11* (5), 1482-1485.

82. Black, F. E.; Hartshorne, M.; Davies, M. C.; Roberts, C. J.; Tendler, S. J. B.; Williams, P. M.; Shakesheff, K. M.; Cannizzaro, S. M.; Kim, I.; Langer, R. Surface Engineering and Surface Analysis of a Biodegradable Polymer with Biotinylated End Groups. *Langmuir* **1999,** *15* (9), 3157-3161.

83. Guerra, G. D.; Cerrai, P.; Tricoli, M.; Maltinti, S. Release of 5-fluorouracil by biodegradable poly(ester-ether-ester)s. Part I: release by fused thin sheets. *Journal of Materials Science: Materials in Medicine* **2001,** *12* (4), 313-317.

84. Li, R.; Li, X.; Xie, L.; Ding, D.; Hu, Y.; Qian, X.; Yu, L.; Ding, Y.; Jiang, X.; Liu, B. Preparation and evaluation of PEG-PCL nanoparticles for local tetradrine delivery. *International Journal of Pharmaceutics* **2009,** *379* (1), 158-166.

85. Jin, J.; Wu, D.; Sun, P.; Liu, L.; Zhao, H. Amphiphilic Triblock Copolymer Bioconjugates with Biotin Groups at the Junction Points: Synthesis, Self-Assembly, and Bioactivity. *Macromolecules* **2011,** *44* (7), 2016-2024.

86. Chen, C.; Yu, C. H.; Cheng, Y. C.; Yu, P. H. F.; Cheung, M. K. Biodegradable nanoparticles of amphiphilic triblock copolymers based on poly(3-hydroxybutyrate) and poly(ethylene glycol) as drug carriers. *Biomaterials* **2006,** *27* (27), 4804-4814.

87. Chen, C.; Yu, C. H.; Cheng, Y. C.; Yu, P. H. F.; Cheung, M. K. Preparation and characterization of biodegradable nanoparticles based on amphiphilic poly(3-hydroxybutyrate)-poly(ethylene glycol)-poly(3-hydroxybutyrate) triblock copolymer. *European Polymer Journal* **2006,** *42* (10), 2211-2220.

88. Li, Y.; Kissel, T. Synthesis, characteristics and in vitro degradation of star-block copolymers consisting of $_{L}$ -lactide, glycolide and branched multi-arm poly(ethylene oxide). *Polymer* **1998,** *39* (18), 4421-4427.

89. Choi, Y. K.; Bae, Y. H.; Kim, S. W. Star-Shaped Poly(ether-ester) Block Copolymers: Synthesis, Characterization, and Their Physical Properties. *Macromolecules* **1998,** *31* (25), 8766-8774.

90. Wang, F.; Bronich, T. K.; Kabanov, A. V.; Rauh, R. D.; Roovers, J. Synthesis and Evaluation of a Star Amphiphilic Block Copolymer from Poly(ε-caprolactone) and Poly(ethylene glycol) as a Potential Drug Delivery Carrier. *Bioconjugate Chemistry* **2005,** *16* (2), 397-405.

91. Wang, F.; Bronich, T. K.; Kabanov, A. V.; Rauh, R. D.; Roovers, J. Synthesis and Characterization of Star Poly(ε-caprolactone)-b-Poly(ethylene glycol) and Poly(l-lactide)-b-Poly(ethylene glycol) Copolymers: Evaluation as Drug Delivery Carriers. *Bioconjugate Chemistry* **2008,** *19* (7), 1423-1429.

92. Gou, P. F.; Zhu, W. P.; Shen, Z. Q. Synthesis, Self-Assembly, and Drug-Loading Capacity of Well-Defined Cyclodextrin-Centered Drug-Conjugated Amphiphilic A14B7 Miktoarm Star Copolymers Based on Poly(ε-caprolactone) and Poly(ethylene glycol). *Biomacromolecules* **2010,** *11* (4), 934-943.

93. Khoee, S.; Rahimi, H. B. Intermolecular interaction and morphology investigation of drug loaded ABA-triblock copolymers with different hydrophilic/lipophilic ratios. *Bioorganic & Medicinal Chemistry* **2010,** *18* (20), 7283-7290.

94. R.van Dijkhuizen-Radersma, R.; Metairie, S.; Roosma, J. R.; de Groot, K.; Bezemer, J. M. Controlled release of proteins from degradable poly(ether-ester) multiblock copolymers. *Journal of Controlled Release* **2005,** *101* (1-3), 175-186.

95. R.van Dijkhuizen-Radersma, R.; Roosma, J. R.; Kaim, P.; Metairie, S.; Peters, F. L. A. M.; de Wijn, J.; Zijlstra, P. G.; de Groot, K.; Bezemer, J. M. Biodegradable poly(ether-ester) multiblock copolymers for controlled release applications. *Journal of Biomedical Materials Research Part A* **2003,** *67A* (4), 1294-1304.

96. Wang, L. c.; Chen, J. w.; Liu, H. l.; Chen, Z. q.; Zhang, Y.; Wang, C. y.; Feng, Z. g. Synthesis and evaluation of biodegradable segmented multiblock poly(ether ester) copolymers for biomaterial applications. *Polym. Int.* **2004,** *53* (12), 2145-2154.

97. Hwang, S. Y.; Jin, X. Y.; Yoo, E. S.; Im, S. S. Synthesis, physical properties and enzymatic degradation of poly (oxyethylene-b-butylene succinate) ionomers. *Polymer* **2011,** *52* (13), 2784-2791.

98. Voronov, A.; Kohut, A.; Peukert, W.; Voronov, S.; Gevus, O.; Tokarev, V. Invertible Architectures from Amphiphilic Polyesters. *Langmuir* **2006,** *22* (5), 1946-1948.

99. Vassiliou, A. A.; Papadimitriou, S. A.; Bikiaris, D. N.; Mattheolabakis, G.; Avgoustakis, K. Facile synthesis of polyester-PEG triblock copolymers and preparation of amphiphilic nanoparticles as drug carriers. *Journal of Controlled Release* **2010,** *148* (3), 388-395.

100. Soppimath, K. S.; Aminabhavi, T. M.; Kulkarni, A. R.; Rudzinski, W. E. Biodegradable polymeric nanoparticles as drug delivery devices. *Journal of Controlled Release* **2001,** *70* (1-2), 1-20.

101. Dalton, P. D.; Lleixa Calvet, J.; Mourran, A.; Klee, D.; Möller, M. Melt electrospinning of poly-(ethylene glycol-block-ε-caprolactone). *Biotechnology Journal* **2006,** *1* (9), 998-1006.

102. Kim, K.; Yu, M.; Zong, X.; Chiu, J.; Fang, D.; Seo, Y. S.; Hsiao, B. S.; Chu, B.; Hadjiargyrou, M. Control of degradation rate and hydrophilicity in electrospun non-woven poly($_{D\ L}$-lactide) nanofiber scaffolds for biomedical applications. *Biomaterials* **2003,** *24* (27), 4977-4985.

103. Yang, D. J.; Zhang, L. F.; Xu, L.; Xiong, C. D.; Ding, J.; Wang, Y. Z. Fabrication and characterization of hydrophilic electrospun membranes made from the block copolymer of poly(ethylene glycol-co-lactide). *Journal of Biomedical Materials Research Part A* **2007,** *82A* (3), 680-688.

104. Sun, J.; Bubel, K.; Chen, F.; Kissel, T.; Agarwal, S.; Greiner, A. Nanofibers by Green Electrospinning of Aqueous Suspensions of Biodegradable Block Copolyesters for Applications in Medicine, Pharmacy and Agriculture. *Macromol. Rapid Commun.* **2010,** *31* (23), 2077-2083.

105. Soccio, M.; Lotti, N.; Finelli, L.; Gazzano, M.; Munari, A. Aliphatic poly(propylene dicarboxylate)s: Effect of chain length on thermal properties and crystallization kinetics. *Polymer* **2007,** *48* (11), 3125-3136.

106. Goodman I. Encyclopedia of polymer science and engineering. Wiley: 1988; pp 1-75.

107. Plage, B.; Schulten, H. R. Thermal degradation and mass-spectrometric fragmentation processes of polyesters studied by time/temperature-resolved pyrolysis-field ionization mass spectrometry. *Macromolecules* **1990,** *23* (10), 2642-2648.

108. Miyata, T.; Masuko, T. Crystallization behaviour of poly(tetramethylene succinate). *Polymer* **1998,** *39* (6-7), 1399-1404.

109. Cohen, L.; Rocco, A. Study of the Crystallization Kinetics. Poly(ethylene oxide) and a blend of poly(ethylene oxide) and poly(bisphenol A-co-epichlorohydrin). *Journal of Thermal Analysis and Calorimetry* **2000,** *59* (3), 625-632.

110. Silva, V. P. R.; Silva, G. G.; Caliman, V.; Rieumont, J.; de Miranda-Pinto, C. O. B.; Archanjo, B. S.; Neves, B. R. A. Morphology, crystalline structure and thermal properties of PEO/MEEP blends. *European Polymer Journal* **2007,** *43* (8), 3283-3291.

111. Cheng, S. Z. D.; Wunderlich, B. Molecular segregation and nucleation of poly(ethylene oxide) crystallized from the melt. I. Calorimetric study. *J. Polym. Sci. B Polym. Phys.* **1986,** *24* (3), 577-594.

112. Cheng, S. Z. D.; Wunderlich, B. A study of crystallization of low-molecular-mass poly(ethylene oxide) from the melt. *Macromolecules* **1989,** *22* (4), 1866-1873.

113. Alexandridis, P. Structural Polymorphism of Poly(ethylene oxide)Γêþoly(propylene oxide) Block Copolymers in Nonaqueous Polar Solvents. *Macromolecules* **1998,** *31* (20), 6935-6942.

114. Gabarayeva, N. I.; Grigorjeva, V. V. Sporoderm ontogeny in Chamaedorea microspadix (Arecaceae): self-assembly as the underlying cause of development. *Grana* **2010,** *49* (2), 91-114.

115. A.Romo-Uribe Hybrid - block copolymer nanocomposites. characterization of nanostructure by small-angle X-ray scattering (SAXS). *REVISTA MEXICANA DE FI´SICA* **2007,** *53* (3), 171-178.

116. Hamley, I. W. Melt phase behaviuor of block copolymers. In *The Physics of Block Copolymers*, Oxford University Press: 1998; p 24.

117. Loo, Y. L.; Register, R. A. Crystallization Within Block Copolymer Mesophases. In *Developments in Block Copolymer Science and Technology*, John Wiley & Sons, Ltd: 2004; pp 213-243.

118. Göpferich, A. Mechanisms of polymer degradation and erosion. *Biomaterials* **1996,** *17* (2), 103-114.

119. Langer, R.; Peppas, N. Chemical and Physical Structure of Polymers as Carriers for Controlled Release of Bioactive Agents: A Review. *Journal of Macromolecular Science, Part C: Polymer Reviews* **1983,** *23* (1), 61-126.

120. Langer, R. New methods of drug delivery. *Science* **1990,** *249* (4976), 1527-1533.

121. Vacanti, C. A.; Vacanti, J. P.; Langer, R. Tissue Engineering Using Synthetic Biodegradable Polymers. In *Polymers of Biological and Biomedical Significance*, 540 ed.; American Chemical Society: 1993; pp 16-34.

122. Taniguchi, I.; Nakano, S.; Nakamura, T.; El-Salmawy, A.; Miyamoto, M.; Kimura, Y. Mechanism of Enzymatic Hydrolysis of Poly(butylene succinate) and Poly(butylene succinate-co-L-lactate) with a Lipase from Pseudomonas cepacia. *Macromol. Biosci.* **2002,** *2* (9), 447-455.

123. Shih, Y. F.; Wu, T. M. Enzymatic degradation kinetics of poly(butylene succinate) nanocomposites. *Journal of Polymer Research* **2009,** *16* (2), 109-115.

124. Ding, M.; Zhang, M.; Yang, J.; Qiu, J. h. Study on the enzymatic degradation of PBS and its alcohol acid modified copolymer. *Biodegradation* **2011,** 1-6.

125. Park, S. Y.; Bae, Y. H. Novel pH-sensitive polymers containing sulfonamide groups. *Macromol. Rapid Commun.* **1999,** *20* (5), 269-273.

126. Kang, S. I.; Na, K.; Bae, Y. H. Sulfonamide-containing polymers: a new class of pH-sensitive polymers and gels. *Macromol. Symp.* **2001,** *172* (1), 149-156.

127. Kang, S. I.; Bae, Y. H. pH-Induced Volume-Phase Transition of Hydrogels Containing Sulfonamide Side Group by Reversible Crystal Formation. *Macromolecules* **2001,** *34* (23), 8173-8178.

128. Kang, S. I.; Bae, Y. H. pH-Induced solubility transition of sulfonamide-based polymers. *Journal of Controlled Release* **2002,** *80* (1-3), 145-155.

129. Hong, S. W.; Ahn, C. H.; Huh, J.; Jo, W. H. Synthesis of a PEGylated Polymeric pH Sensor and Its pH Sensitivity by Fluorescence Resonance Energy Transfer. *Macromolecules* **2006,** *39* (22), 7694-7700.

130. Robert M.Silverstein; Francis X.Webster; David J.Kiemle *Spectrometric identification of organic compounds;* 7th ed.; John Wiley & Sons: 2005.

131. Kalyanasundaram, K.; Thomas, J. K. Environmental effects on vibronic band intensities in pyrene monomer fluorescence and their application in studies of micellar systems. *Journal of the American Chemical Society* **1977,** *99* (7), 2039-2044.

132. Kalyanasundaram, K.; Thomas, J. K. Solvent-dependent fluorescence of pyrene-3-carboxaldehyde and its applications in the estimation of polarity at micelle-water interfaces. *The Journal of Physical Chemistry* **1977,** *81* (23), 2176-2180.

133. Wilhelm, M.; Zhao, C. L.; Wang, Y.; Xu, R.; Winnik, M. A.; Mura, J. L.; Riess, G.; Croucher, M. D. Poly(styrene-ethylene oxide) block copolymer micelle formation in water: a fluorescence probe study. *Macromolecules* **1991,** *24* (5), 1033-1040.

134. Zana, R.; In, M.; Levy, H.; Duportail, G. Alkanediyl--α,ω-bis(dimethylalkylammonium bromide). 7. Fluorescence Probing Studies of Micelle Micropolarity and Microviscosity. *Langmuir* **1997,** *13* (21), 5552-5557.

135. Nakahara, Y.; Kida, T.; Nakatsuji, Y.; Akashi, M. New Fluorescence Method for the Determination of the Critical Micelle Concentration by Photosensitive Monoazacryptand Derivatives. *Langmuir* **2005,** *21* (15), 6688-6695.

136. Bandyopadhyay, P.; Ghosh, A. K. Reversible Fluorescence Quenching by Micelle Selective Benzophenone-Induced Interactions between Brij Micelles and Polyacrylic Acids: Implications for Chemical Sensors. *The Journal of Physical Chemistry B* **2010,** *114* (35), 11462-11467.

137. Chattopadhyay, A.; London, E. Fluorimetric determination of critical micelle concentration avoiding interference from detergent charge. *Analytical Biochemistry* **1984,** *139* (2), 408-412.

English Summary

Different biodegradable amphiphilic block copolymers were prepared by melt-polycondensation. These block copolymers are composed of different molar ratio of two segments, 1st is hydrophilic block which is methoxy poly(ethylene oxide) MPEO of two different molecular weights, (5000 and 2000 g/mol). The hydrophobic segments are aliphatic poly ester of poly hexylene adipate PHA, polybutylene succinate PBS, polyhexylene succinate PHS and polybutylene adipate PBA. Full characterization of these block copolymers have been achieved using GPC, NMR, Thermal analysis, and X-ray analysis. Hydrolytic and enzymatic degradation have been done. Loading of PHA-b-MPEO5 with pH sensitive moiety is also achieved. Values of cmc of two commercially available surfactants as well as two samples of our polymers were measured by fluorescence spectroscopy using pyrene as a probe as detailed in the next points:

1- At first, the block copolymer composition was determined by NMR after thorough purification of the polymers. It was found that in the molar composition of the block segments, there is a deviation from the feed molar ratio in the final molar ratio. This deviation is increased by increasing of the amount of MPEO in the feed molar ratio. This behavior was attributed to the higher viscosity of the reaction medium during the polycondensation, consequently the movement of MPEO polymer chains becomes difficult and they could not contribute easily in the polycondensation reaction via their chain end groups. Conversions by weight are satisfactory with average value of 85 %.
2- Moderate molecular weight was obtained for most of the polymers. For the block copolyesters that contain more MPEO segments, the obtained molecular weight is somewhat lower, this low value because in presence of higher amount of MPEO in the reaction medium, it has bigger chance to react with the growing PE chains at earlier stage, i.e. before PE forms longer chains, resulting in a fixed MPEO chain length and lower PE chain length and the overall molecular weight is reduced. All the obtained block copolyesters have mono-modal GPC curves, with slight shift of the polymers containing larger amount of MPEO to higher elution volume i.e. lower molecular weight.

3- The thermal properties of the prepared block copolymers were investigated by TGA and DSC. In TGA it was found that one-step degradation is observed in all curves. Also the initial decomposition temperature (0 % decomposition) is ranging from 320 to 350 ^{o}C, indicating high thermal stability of the whole block copolymer categories.

4- DSC measurement were carried out for both homopolymers PHA and PBS as well as the prepared block copolymers and the data were extracted from both the heating and cooling cycles as described in details in the body of the thesis. In the heating cycle Tm are observed at 56, 60, and 116 °C for MPEO, PHA and PBS respectively. In addition an exothermic peak (Texo) at 94 °C could be observed for PBS exactly as observed in the literaure.[108] Tg could be obtained only for the semi-crystalline polymers PHA and PBS at -60 and -37 °C respectively, while for PEO it was not possible to detect any Tg, as PEO is mostly crystalline polymer (70-80 %).[109] No significant difference in the value of Tg, Tcc and heat of fusion (Δ Hm) for adipate based block copolymers. But a slight reduction in melting point Tm was observed in case of polymer containing more % of MPEO. This reduction in melting point may because the MPEO homopolymer itself has lower melting than PHA; therefore it lowers the overall melting of the block copolymer when it exists in larger amounts. In block copolymers with fewer amounts of MPEO and due to the comparable values of Tm of both MPEO and PHA, a merging of the two melting peaks could be possible during the heating cycle, while two melting peaks could be observed in case of block copolymer containing more amount of MPEO. The same behavior could be observed in the succinate based system, Tm of succinate moiety is ranging from 112-116 ^{o}C, while those of MPEO segments are in the range from 32-40 ^{o}C. For the block copolymers PBA-b-MPEO and PHS-b-MPEO, the melting points at around 55 ^{o}C is split into two peaks that represents the two segments, however the splitting is more distinct in case of PHS-b-MPEO.

5- The WAXD patterns have shown that by altering the MPEO/PE molar ratio, the crystal structure exhibit different behavior. For example, in the WXRD patterns of the block copolymers PHA-b-MPEO of both MPEO5 and MPEO2, by increasing the amount of PHA segments in the block copolymers, the main PEO diffraction peaks exhibited differences in shape and position in which the intensity of the characteristic peaks at 2θ:

19.68 and 23.81 were decreased or even diminished at the least amount of MPEO in the block copolymers which reflect a change in the crystalline structure of the MPEO in these materials. The same behavior could be observed in the remaining polymers, where a rearrangement of crystal structure of both hydrophilic and hydrophobic segments.

6- The stress–strain properties of the block copolymers show good properties in case of block copolymers contain less amount of MPEO. As the amount of MPEO increase the consistency of the polymer films become very weak and the stress strain curves could not be measured. These results could be attributed to the microphase separation caused by segments segregation that takes place in presence of sufficient amount of MPEO.

7- Hydrolytic degradation is achieved using potassium hydroxide solution of concentration 5 % and 10%, and all polymers are hydrolyzed by attacking the ester linkage of the hydrophobic segments.

8- Enzyme catalyzed degradation is also achieved using lipase from *pseudomonas cepacia* enzyme. This enzyme is suitable to degrade PHA, PBA and PHS. But it is not efficient for PBS based polymers

9- Degradation mechanism was via surface erosion and the order of degradability could be arranged as follow PBA=PHS > PHA> PBS.

10- Synthesis of pH responsive polymer from the prepared block copolymers was achieved by immobilizing a pH-responsive (Sulfadimethoxine, SD) moiety to the chain end of polymers and the structure was proofed using NMR, IR and UV spectroscopy

11- Low temperature, longer reaction time and using proper solvent (THF) are required to obtain well-functionalized chain ends without sacrificing the polymer properties specially molecular weight, where higher temperatures in absence of solvent lead to polymer degradation

12- The SD-loaded polymer exhibit pH transition as proofed by turbidity measurements and the pKa of the loaded polymers ranged from 5.6 to 6, which is close to the pKa of the SD itself (5.9).

13- cmc of SD loaded polymer and SD-free polymer was determined using fluorescence spectroscopy. At first the cmc of two commercial surfactants were measured, the value obtained is matching with those reported in the literature. For our polymer, PHA-b-MPEO5 (1:1) both SD-free and SD-loaded were selected for cmc measurements. The

value of cmc of SD-free sample is 0.4 g/L while this of SD-loaded sample is 0.75 g/L which differ from the value of SD-free polymer because both polymers have different molecular weights.

Zusammenfassung

(German Summary)

Verschiedene bioabbaubare amphiphile Blockcopolymere wurden durch Schmelz-polykondensation hergestellt. Diese Blockcopolymere bestehen aus zwei unterschiedlichen Segmenten. Das 1. Segment besteht aus einem hydrophilen Block, Methoxypolyethylenoxid (MPEO) besitzt zwei unterschiedliche Molekulargewichte (5000 und 2000 g/mol). Die hydrophoben Segmente sind aliphatische Polyester von Poly hexyleneadipate PHA, polybutylenesuccinate (PBS), Polyhexylenesuccinate, (PHS) und Polybutyleneadipate (PBA). Die vollständige Charakterisierung dieser Blockcopolymere wurden erreicht mit GPC, NMR, thermische Analyse und die Röntgenstrukturanalyse. Hydrolytischer und enzymatischer Abbau wurden durchgeführt. PHA-b-MPEO5 werden mit pH-empfindlichen Einheit beladen. Werte von cmc von zwei kommerziell erhältlichen Tensiden sowie zwei Beispiele unserer Polymere wurden durch Fluoreszenz-Spektroskopie mit Pyren als Sonde gemessen, wie in den folgenden Punkten beschrieben.

1. Zuerst, die Blockcopolymer-Zusammensetzung wurde durch NMR nach gründlicher Reinigung der Polymere bestimmt. Es wurde festgestellt, dass in den erhaltenen Polymeren verschedene molaren Zusammensetzung des Blocks nicht dem eingestzen v-Molverhältnis in den finalen Molverhältnis. Diese Abweichung ist durch die Erhöhung der Menge von MPEO im Feed-Molverhältnis erhöht. Dieses Verhalten lässt sich durch die höhre Viskosität des Reaktionsmediums während der Polykondensation erklären. Die Bewegung der MPEO Polymerketten wurde schwieriger, wodurch, schlechter in der Polykondensationsreaktion über ihre Endgruppen reagieren konnten. Die Ausbeuten sind zufriedenstellend mit einem durchschnittlichen Wert von 85%.
2. Für die meisten der erhaltenen Polymere, wurde einmäßiges Molekulargewicht erreicht. Für die Block Copolyester, die mehr MPEO Segmente enthalten, ist das erhaltene Molekulargewicht etwas niedriger. Dieser niedrige Wert kann daran liegen, dass größere Mengen von MPEO im Reaktionsmedium, eine größere Chance haben mit den wachsenden PE-Ketten bei früheren Stufe der Polykondensation zu reagieren. Bei einer festen MPEO Kettenlänge wurden PE Kettenlängen gebildet und das gesamte Molekulargewicht reduziert. Alle erhalten Blockcopolyester haben monomodal GPC-

Kurven, mit leichten Verschiebung der Polymere, die größere Menge an MPEO haben zu höheren Elutionsvolumen.

3. Die thermischen Eigenschaften der hergestellten Blockcopolymere wurden durch TGA und DSC untersucht. In der ein Ein-Schritt-Abbau in allen Kurven zu beobachtet. Die initiale Dekompositionstemperatur (0 % Dekomposition) ist von 320 bis 350 ^{o}C, dh alle Blockcopolymere Kategorien besitzen eine hohe thermische Stabilität.
4. Sowohl von den Homopolymeren (PHA und PBS) als auch von den hergestellten Blockcopolymeren wurden DCS-Messungen durchgeführt. Die Daten der Heiz- und Abkühlkurven wurden, wie im Hauptteil der Arbeit beschrieben, gesondert ausgewertet. In den heizkurven wurden für MPEO, PHA und PBS Schmelztemperaturen von 56, 60 und 116 °C ermittelt. Analog zur Literatur wurde für PBS zusätzlich ein exothermer Peak (Texo) bei 94°C beobachtet. Für die teilkristallinen Polymere PHA und PBS wurden Tg bei 60 und -37 °C bestimmt. Für PEO konnte kein Tg bestimmt werden, weil PEO mit 70-80% eine starke Kristallinität aufweist. Es konnte kein signifikanter Unterschied in den Werten der Tg, Tcc und Schmelzenthalpie (Δ Hm) zu Adipat Blockcopolymeren festgestellt werden. Die Schmelztemperaturen der Copolymere mit größerem prozentualem Anteil an MPEO sanken leicht. Eine mögliche Erklärung hierfür ist, dass das MPEO-Homopolymer eine niedrigere Schmelztemperatur als PHA aufweist und somit die die Schmelztemperatur des gesamten Polymers herabsetzt. In Blockcopolymeren mit geringeren Anteilen an MPEO konnte durch die ähnlichen Tm nur ein überlagerter Schmelzpeaks beider Polymerblöcke in der Heizkurve beobachtet werden. Zwei getrennte Schmelzpeaks wurden bei den Blockcopolymeren mit größeren Anteilen an MPEO beobachtet. Das gleiche Verhalten wurde bei Succinat basierten Systemen beobachtet. Die Tm der Succinat Reste lag im Bereich von 112-116 °C und die der MPEO-Segmente bei 32-40 °C. Für die Blockcopolymere PBA-b-MPEO und PHS-b-MPEO ist der Schmelzpeak bei ca. 55 °C in zwei Peaks aufgespalten. Diese Peaks repräsentieren die Schmezlpeaks der beiden Polymerblöcke, wobei der Aufspaltung bei dem PHS-b-MPEO deutlicher zu sehen ist.
5. Die WAXD-Profile haben gezeigt, dass die Polymeren durch die Veränderung der molaren Verhältnisse von MPEO/PE eine Veränderung der kristallstruktur aufweisen. Zum Beispiel sind für die Hauptpeaks von PEO in den WXRD-Profilen der

Blockcopolymere PHA-b-MPEO von MPEO5 und MPEO2 durch Zunahme der PHA-Segmente Unterschiede in Form, Position. Die Intensität der charakteristischen Peaks bei 2θ 19.68 ° und 23.81 ° wurde verringert oder bei den geringsten Mengen an MPEO im Blockcopolymer sogar unterdrückt. Diese Beobachtungen spiegeln die Veränderung der kristallstruktur von MPEO in den Copolymeren wieder. Das gleiche Verhalten konnte bei den anderen Polymeren beobachtet werden, bei denen eine Veränderung in der Kristallstruktur sowohl der hydrophilen als auch durch die hydrophoben Segmente auftrat.

6. Die Copolymere mit einer geringen Menge an MPEO zeigten gute Zug-Dehnungs-Eigenschaften. Mit Erhöhung des MPEO-Anteils wurden die Filme immer brüchiger so das keine Zug-Dehnung gemessen werden konnte. Dies könnte an der Mikrophasenseparation durch Segmenttrennung liegen, die bei ausreichenden Mengen an MEOP auftritt.
7. Der hydrolytische Abbau erfolgte über wässrige KOH (5% und 10%). Alle Polymere wurden durch Estherspaltung hydrolysiert.
8. Enzymatischer Abbau wurde mit Lipase aus Pseudomona cepacia durchgeführt. Dieses Enzym ist für den Abbau von PHA, PBA und PHS geeignet, aber ungeeignet für den Abbau von PBS.
9. Der Abbau fand durch Oberflächenerosion statt. Die Reihenfolge der Abbaubarkeit ist PBA = PHS > PHA > PBS.
10. Die Synthese von pH-responsiven Polymeren wurde durch Funktionalisierung der Blockcopolymere mit Sulfadimethoxin (SD) als Endgruppe realisiert. Die funktionalisierung wurde durch NMR-, IR- und UV-Spektroskopie belegt.
11. Für eine gute Funktionalisierung der Kettenenden wurde die Reaktion in geeignetem Lösungsmittel (THF) bei niedriger Temperatur und für lange Zeit durchgeführt. Hohe Temperaturen und Substanzreaktionen führen zum Polymerabbau.
12. Der pH-Übergang der SD-beladenen Polymere wurden durch Trübungsmessungen getestet. Der pKa-Wert der beladenen Polymere liegt zwischen 5.6 und 6.0, was ähnlich dem pKa des reinen SD (5.9) ist.
13. Die cmc-Werte des SD beladenen Polymers und des reinen Polymers wurden mittels Fluoreszenz-Spektroskopie bestimmt. Zunächst wurden zwei handelsübliche Tenside in

Übereinstimmung mit der Literatur vermessen. Es wurden SD-freie und SD-beladene Blockcopolymere (PHA-b-MPEO5 1:1) gemessen. Die cmc des SD-freien Polymers beträgt 0.4 g/l und die des SD-funktionalisiertem 0.75 g/L. Der Unterschied in der cmc kommt durch das unterschiedliche Molekulargewicht der eingesetzten Polymere.